

# Voltammetric determination of metformin and its derivatives using Cu modified polymer electrode.



**UNIVERSITY** *of the*  
**WESTERN CAPE**

*By*

**Andisiwe Ngwekazi**

A thesis submitted in partial fulfilment of the requirement for the degree of

**Magister in Scientiae**

Faculty of Natural Science

Chemistry Department

University of the Western Cape

Cape Town, South Africa

Prof PGL Baker (**Supervisor**)

Dr L.P Mciteka (**Co-supervisor**)

March 2020

## KEYWORDS

Metformin

Metformin analogues

Type II diabetes mellitus

Polypyrrole

Copper nanoparticles

Electrochemistry

Metformin derivatives

Cyclic Voltammetry

Fourier Transform Infrared

Scanning Electron Microscopy

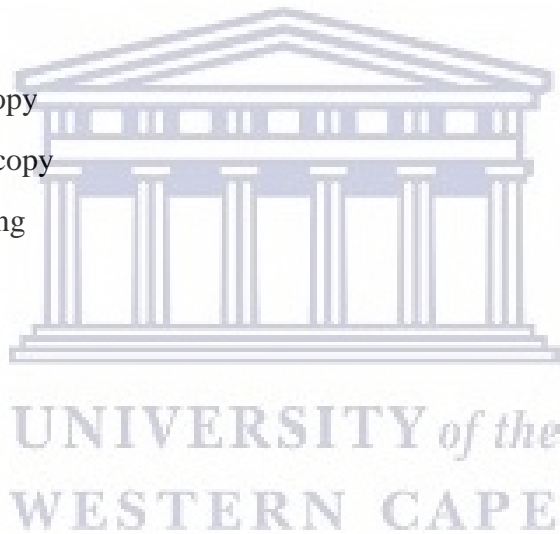
Transform Electron Microscopy

Small-Angle X-ray Scattering

Glassy Carbon Electrode

Limit of detection

Limit of quantification



## ABSTRACT

Diabetes, a worldwide disease, is classified into two types, type 1 or insulin-dependent and type 2 or noninsulin-dependent. Based on reports published by the International Diabetes Federation, the total number of those suffering from diabetes is growing every year. Statistics predict that type 2 diabetes, currently affecting about 8% of the adult population, would spread at such a pace that by 2030, more than 40 million cases of diabetes would be found throughout the world. On the other hand, studies revealed that patients with type 2 diabetes mellitus (T2DM) have a lower incidence of tumour development than healthy controls and that patients diagnosed with cancer have a lower risk of mortality when treated with metformin. However, the frequent use of metformin with low oral bioavailability ranging between 40-60% in the intestinal environment leads to large accumulation on the enterocytes. Consequently, metformin or its metabolites will then be excreted in the effluent and reach the wastewater treatment plant. Thus, metformin is regarded as one of the pharmaceuticals of emerging concern, found in high abundance in wastewater treatment plant (WWTP) effluent and surface water. Literature reports that metformin does not remain active for a long time in an aqueous medium but gets converted to its metabolites which subsequently remain in wastewater for a very long time. Thus, designing metformin analogue with improved oral bioavailability is of great interest.

Quite a lot of methods are used to detect the level of metformin in wastewater nonetheless they suffer from numerous disadvantages which include long chromatographic run time, low sensitivity, large consumptions of sample volumes, and cost-effectiveness. Electrochemical sensors, on the other hand, are simple systems, with high selectivity and sensitivity for individual measurements and cost-effectiveness. In this work, electrochemical sensors will be used for the early detection of metformin in aqueous matrices. The first part of this study looked at the need to synthesize metformin analogues with improved bioavailability and harmless metabolites. However, the synthesis proved very complicated and costly and could not be explored to completion. The second part addressed the design of highly sensitive electrochemical sensors for qualification and quantification of metformin in aqueous matrices. Copper nanoparticles were successfully synthesized and characterized with scanning electron microscopy (for morphology), energy-dispersive x-ray spectroscopy (chemical composition), transmission electron microscopy

(size of nanoparticles and morphology), small-angle x-ray scattering (particle size), and fourier transform infrared (functional groups). The modified electrode was characterized by a cyclic voltammetry as well as square wave voltammetry. The novel electrode (CuNP-PPy/GCE) was prepared by electrochemically depositing copper nanoparticle-polypyrrole on a glassy carbon electrode, using 6 cycles at a potential of -0.4 to 1.0 V at  $50 \text{ mVs}^{-1}$ . The novel electrode was then characterized by cyclic voltammetry (CV) and square wave voltammetry (SWV). The bare and modified electrodes were used to detect metformin electrochemically in aqueous solution using CV and SWV and their analytical performance is reported in this thesis. The obtained diffusion coefficient ( $D_0$ ) for the bare glassy carbon electrode was  $1.4157 \times 10^{-3} \text{ cm}^2/\text{s}$ ,  $3.9821 \times 10^{-3} \text{ cm}^2/\text{s}$  for glassy carbon electrode modified with polypyrrole (PPy-GCE) and  $5.0185 \times 10^{-5} \text{ cm}^2/\text{s}$  for CuNP-PPy.



## DECLARATION

I hereby declare that “**Voltammetric determination of metformin and its analogues using a copper modified polymer electrode**” submitted to the University of the Western Cape is my work, except where indicated by referencing which are completely and accurately reported.

**Andisiwe Ngwekazi**

Signature: .....

Supervisor: Prof. Priscilla G.L Baker

Co-supervisor: Dr L.P. Mciteka

**March 2020**

The logo of the University of the Western Cape, featuring a classical building with a pediment and columns.

UNIVERSITY *of the*  
WESTERN CAPE

## ACKNOWLEDGEMENTS

I would like to take this opportunity and extend my gratitude to the following individuals for their assistance, support, and encouragement throughout my entire academic life. Without their support, I do not think it would be possible for me to complete this thesis.

- To **God** above, for the strength, wisdom, and provision throughout this journey words are not enough to thank you all I can say is I am grateful. “I will give thanks to you, Lord, with all my heart; I will tell of all your wonderful deeds” Psalms 9:1.
- To my supervisors, Prof Priscilla G.L Baker and Dr. L.P Mciteka thank you very much for your supervision, encouragement, guidance, support, and most importantly for believing in me. Your teachings and advice mean everything to me.
- To Dr. S. Hamnca, Dr. X. Ngema, and Dr. A. Faro, thank you very much for your assistance and support through this work. Your efforts are highly appreciated.
- To my colleagues in Sensor lab and organic labs, I thank you for welcoming me, helping to complete this work. Special thanks to Prof F. Ajayi and Dr. N Ntshongontshi.
- To my organic colleagues (Masande Yalo and Masixole Makhaba), I would like to express my gratitude for your assistance and support during the synthesis process.
- To my mother Nobulali Ngwekazi, my father Melusi Ngwekazi, my sister Thobeka Ngwekazi, my brother Ovayo Ngwekazi, my late grandmother Nobanzi Deliwe, my cousins Fundiswa Rungqu & Sibongiseni Ngwekazi thank you very much for your love, care, kindness, support. Your prayers kept me going when I needed strength and for that, I owe it all you.
- To my friends (Noloyiso Vondo, Siyasanga Booysen, Sinazo Nqeketo, Clementine Louw, and Akheke Mehlomakhulu) and my family in Christ, thank you very much your support was amazing. Your motivations, encouragements did not go unnoticed, I am grateful.
- Last but not least, to the Chemistry Department, University of the Western Cape, and most importantly the National Research Foundation (Grant) for funding my studies. Thank you very much.

# DEDICATION

This project is dedicated

To

My parents and my late grandmother (Nobanzi Christina Deliwe)



UNIVERSITY *of the*  
WESTERN CAPE

## CONFERENCES

**Andisiwe Ngwekazi**, Priscilla G.L Baker, Lulama P. Mciteka. “*Voltammetric determination of metformin using modified polymer electrodes*” 70<sup>th</sup> Annual Meeting of the International Society of Electrochemistry, 03 -10 August 2019, Durban, SOUTH AFRICA. (poster)



UNIVERSITY *of the*  
WESTERN CAPE



# CONTENTS

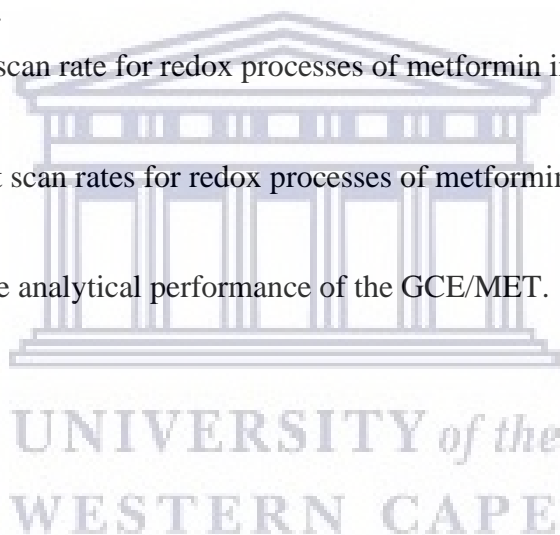
|  |           |
|--|-----------|
| <b>KEYWORDS</b>                              | 2         |
| <b>ABSTRACT</b>                              | 3         |
| <b>DECLARATION</b>                           | 5         |
| <b>ACKNOWLEDGEMENTS</b>                      | 6         |
| <b>DEDICATION</b>                            | 7         |
| <b>CONFERENCES</b>                           | 8         |
| <b>CONTENTS</b>                              | 9         |
| <b>LIST OF FIGURES</b>                       | 13        |
| <b>LIST OF ABBREVIATIONS</b>                 | 16        |
| <b>CHAPTER 1</b>                             | 17        |
| 1.1 Introduction                             | 17        |
| 1.2 Management of type 2 diabetes            | 20        |
| 1.3 Anti-diabetic agents                     | 21        |
| 1.3.1 Sulfonylureas                          | 21        |
| 1.3.2 Meglitinides                           | 22        |
| 1.3.3 Thiazolidinedione (TZD)                | 23        |
| 1.3.4 Alpha-Glucosidase Inhibitors           | 23        |
| 1.3.5 Dipeptidyl-Peptidase IV Inhibitors     | 24        |
| 1.3.6 Insulin                                | 24        |
| 1.3.7 Biguanides                             | 25        |
| 1.3.7.1 Metformin                            | 25        |
| 1.3.7.2 Pharmacokinetic Profile of metformin | 26        |
| 1.3.7.2.1 Intestinal action of metformin     | 27        |
| 1.3.7.2.2 Hepatic action of metformin        | 29        |
| 1.3.7.3 Metformin Derivatives                | 29        |
| 1.4 Problem Statement                        | 30        |
| 1.5 Aims and Objectives                      | 33        |
| 1.5.1 Aim                                    | 33        |
| 1.6 Thesis lay-out.                          | 34        |
| <b>CHAPTER 2</b>                             | <b>36</b> |

|   |           |
|---|-----------|
| 2.1 Introduction  | 36        |
| 2.1.1 Analytical Techniques                               | 36        |
| 2.2 Electrochemistry of metformin                         | 36        |
| 2.3 Polymers  | 39        |
| 2.4 Polymer Nanocomposite                                 | 41        |
| 2.5 Biosensors for metformin detection                    | 43        |
| 2.5.1 Copper binding properties towards metformin         | 45        |
| 2.6 Conceptual diagrams                                   | 47        |
| <b>CHAPTER 3</b>  | <b>49</b> |
| 3.1 Introduction  | 49        |
| 3.1.1 Spectroscopic Technique                             | 50        |
| 3.1.1.1 Fourier Transform Infrared spectroscopy (FTIR)    | 51        |
| 3.1.1.2 Small Angled X-ray Scattering (SAXS)              | 51        |
| 3.1.1.3 Nuclear Magnetic Resonance                        | 52        |
| 3.1.1.4 Ultraviolet Spectroscopy                          | 53        |
| 3.1.2 Microscopic Techniques                              | 54        |
| 3.1.2.1 Scanning Electron Microscope (SEM)                | 54        |
| 3.1.2.2 Transmission Electron Microscopy (TEM)            | 56        |
| 3.1.3 Electrochemical characterization                    | 56        |
| 3.1.3.1 Cyclic Voltammetry                                | 57        |
| 3.1.3.2 Square Wave Voltammetry                           | 59        |
| 3.1.3.3 Capillary electrophoresis                         | 60        |
| <b>CHAPTER 4</b>  | <b>61</b> |
| 4.1 Chemical Reagents                                     | 61        |
| 4.2 Chromatography  | 61        |
| 4.2.1 Column Chromatography (CC)                          | 62        |
| 4.2.2 Thin Layer Chromatography (TLC)                     | 63        |
| 4.3 Nuclear Magnetic Resonance (NMR)                      | 64        |
| 4.4 Synthesis of metformin and its analogues              | 65        |
| 4.4.1 Column Chromatography of alpha-bromoisovaleric acid | 69        |
| <b>CHAPTER 5</b>  | <b>78</b> |
| 5.1 Materials   | 78        |

|  |            |
|--|------------|
| 5.2 Methods  | 78         |
| 5.2.1 Preparation of HCl solution                                      | 78         |
| 5.2.2 Preparation of metformin solution                                | 78         |
| 5.2.3 Electropolymerization of pyrrole                                 | 79         |
| 5.3 Spectrochemical characterisation of copper nanoparticles           | 82         |
| 5.3.1 Ultraviolet-Visible analysis                                     | 82         |
| 5.3.2 Fourier Transform Infrared                                       | 84         |
| 5.4 Microscopic characterisation of copper nanoparticles               | 86         |
| 5.4.1 Scanning Electron Microscopy (SEM) analysis                      | 86         |
| 5.4.2 Transmission Electron Microscopy (TEM)                           | 88         |
| 5.4.3 SAX Space  | 89         |
| 5.5 Electrochemical characterisation                                   | 90         |
| 5.5.1 Concentration profile of metformin                               | 91         |
| 5.5.2 Characterisation of metformin on GCE                             | 92         |
| 5.5.3 Characterisation of PPy-GCE                                      | 94         |
| 5.5.4 Electrodeposition of copper nanoparticles on PPy-GCE             | 98         |
| 5.5.5 Characterisation of metformin in hydrochloric acid at Cu-PPy/GCE | 99         |
| <b>CHAPTER 6</b>   | <b>105</b> |
| 6.1 UV-Vis of metformin  | 105        |
| 6.1.1 Sample preparation   | 105        |
| 6.2 Electrochemical detection of metformin                             | 107        |
| 6.3 Electrochemical detection of metformin on PPy/GCE                  | 111        |
| 6.4 Electrochemical detection of metformin on CuNP-PPy/GCE             | 114        |
| Conclusion   | 118        |
| Future works   | 120        |
| References   | 121        |

## LIST OF TABLES

|  |     |
|--|-----|
| Table 1:Amino acids side chains  | 67  |
| Table 2: Fractionation of 2-Bromo-3-methylbutanoic acid (9.0g)   | 74  |
| Table 3:Combination of main fractions of alpha-bromoisovaleric acid.   | 76  |
| Table 4: NMR data for alpha-bromoisovaleric acid in CDCl <sub>3</sub> .  | 78  |
| Table 5:NMR data for 2-amino-3-methylbutanoic acid in CDCl <sub>3</sub>  | 82  |
| Table 6: Fourier Transform Infrared peak assignment for copper nanoparticles.  | 92  |
| Table 7: Percentage (%) of elements present in copper nanoparticles.   | 94  |
| Table 8: Effect of different scan rates for redox processes of metformin in 0,1M HCl at glassy carbon electrode at 50mV/s. | 100 |
| Table 9: Effect of different scan rate for redox processes of metformin in 0,1M HCl at PPy/GCE.                            | 103 |
| Table 10: Effect of different scan rates for redox processes of metformin in 0,1m HCl at CuNP-PPy/GCE.                     | 109 |
| Table 11: Comparison of the analytical performance of the GCE/MET.   | 119 |



## LIST OF FIGURES

|   |    |
|---|----|
| Figure 1:Summary of diabetes mellitus in the African region.....  | 19 |
| Figure 2:Chemical Structure of Metformin. ....  | 26 |
| Figure 3:Typical metformin mechanism in the abdomen (Han et al, 2015). ....   | 27 |
| Figure 4:Electrochemical synthesis of polypyrrole from pyrrole monomer.....   | 41 |
| Figure 5:Cyclic Voltammograms corresponding to: (A) 10 $\mu$ M MET at Fe-Cu/TiO <sub>2</sub> -CPE. With the following measurement conditions: pH 12, scan rate= 100mVs-1 and (B) 10uM MET at (a) CPE, (b) Fe/TiO <sub>2</sub> -CPE and (c) Fe-Cu/TiO <sub>2</sub> -CPE at the same conditions mentioned above (Gholivand et al, 2014). .... | 43 |
| Figure 6:Flow diagram of the thesis for organic synthesis (Part A) and electroanalytical behaviour of metformin on the modified electrode. ....   | 48 |
| Figure 7:Nuclear magnetic resonance (NMR) instrument (Bruker-400 MHz). ....   | 53 |
| Figure 8:Nicolet evolution 100 UV-Vis instrument. ....  | 54 |
| Figure 9:Schematic diagram of scanning electron (SEM). ....   | 55 |
| Figure 10:A typical diagram of cyclic voltammogram.....   | 58 |
| Figure 11:A typical Column Chromatography. ....   | 63 |
| Figure 12:A typical Thin Layer Chromatography (TLC). ....   | 64 |
| Figure 13: $\alpha$ - bromoisovaleric acid.....   | 70 |
| Figure 14:Flash Column for the crude product ( $\alpha$ -bromoisovaleric acid) with the solvent system of 9:1 (Hex: EtOAc). ....  | 70 |
| Figure 15:Thin layer chromatograms of fractions obtained from column chromatogram of alpha-bromoisovaleric acid. ....   | 72 |
| Figure 16: <sup>13</sup> C NMR of $\alpha$ -bromoisovaleric acid G in CDCl <sub>3</sub> . ....  | 74 |
| Figure 17: <sup>1</sup> H NMR of $\alpha$ -bromoisovaleric acid G in CDCl <sub>3</sub> . ....   | 75 |
| Figure 18: <sup>1</sup> H NMR of 2-amino-3-methylbutanoic acid G in CDCl <sub>3</sub> . ....  | 76 |
| Figure 19:Electrochemical synthesis of polypyrrole (PPy) thin film. ....  | 79 |
| Figure 20:Electro polymerization of polypyrrole at glassy electrode carbon electrode glassy (GCE) for (A) 5 Cycles, (B) 10 cycles and (C) 15 cycles in a 0,1M HCl at 50 mV/s. ....  | 80 |

|  |     |
|--|-----|
| Figure 21:Electrochemical synthesis of polypyrrole from pyrrole monomer.....   | 81  |
| Figure 22:UV-Visible spectra of copper nanoparticles synthesised by chemical reduction method<br>(A) immediately after synthesis (B) 24 hours after synthesis..... | 83  |
| Figure 23: FTIR Spectrum of copper nanoparticles. ....   | 84  |
| Figure 24: SEM image of copper nanoparticles. ....   | 86  |
| Figure 25:EDS of copper nanoparticles.....   | 87  |
| Figure 26:TEM (A) and SAED (B) images for copper nanoparticles.....  | 88  |
| Figure 27:Distribution curves of copper nanoparticles (A, B) distribution by number (C) PDDF.<br>.....   | 89  |
| Figure 28:Concentration dependent cyclic voltammogram of metformin at GCE in 0,1 M HCl at<br>50 mV/s.....  | 91  |
| Figure 29:Multi-scan voltammogram of metformin at bare GC electrode in 0,1M HCl at 10 to 60<br>mV/s.....   | 92  |
| Figure 30:Randles Sevçik plot of MET.....  | 94  |
| Figure 31:Cyclic voltammogram showing polymer growth during 10 cycles of polymerization of<br>pyrrole at GCE in 0,1M HCl, at 10-100 mV/s.....                      | 95  |
| Figure 32:Randles Sevçik plot of PPy.....  | 97  |
| Figure33:Cyclic voltammogram corresponding to commercial copper and synthesised copper<br>nanoparticles Cu NP in 0.1 M HCl at a bare GCE, 50 mV/s scan rate.....   | 98  |
| Figure 34:Multi-scan voltammogram of metformin in 0,1M HCl at Cu-PPy/GCE, 10-100 mV/s.<br>.....  | 100 |
| Figure 35:Suggested oxidation mechanism of metformin.....  | 101 |
| Figure 36:Randles Sevçik plot of PPy-CuNP.....   | 103 |
| Figure 37:UV-Vis absorption spectra of metformin at $\lambda=232\text{nm}$ .....   | 106 |
| Figure38:Calibration curve for the detection of metformin (83,408 – 0.3175 mM) by UV-Vis, at<br>maximum wavelength of 232 nm. ....                                 | 106 |
| Figure 39:Full calibration curve of UV-Vis for different concentrations of metformin at maximum<br>wavelength of 232 nm.....                                       | 107 |
| Figure 40:Concentration-dependent cyclic voltammogram (A) and square wave voltammogram<br>(B) of metformin at a bare GCE in 0,1 M HCl, scan rate of 50 mV/s.....   | 108 |

Figure 41: Calibration curve for the detection of metformin (0.01 - 0.13 mM) at bare GC electrodes, at a potential between -0.4 to 1.0 V (Ag/AgCl), 50 mV/s in 0.1 M HCl..... 109

Figure 42: Linear plot of the current response of metformin within the concentration range of 0.01- 0, 13 mM at GCE in HCl, scan rate of 50 mV/s. .... 109

Figure 43: Concentration dependent cyclic voltammogram (A) of metformin on PPy/ GCE in 0,1 M HCl at 50 mV/s..... 111

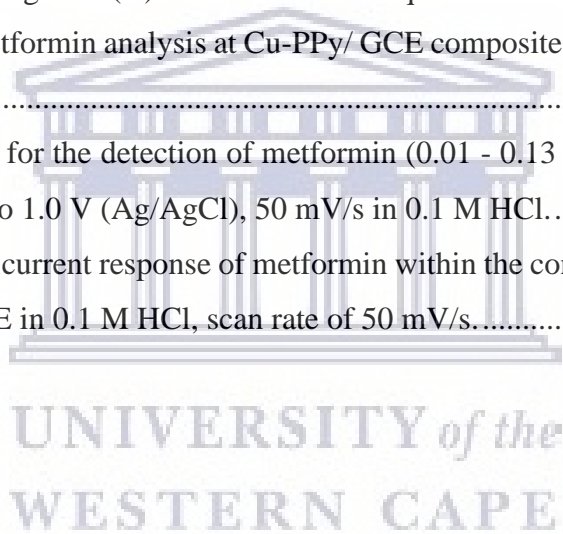
Figure 44: Calibration curve for the detection of metformin (0.33 – 3.66 mM) at PPy/GCE electrodes, at a potential range of -0.4 to 1.0 V (Ag/AgCl), 50 mV/s in 0.1 M HCl..... 112

Figure 45: Linear plot of the current response of metformin within the concentration range of 0.33- 3.66 Mm at PPy/GCE in HCl, scan rate of 50 mV/s..... 113

Figure 46: Cyclic voltammogram (A) and oxidative square wave voltammogram (B) of concentration dependent metformin analysis at Cu-PPy/ GCE composite in 0,1 M HCl at 50 mV/s. .... 114

Figure 47: Calibration curve for the detection of metformin (0.01 - 0.13 mM) at CuNP-PPy/GCE, at a potential between -0.4 to 1.0 V (Ag/AgCl), 50 mV/s in 0.1 M HCl..... 115

Figure 48: Linear plot of the current response of metformin within the concentration range of 0.33- 3,66 Mm at CuNP-PPy/GCE in 0.1 M HCl, scan rate of 50 mV/s..... 116



## LIST OF ABBREVIATIONS

CDCl<sub>3</sub>: Deuterated chloroform

Cu-Np: Copper nanoparticles

CV: Cyclic Voltammetry

CC: Column Chromatography

D<sub>0</sub>: Diffusion Coefficient

FTIR: Fourier Transformer Infrared

GCE: Glassy carbon electrode

GUU: Guanylurea

HCl: Hydrochloric acid

LOD: Limit of detection

M: Molar

nm: Nanometre

NMR: Nuclear Magnetic Resonance

PEG: Polyethylene Glycol

PPy: Polypyrrole

SAXS: Small-angle X-ray scattering

SEM: Scanning electron microscopy

TEM: Transmission electron microscopy

TLC: Thin layer Chromatography

UV: Ultraviolet-visible

Vis: Visible

WWTP: Wastewater Treatment Plant



UNIVERSITY of the  
WESTERN CAPE



# CHAPTER 1

*This chapter offers a brief introduction to diabetes mellitus (type 2) and provides background about all the types of drugs used to treat diabetes and their drawbacks.*

## 1.1 Introduction

Recently diabetes mellitus has been classified as a major health problem that affects approximately 350 million people worldwide. The increasing number of people affected by this metabolic disorder can be linked to sedentary lifestyle patterns such as unhealthy diet and lack of physical activity, which in turn contribute to increasing chronic disease rates. The International Diabetes Federation (IDF) discovered a rapid increase in the prevalence of diabetes worldwide. Statistically worldwide, the number of people suffering from diabetes mellitus was observed and recorded each year. Approximately 9% of people aged 30 years and older were reported to have diabetes in 2009, increasing with two-fold since 2000 when Bradshaw *et al* reported a prevalence of 5.5%. In the last decade, it was reported that 285 million people had both type 1 and type 2 diabetes with the considerable disparity between populations and regions. The pattern of diabetes differs for each country according to its economic status. The majority of people with diabetes were found to be over 60 years of age for the developed countries, while most people with diabetes in developing countries were at their working-age between 40 and 60 years (Shaw, et al, 2010). In 2011, the global statistics reported 366 million people to be suffering from diabetes mellitus, and this prevalence is expected to increase in the next coming years (Whitting et al, 2011). The International Diabetes Federation (IDF) predicted that the biggest potential increase in the prevalence of diabetes mellitus will occur in Africa (Kibirigel et al,2019). Statistics reports, revealed that the majority of people with diabetes are from the African continent and the global projections show that it will experience the greatest increase of about 156% by 2045 (Kibirige et al, 2019).

The statistics presented above confirm the large and growing burden of diabetes in the world with the African region as the large contributor (Guariguata et al, 2014). On the African continent, South Africa was reported to be amongst the countries which contribute largely to the increase of people affected with diabetes. More than half (61.1%) of the 2.3 million populace with diabetes in South Africa were found undiagnosed (Abdulfatai et al, 2012). Thus, approximately 74.9 thousand deaths in 2013 were related to cases of undiagnosed diabetes mellitus. The number of people suffering from this metabolic disease increased with 15.8 million to a total of 381.8 million in Africa by 2013. Statistical reports of 2015 showed that one death every six seconds occurred due to diabetes, overtaking the number of deaths related to HIV/AIDS, tuberculosis, and malaria combined (Kaul, et al, 2012). The African region remains the highest with adults suffering from diabetes making it the seventh leading cause of death (Dwyer-Lindgren et al, 2016). Controlling the spread of this pandemic disease is a challenge as the statistics of diabetes were observed to increase every year.

Furthermore, in 2015, the International Diabetes Federation estimated the prevalence of diabetes to increase by 55% by 2040 affecting more than half of adults globally (Labuschagne, et al, 2017). The International Diabetes Federation (IDF) in 2017 reported 451 million adults worldwide had diabetes, and predictions of 693 million new cases by 2045 (Pheiffer et al, 2018). More than 500 million prevalent cases of type 2 diabetes mellitus were reported in 2018 and the prevalence is comparable between high- and low-income countries of the African continent. The highest growth was found to be in countries with lower incomes (Pettit et al, 2014).

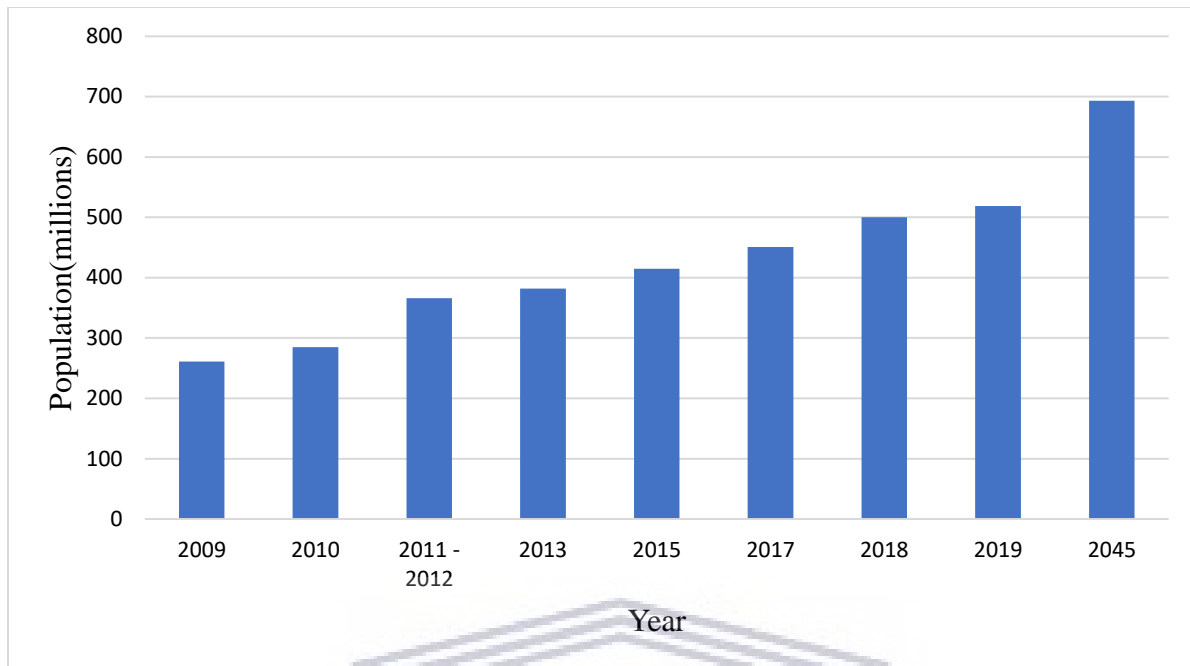


Figure 1: Summary of diabetes mellitus in the African region.

The above-reported statistics (Figure 1) suggest that the burden of diabetes mellitus has increased to epidemic proportions globally. Hyperglycaemia and diabetes were discovered to be the major cause of global morbidity and premature mortality (which are due to microvascular complications and impaired regulation glycaemia) on individuals with diabetes mellitus. Mortality incidence differs extensively across the continent due to variability of the population studied in terms of glycaemic control, accompanying risk factors such as hypertension or smoking, among other variables, the type diabetes, and duration of diabetes mellitus (Douros et al, 2018).

There are different types of diabetes mellitus: type 1, type 2 diabetes mellitus, which are triggered by a complex interaction between environmental and genetic factors. Type 2 diabetes mellitus is a metabolic disorder characterized by insulin resistance in the liver and pancreatic  $\beta$ -cell dysfunction due to unsettled hyperglycaemia while type 1 diabetes mellitus is a result of autoimmune destruction of pancreatic  $\beta$ -cells that leads to insulin deficiency. Type 2 diabetes accounts for 90% of all diabetes cases, nonetheless, its incidence is increasing steadily among children and adolescents and that is attributed to the increase in urbanization, and obesogenic (tending to cause

obesity) environments (Rena et al, 2017). The prevalence of type 2 diabetes (T2D) has reached epidemic proportions in many countries worldwide and has been linked to the risk for cardiovascular diseases and early mortality (Rena et al, 2017).

Management of type 2 diabetes entails lifestyle changes supplemented by effective treatment to promote efficient insulin availability in controlling blood sugar levels. Several pharmacological agents have been used in managing diabetes, but due to some serious side effects, they have been withdrawn from being used. Metformin (biguanide) defined as an anti-hyperglycaemic agent was introduced in 1958 by the American Diabetes Association to control blood glucose levels in people. Metformin is an old and widely accepted first-line agent for type 2 diabetes mellitus and its glycaemic control includes improvements in endothelial dysfunction and insulin resistance. Increased awareness, early diagnosis of diabetes, and improved management of diabetes has resulted in a reduction of premature mortality (Chatterjee et al, 2017).

## **1.2 Management of type 2 diabetes**

The management and treatment of T2D include increasing insulin secretion and enhancing insulin sensitivity and hyperglycaemia. Diabetes mellitus is referred to as a chronic disease initiated by inherited and/or developed deficiency in production of insulin by the pancreas, or by the ineffectiveness of the insulin produced (Rena et al, 2017). The increased concentrations of glucose in the blood results in damage to the blood vessels and nerves. However, type 2 diabetes is a metabolic disease that can be controlled through lifestyle modification, such as exercise and diet. In controlling this emerging disease, educating the individuals suffering from type 2 diabetes is crucial (Naveed, 2014).

Recent studies show a significant reduction in the incidence of type 2 diabetes mellitus when a body mass index of 25 kg/m<sup>2</sup> is maintained and a diet rich in fibre and unsaturated fat is followed. This treatment regime is enhanced when supplemented by regular exercise, abstinence from smoking, and moderate consumption of alcohol (McCreight et al, 2016). This treatment regime is improved when complemented by consistent exercise, abstinence from smoking, and moderate intake of alcohol. Moreover, the effective management and control of diabetes mellitus requires a

multidisciplinary approach which includes medical intervention and educating people regarding self-management. Fundamentally, the self-management plan should be based on a medical nutrition evaluation which include strict control of food intake, provided by a registered dietician, as well as consistent monitoring of blood sugar with lifestyle changes. Occasionally, this is useful for managing the diabetic condition; however, in most cases where there are inadequate glycaemic regulations, pharmaceutical intervention in the form of an antidiabetic agent is required.

### **1.3 Anti-diabetic agents**

In the past years, several antidiabetic agents have emerged intending to improve type 2 diabetes by exerting their influence through biological targets and allowing a complementary combination of pharmaceutical agents to be used. This contrast dramatically with the preceding pharmaceutical strategies where sulfonylureas were the only antidiabetic agents available for treating T2D in the U.S before 1995 (Devine, 2013).

#### **1.3.1 Sulfonylureas**

Sulfonylureas are regarded as anti-diabetic drugs that were discovered and developed in the 1950s and are recommended as a second line of treatment in patients with type 2 diabetes. Notwithstanding the recent approval of many new medications, sulfonylureas remain the most prescribed anti-diabetic medication after metformin, hence it is regarded as the second line of treatment (Douros et al, 2018). Sulfonylureas are divided into two generations (1<sup>st</sup> and 2<sup>nd</sup> generation) (Evans, 2006). The first generation of sulfonylureas (acetohexamide, chlorpropamide, tolazamide, and tolbutamide) was discovered to have a lower binding affinity for the ATP-sensitive potassium channel, their molecular target (*vide infra*), and hence higher doses are required to achieve efficacy (Douros et al, 2018). These first-generation sulfonylureas are hardly used anymore. In the 1980s a 2nd generation sulfonylurea that includes glyburide (glibenclamide), glipizide, and glimepiride; were developed and are now widely used. They act by increasing insulin release from the beta cells in the pancreas (Douros et al, 2017) however, they carry a risk of hypoglycaemia due to their endogenous insulin secretion but are nonetheless well tolerated. Sulfonylureas function by increasing insulin release from the beta cells of the pancreas and may improve insulin resistance in peripheral target tissues. On average, this class reduces

glycosylated haemoglobin A<sub>1c</sub>(HbA<sub>1c</sub>) levels by 0.8 to 2.0% and fasting plasma glucose (FPG) concentrations by 60 to 70 mg per dL (3.3 to 3.9 mmol per L), with the greatest reductions observed in patients with the highest FPG concentrations at the initiation of therapy (Abdelmoneim et al, 2012). Higher rates of hypoglycaemia are associated with the use of glyburide compared to glipizide. Hence sulfonylureas are not highly recommended in an elderly population where the risks of hypoglycaemia are high, due to an increased risk of stroke, in susceptible populations (Mazzola, 2012). Sulfonylureas are less effective for obese patients who are also insulin resistant. In this case, medications aimed at weight loss, are used in parallel with sulfonylureas. These disadvantages have resulted in the nearly complete withdrawal of sulfonylureas as an effective anti-diabetic drug.

### **1.3.2 Meglitinides**

Meglitinides (repaglinide, nateglinide) are shorter-acting insulin secretagogues compared to sulfonylureas, with pre-prandial dosing achieving more available insulin release and less risk for hypoglycaemia. Unlike sulfonylureas, repaglinide and nateglinide stimulate first-phase insulin release in a glucose-sensitive manner, theoretically reducing the risk of hypoglycaemic events (Abdufatai et al, 2012). Moreover, studies have shown that comparing meglitinide action to placebo cases, both repaglinide and nateglinide resulted in a reduction in glycosylated haemoglobin (0.1% to 2.1% reduction in HbA<sub>1c</sub> for repaglinide: 0.2% to 0.6% for nateglinide) (Mohanty, 2018). It has been discovered that weight gain and hypoglycaemia have been identified as the major drawbacks associated with these drugs, but less so, compared to sulfonylureas. Meglitinides may offer an alternative oral hypoglycaemic agent of similar potency to metformin and may be indicated where side effects of metformin are intolerable or where metformin is contraindicated. However, there is no evidence available to indicate what effect meglitinides will have on important long-term outcomes, particularly mortality. Repaglinide is mainly metabolized in the liver with minimal amounts excreted through the kidneys and therefore dose adjustment is not needed in patients with renal insufficiency except in patients with terminal renal disease.

### **1.3.3 Thiazolidinedione (TZD)**

Thiazolidinedione is an insulin sensitizer and among the first drugs used to address the basic issue of insulin resistance in type 2 Diabetes Mellitus patients. Thiazolidinedione (glitazones) are a class of oral hypoglycaemic drugs which are used for the treatment of type 2 diabetes (Abdulfatai, 2012). Thiazolidinedione class presently incorporates mainly pioglitazone after the limited utilization of rosiglitazone prescribed by the Food and Drug Administration (FDA). Rosiglitazone was withdrawn due to the risk of higher associated cardiovascular occasions. Pioglitazone use is not related to hypoglycaemia and can be utilized in instances of renal weakness and thus well tolerated in older adults (Yoon, et al, 2006). Individuals with congestive heart failure and class III-IV heart failure should avoid pioglitazone.

### **1.3.4 Alpha-Glucosidase Inhibitors**

Alpha-glucosidase inhibitors (AGIs) are a class of oral glucose-lowering drugs (OGLDs), used exclusively in treatment for type 2 diabetes mellitus. Largely, they act by altering the intestinal absorption of carbohydrates by inhibiting their conversion into simple sugars (monosaccharides). Hence, alpha-glucosidase inhibitors significantly lower the blood glucose levels contributed by carbohydrates. The three AGIs used in clinical practice are acarbose, voglibose, and miglitol. There is no other AGI currently in active clinical trials. Their use is usually limited due to high rates of side-effects such as diarrhoea and abdominal distension (accumulation of air or fluid in the abdomen leading to expansion). Alpha-glucosidase inhibitors functions by inhibiting the enzyme alpha-glucosidase found in the brush border cells that line the small intestine, which cleaves more complex carbohydrates into sugars. Since they prevent the breakdown and ensuing absorption of carbohydrates (maltose, sucrose, and starch; no effect on glucose) from the gut following meals, the largest impact of these drugs is on postprandial hyperglycaemia. They have been associated with a reduction in HbA<sub>1c</sub> by 0.7 to 1.0% by 35 to 40 mg per dL (1.9 to 2.2 mmol per L) (Mohanty, 2018). Thus, these agents are most useful in patients with predominant postprandial hyperglycaemia.

### 1.3.5 Dipeptidyl-Peptidase IV Inhibitors

They are effective as monotherapy in patients inadequately controlled with diet and exercise and as add-on therapy in combination with metformin, thiazolidinedione's, and insulin. The inhibitors of dipeptidyl peptidase 4 (DPP-4) are well-tolerated, carry a low risk of producing hypoglycaemia, and are weight neutral. The long-term durability of effect on glycaemic control and beta-cell morphology and function remains to be established. In practice, DPP-4 inhibitors increase concentrations of both active incretin hormones, glucagon-like peptide-1 (GLP-1) and glucose-dependent insulintropic polypeptide (secreted by the enteroendocrine L and K cells, respectively, which are substrates for DPP-4). This results in improved-cell responsiveness to prevailing glucose concentrations and suppression of glucagon secretion.

### 1.3.6 Insulin

Insulin is a protein hormone that is used as an anti-diabetic medication to treat high blood glucose. It is regarded as the most effective agent of all the anti-diabetic medications in lowering glycemia and likely reduces the elevated HbA1c close to the therapeutic levels especially in type 1 diabetes mellitus (Chaudhury et al, 2017). In type 2 Diabetes Mellitus, it is normally used after the failure of other drugs to accomplish proper control of blood glucose levels. However, relatively large doses (> 1 unit/kg) may be required to overcome the insulin resistance that is observed in type 2 Diabetes Mellitus compared to insulin doses utilized in type 1 diabetes mellitus (Kabel et al, 2017). Insulin comes in about 4 injectable forms which include rapid-acting, short-acting, intermediate-acting, and long-acting. The long-acting structures are less inclined to cause hypoglycaemia contrasted with the short-acting structures. Thus, they are likely used especially in elderly patients with diabetes mellitus (Yakaryılmaz et al, 2017). Nonetheless, insulin treatment with conventional mealtime and basal insulin arrangements has numerous deficiencies. To begin with, the absorption of regular human insulin from the tissues is moderate, and the metabolic interchange makes an impact of about 30–60 min after infusion and starts to be efficient after 2–3 h. Subsequently, the treatment with regular insulin is associated with post-meal hyperglycaemia and an increased risk of postprandial hypoglycaemia (Swinnen et al, 2009). Additionally, the conventional basal neutral protamine Hagedorn (NPH) insulin with a positive effect in lowering glucose and is absorbed from



the tissues at different rates. The major drawback of insulin treatment, weight gain leads to the withdrawal of the treatment especially for the treatment of type 2 diabetes mellitus.

### 1.3.7 Biguanides

The term biguanide refers to a group of oral type 2 diabetes mellitus drugs that work by preventing the production of glucose in the liver, improving the body's sensitivity towards insulin, and reducing the amount of sugar absorbed by the intestines (Thulé, 2012). The main biguanides, which include metformin (dimethyl biguanide) and phenformin (phenethyl biguanide), were introduced in 1957 as glucose-lowering agents for the treatment of non-insulin dependent diabetes mellitus (NIDDM) (Kinaan et al, 2015). Research distributed in 2008 shows a further component of activity of metformin as the enactment of AMP-actuated protein kinase, a chemical that assumes a job in the outflow of hepatic gluconeogenic qualities (Miller et al, 2013). Due to the concern of the development of lactic acidosis, metformin should be used with caution in elderly diabetic individuals with renal impairment. It has a low incidence of hypoglycaemia compared to sulfonylureas.

#### 1.3.7.1 Metformin

Recently metformin is the best recommended pharmacological treatment for individuals suffering from type 2 diabetes, being prescribed to at least 120 million people worldwide (Rojas et al, 2013). The anti-hyperglycaemic effect of metformin was discovered to be mainly due to the inhibition of hepatic glucose output, and therefore, the liver is probably the primary site of metformin function. Literature reports that, metformin belongs to the biguanide class of anti-diabetic drugs. However, the history of biguanides can be outlined from the use of *Galega officinalis* which is commonly known as Galega for treating diabetes in Europe (Abdulfatai et al, 2012). Currently, metformin is discovered to have a superior safety profile compared to phenformin, buformin, and other pharmacological agents which were introduced for diabetes therapy in the late 1950s. Phenformin

and buformin were withdrawn in the early 1970s due to the high risk of lactic acidosis and increased cardiac mortality (Abdulfatai, 2012). At therapeutic doses of metformin, the incidence of lactic acidosis is very rare (Foretz et al, 2014). Reduction of hepatic glucose output, with the successive enhancement of peripheral insulin sensitivity and remarkable cardiovascular safety, are the major clinical advantages of metformin. Literature reports that metformin as being more advantageous than sulfonylurea monotherapy in terms of complications associated with cardiovascular which then lead to mortality.

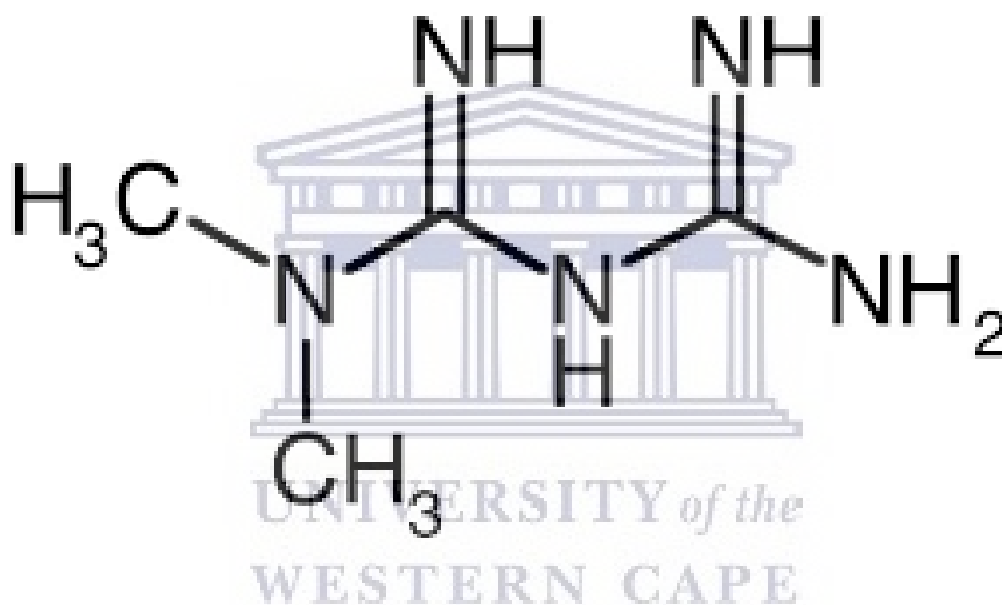


Figure 2:Chemical Structure of Metformin.

### 1.3.7.2 Pharmacokinetic Profile of metformin

Metformin is a derivative of guanidine, the active ingredient in goat's rue that had empirically been used as a treatment for diabetes in the middle ages. The main mechanism of metformin is to decrease high blood sugar, primarily by suppressing liver glucose production

(hepatic gluconeogenesis) (Foretz et al, 2014). Reduced appetite is a convenient action of metformin, contributing to weight loss, which is beneficial, given that most patients are obese. The optimal oral metformin dose for many diabetic patients is ~2 g/day. After a single oral dose, metformin is rapidly distributed to many tissues, but the luminal concentration in the gastrointestinal tract remains high. However, in the digestive tract, metformin is partially absorbed by the small intestine (Shekhawat et al, 2017) Figure 2.

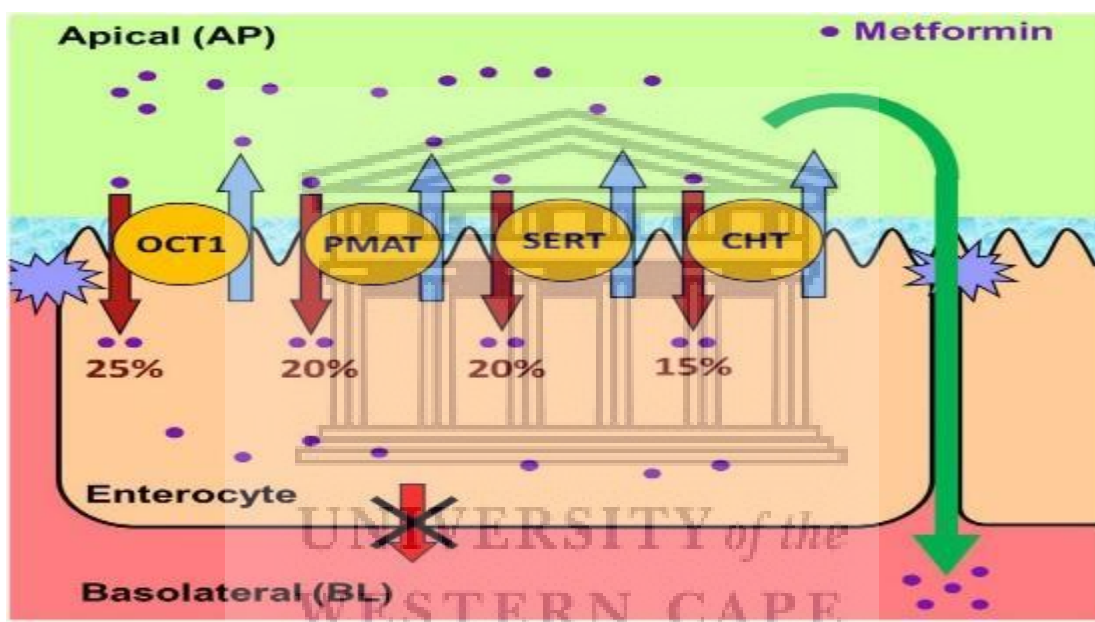


Figure 3: Typical metformin mechanism in the abdomen (Han et al, 2015).

### 1.3.7.2.1 Intestinal action of metformin

Metformin is usually taken orally as the hydrochloride salt, in a tablet formulation most preferably Glucophage. Chemically, metformin is a hydrophilic base that exists at physiological pH as the cationic species. Thus, its passive diffusion through cell membranes in the human system is limited. Due to its oral bioavailability which ranges between 40% and 60%, metformin is absorbed predominantly from the small intestine hence it is excreted unchanged in urine (Shekhawat et al, 2017). Moreover, oral absorption, hepatic uptake, and renal excretion of metformin are mediated

very largely by organic cation transporters which are likely expressed on the basolateral membrane of enterocytes (Figure 3). Due to the low permeability of metformin across the cell membranes and high aqueous solubility, it is classified as a Class 3 compound according to Biopharmaceutics Classification System (BCS). However, absorption of metformin is mostly confined to the small intestine with insignificant absorption in the stomach or large intestine (Han et al, 2015).

The bioavailability of metformin is affected by gastric motility and may be reduced by high-fat meals. Its incomplete absorption is improved by using convenient drug delivery systems, such as bio adhesive and gastro retentive drug delivery systems. Its biological half-life ( $t_{1/2}$ ) is in the range of 0.9–2.6 h. Therefore, repeated applications of high doses of metformin (500 mg two or three times daily, or 850 mg once or twice daily with or after meals) are needed for the effectiveness of the drug. As a result, patient compliance is reduced, and/or the incidence of side effects, such as diarrhoea, nausea, anorexia, vomiting, weight loss, and taste disturbance is increased (Wang et al, 2017).

The concentration of metformin in the small intestine at the dosage of 500  $\mu\text{g/g}$ , is 30–300 times greater than plasma concentrations, highlighting the small intestine as an important site of metformin uptake (McCreight et al, 2016). Metformin modified-release formulations have been established to spread the absorption of metformin along the gut and thereby reducing local concentrations of the drug, to increase its tolerability. The dual polymer matrix uses metformin MR (modified release) to interrupt the transit and slow the release of metformin in the gut. On contact with fluid from the GI tract, the tablet swells, and the metformin is released as the polymer gradually breaks down. A new metformin formulation has recently been developed, metformin DR (delayed-release), which is formulated to target the ileum through the pH-dependent dissolution of the tablet. Compared with metformin IR (immediate-release) or metformin XR (extended-release), the bioavailability of metformin DR is lower, yet its glucose-lowering efficacy is similar, despite lower systemic metformin exposure. This again highlights the ileum as a site of uptake and as a significant site of action of metformin in lowering blood glucose. The development of novel formulation strategies for metformin might be useful to improve its bioavailability, to

reduce the dosing frequency, and to decrease gastrointestinal side effects and toxicity (Cetin, 2015).

#### **1.3.7.2.2 Hepatic action of metformin**

The metformin molecule works in the humans' bodies at the level of the liver and peripheral tissues, basically, by downsizing the glucose output from the liver, as well as by enhancing the utilization at the peripheral tissues (muscles). This process takes place through the activation of adenosine monophosphate-activated protein kinase (AMPK) (Stephenie et al, 2011) (Rena et al, 2017). The AMPK is the cell regulatory pathway that reduces the energy expenditure at the cellular level. In humans, AMPK is essential for the metabolism of glucose and fatty acids, through reduction of the gluconeogenesis and fatty acids synthesis in the liver, and enhancing glucose uptake, and the oxidation of the fatty acids by peripheral tissues (Viollet, 2011). Between oral dose and drug absorption, a negative correlation has been discovered. Metformin is promptly dispersed, without binding to plasma proteins and it does not metabolize in the liver hence it become excreted unchanged by the kidneys (Graham et al, 2011). Thus, the continuous use of metformin in managing type II diabetes will result in being regarded as an emerging pollutant in the environment (water bodies) in the near future. This presents the opportunity to synthesize new analogues of metformin which will be absorbed by the intestine and reduce the level of it being excreted.

#### **1.3.7.3 Metformin Derivatives**

An analogue is generally characterized as modifying a drug molecule or other bioactive compound to create a new molecule that shows chemical and biological similarity to the original compound of a model. Generally, the analogue is supposed to display some changes over the original drug. Metformin analogue is an antidiabetic drug that is substantially similar to metformin but with different chemical and biological properties. To date not much has been reported on metformin analogues. However, two metformin derivatives (sulfenamide and sulfonamide) have been recently reported in literature (Markowicz-piasecka et al, 2019). Sulfenamide derivatives of metformin are bio-reversible guanidine's (N-S) with prodrug properties, while sulfonamide derivatives were designed to remain intact in the bloodstream until they are conveyed into the

hepatocytes where they can be bio converted to metformin. Chemical modification of the metformin scaffold into sulfenamide with a variety of alkyl substituents as well as sulfonamides with a nitro group in the aromatic ring assists to acquire the potential agents with more clearly marked anticoagulant properties than their parent drug, metformin. The properties of the metformin derivatives presented above towards endothelial cells (EC) are determined by the alkyl chain length in sulfenamide. However, the examined metformin derivatives, sulfenamide and sulfonamide suggested a varied effect on the role of endothelial cells (ECs) (Bakhashab et al, 2018). The comparable sulfenamide with (n-butyl alkyl chain), to metformin, failed to contribute to the alterations in endothelial integrity across the entire concentration range. The functionality of the developed analogues of metformin was evaluated in vivo to assess the improvement of bioavailability of the new drugs; the bioavailability of the analogues was discovered to be improved from 40 to 60% in the human body (Huttunen, 2009).

#### **1.4 Problem Statement**

Managing type 2 diabetes entails effective treatment to lower glycaemic index and cardiovascular risk factors. Several pharmacological agents have been synthesized for managing diabetes nonetheless, due to complications they convey to patients, they have been withdrawn. Accordingly, in recent times, metformin (biguanide) has become the preferred anti-diabetic drug; it was introduced by the American Diabetes Association to control blood glucose levels in the human body. Metformin hydrochloride (MET) is a biguanide that is an amino group-rich compound and is effectively used for the treatment of type 2 diabetes mellitus (non-insulin dependent) (Figure 3) (Gholivand, 2013). Due to the low risk of hypoglycaemia offered by metformin, it has been widely accepted as a first-line anti-diabetic drug for type 2 diabetes mellitus. Furthermore, it was recently discovered that patients diagnosed with cancer have a lower risk of mortality when treated with metformin. The association of metformin with a 23% decrease in the risk of cancer, particularly breast and pancreatic cancer will lead to the frequent use of this drug as a treatment option for a broadening variety of health problems worldwide (Zi, 2018). This would lead to metformin being introduced in the environment and be considered as one of the groups of an emerging pollutant.

Pharmaceuticals are increasingly found in wastewater and surface waters around the world, often due to incomplete metabolism in humans and subsequent excretion in human waste unaltered. Metformin (the medicine most prescribed for treatment of Type II diabetes worldwide) was discovered to escape the wastewater treatment plant (WWTP) effluent due to its hydrophilic nature and end up on the surface waters. Accordingly, levels of metformin in wastewater treatment plant (WWTP) effluent and surface waters, will likely continue to increase due to the above-mentioned challenge. Metformin was discovered to primarily biodegrade in WWTP effluent to its metabolite (Tisler et al,2018), guanylate (GUU) which was proposed to be persistent in and cause potential concern for the environment (Straub et al,2019). Metformin metabolite, guanylate (GUU) was found to be very stable in photolysis and consequently in technical irradiation in improved water treatment, indicating that it is not anticipated to be eliminated in wastewater and water treatment plants (Trautwein et al, 2011). Therefore, the use of metformin poses a huge threat to the ecosystem worldwide to an extent that it is recently discovered as an emerging pollutant in wastewater.

The effects of pharmaceuticals, particularly metformin on wildlife have received increased attention in the literature in recent years, with emphasis on those that affect endocrine function. However, metformin's impact on aquatic life is poorly understood, having been addressed in a limited number of studies exploring its metabolic effects in the contexts of aquaculture and drug screening. A recent study of fathead minnows' fish (*Pimephales promelas*) exposed to the drug revealed that metformin treatment-induced molecular genetic changes indicative of endocrine disruption. Males exposed to the drug for four weeks at a level like the average found in WWTP effluent (40 µg/L) experienced significant up-regulation of mRNA encoding the egg-protein vitellogenin (VTG), a well-established indication of endocrine disruption (Niemuth et al, 2015). The authors suggest these changes offer the potential for greater hormone, health- and behaviour-disrupting impacts from extended exposure, as occurs in nature. Studies of the effects of metformin at higher doses, over longer periods of exposure, and in other species are needed to better assess the impacts of the drug in nature. A study by MacLaren, 2018 indicates the concentrations of metformin in freshwater systems and waste-water effluent (40 µg/L) to affect the behaviour in adult male fish *Betta splendens* (popular fish in the aquarium trade). The harmful effects of metformin provide a long list of contraindications, such as the contamination and accumulation in wastewater and the possibility of causing endocrine disorders, show the importance of quantifying

metformin in the environment (Machini et al, 2019). In the past years, different strategies have been developed for the quantification of MET in wastewater, among them stand out conductometry, gas chromatography coupled to different detectors, high-performance liquid chromatography coupled to different detectors, electrophoresis, UV-Vis, infrared, nuclear magnetic resonance spectroscopy (Gholivand, 2013). However, some of these methods suffer from several disadvantages, such as long chromatographic run times, low sensitivity, large consumption of sample volumes, and complicated sample preparation procedures before analysis, which prevents their use for routine sample analysis. Electroanalytical methods, on the other hand, are highly sensitive, simple, and need only low-cost instrumentation.





## 1.5 Aims and Objectives

### 1.5.1 Aim

To use electrochemical sensor systems for the qualification and quantification of metformin in aqueous systems, with a view to determine its aqueous concentration profile.

*Objective 1:* Understanding the metformin synthetic pathway with a view to propose new drug derivatives

*Objective 2:* Preparation and electrochemical characterization of polypyrrole (PPy) for the development of a nanostructured semi conductive polymer transducer platform in the design of metformin sensor systems.

*Objective 3:* Synthesis of copper nanoparticles following the chemical reduction method and characterization using UV-Vis, FTIR for chemical structure, SEM for morphology, EDS for chemical composition, TEM and SAXS for particle size.

*Objective 4:* Combining the advantages of polypyrrole nano polymer and Cu nanoparticles in the preparation of the PPy/CuNP nano sensor for distinguishing electrochemical signals of metformin and its metabolites under controlled conditions of oxidation and reduction.

## 1.6 Thesis lay-out.

### ○ Chapter 1

This chapter provides background information about diabetes mellitus particularly type 2 diabetes mellitus and pharmacological agents utilized to manage this disease. This chapter also provides information about the negative impacts of metformin on the environment.

### ○ Chapter 2

This chapter provides information about different types of sensors and biosensors used in literature to detect metformin. It also provides information about polymers of interest in the preparation of efficient electrochemical transducers in the design of metformin sensors.

### ○ Chapter 3

This chapter provides information on the operating principles of different analytical techniques and instrumentation used to characterize copper nanoparticles as well as polymer.

### ○ Chapter 4

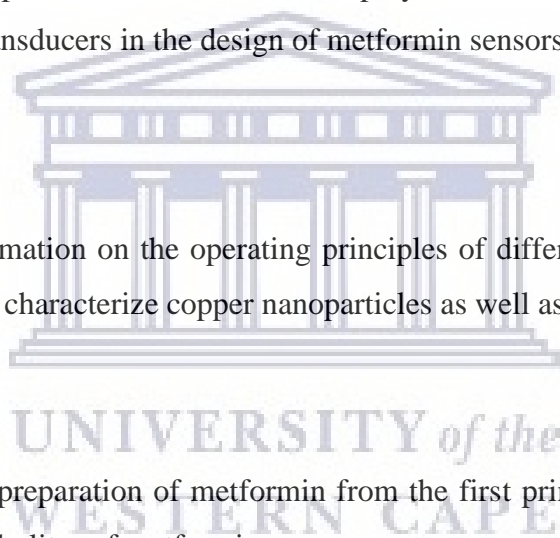
This chapter addresses the preparation of metformin from the first principles to provide insight into the chemistry and metabolites of metformin.

### ○ Chapter 5

The analytical performance of the sensor developed from polymer nanocomposite and Cu nanoparticle will be evaluated in terms of efficiency and sensitivity of the analysis.

### ○ Chapter 6

This chapter provides information about the synthetic route adopted in the synthesis of metformin and highlights the possibilities of new drug synthesis options. Preliminary steps and products are detailed and characterized.



- **Chapter 7**

Presents the summary and the most significant conclusions of the work done as well as the results obtained.



UNIVERSITY *of the*  
WESTERN CAPE

# CHAPTER 2

*This chapter provides a literature overview of the electrochemical sensor and biosensors that have been applied to the detection of metformin in aqueous systems.*

## **2.1 Introduction**

### **2.1.1 Analytical Techniques**

An analytical technique is a method that is used to determine the concentration of a chemical compound or chemical element. There are a wide variety of techniques used for analysis, from simple weighing gravimetric analysis to very advanced techniques using highly specialized instrumentation (Siddiqui et al,2013). For the evaluation of metformin (MET) specific techniques have been developed, among them stand out conductometry, gas chromatography in combination with different detectors, electrophoresis, UV-Vis, infrared, nuclear magnetic resonance spectroscopy, and electrochemistry. However, their major drawbacks resulted in the above-mentioned techniques to be withdrawn. Electroanalytical techniques gained momentum since they are cost-effectiveness, simple and highly sensitive.

### **2.2 Electrochemistry of metformin**

Electrochemistry is the study of chemical processes involving the movement of electrons. This movement of electrons is called electricity, which can be produced by an electron movement from one element to another in a reaction which is known as an oxidation-reduction (redox) reaction (Bard, 2014). To evaluate the electrochemical behaviour of the analyte of interest, an appropriate electrochemical sensor is required. Electrochemical sensors have been discovered to convert the electrochemical interaction analyte electrode effect into a useful signal. Such effects can be electrically stimulated or may result in a spontaneous interaction at the zero-current condition. Nevertheless, favourable circumstances proposed by electrochemical sensor include low recognition limit, wide direct reaction go, great security and need to small analyte volumes (Attia et al, 2015). Due to the above-mentioned advantages, electrochemical techniques are excellent for

sensitive determination of drugs and related compounds in pharmaceutical dosage forms and biological fluids. The instrumental strategies for quantitation which are most generally utilized in a pharmaceutical lab fall into four essential classes: chromatography, spectrophotometry, electrochemical, and radiometric investigation. However, characterisation techniques such as gas chromatography, HPLC, ultraviolet (UV), Infrared (IR) and NMR suffer from certain disadvantages which include long chromatographic run times, low sensitivity, and large consumption of sample volume. Electro-analytical methods, on the other hand, are cost-effective, highly sensitive and simple; thus, they are of interest in conducting this study (Hadi et al, 2016).

The advances in electrochemical techniques in the field of drug analysis are due to their simplicity, high sensitivity, low cost, and relatively short analysis time compared to the other techniques. Moreover, electrochemistry is most suitable for investigating the redox properties of drugs that can give insight into its metabolic fate. The data obtained from electrochemical techniques are often correlated with molecular structures and pharmacological activities of drugs. However, literature reports limited examples of electrochemical techniques in detecting metformin since it is still a new approach for this study. Electrochemical transducers such as carbon paste electrode and glassy carbon electrode have been used to develop sensors. In Gholivand's paper, designing sensor of carbon paste electrode (CPE) modified with Copper (II)-loaded activated charcoal (Cu-AC) was due to some significant advantages which include wide linear range, the lower limit of detection (LOD) higher sensitivity and increased stability (Gholivand et al, 2013). Electroanalytical techniques such as cyclic voltammetry and differential pulse voltammetry were made in use for characterisation purposes. The electrochemical study of metformin at aqueous medium was performed at Cu-AC-CPE platform using cyclic voltammetry. Based on this article the cyclic voltammograms indicated an anodic peak at 0.75 V and cathodic peak at 0.25 V which corresponds to oxidation of amino group in metformin and reduction of *N*-carbonyl-guanidine. The bare carbon paste electrode (CPE) was less favourable for metformin detection due to slow electron transfer processes, whereas modifying the electrode with Cu-AC produced a better response.

The sensitivity of the sensor was improved due to complex formation between electrode surface copper ions and metformin (Attia et al, 2015). However, the quantity of Cu-AC as a modifier

influences the response of the electrode. Literature reports that as Cu-AC percentages increases from 0-30% the oxidation current of metformin also increases meaning the sensitivity of the electrode increase with the surface area of the modifier. The most preferred oxidation state of copper for the complex formation is Cu (II), the reason being metformin has a high affinity with Cu (II). The selection of proper electrochemical technique is of great significance to achieve a highly sensitive method. Hence differential pulse voltammetry was introduced as a sensitive method for further investigation. In Gholivand's paper, this method demonstrated high selectivity, high sensitivity, and good applicability in detecting metformin in real samples. The limit of detection (LOD) and limit of quantification was found to be 9 nM and 28 nM, respectively. In the electroanalysis, carbon paste electrode has been extensively used due to its ease of fabrication, low cost, high sensitivity for detection and renewable surface.

In Attia's paper, the electropositive behaviour of metformin hydrochloride was evaluated using a pyrogallol modified carbon paste electrode (PYCPE) electrochemical sensor (Attia et al, 2015). Cyclic voltammetry (CV) and Differential Pulse Voltammetry (DPV) were utilized to evaluate the electrochemical behaviour of metformin on pyrogallol modified carbon paste electrode (PYCPE) (Hadi et al, 2016). Accordingly, in this article cyclic voltammogram of metformin on the designed sensor was indicated to exhibit an anodic peak at a forward scan and a cathodic peak at the reverse scan which was associated to the oxidation and reduction of pyrogallol (PY). However, it was discovered that the PYCPE in metformin hydrochloride solution indicated an irreversible oxidation behaviour over a wide pH interval of 2-9, due to the electrochemical oxidation of an amino group in guanidine group to *N*-hydroxyl amino group. The observed analytical performance of a sensor in an anticipated voltammetry method was acknowledged. The limit of detection and quantification was found to be  $9.14 \times 10^{-8}$  mol/L and  $3.05 \times 10^{-7}$  mol/L, respectively.

On the other hand, Hadi et al, 2016, proposed a highly sensitive electrochemical sensor by modifying glassy carbon with Copper-based metal-organic frameworks (Cu-BTC) nanocrystals or multi-walled CNTs hybrid nanostructure. The advantage of using multi-walled CNT as a modifier is that its large surface area could increase the electron transfer rate and produce higher response sensitivity because of high adsorption capability to target analyte molecules. The Cu-based metal-organic framework (MOF) has been regarded as an efficient electrode modifier for metformin

detection since it provides higher electrocatalytic performance and wider linear range. In Hadi's paper, the sensor was reported to have a long linear dynamic range of 0.50 –25.00 $\mu$ M and a low detection limit of 0.12  $\mu$ M. The electro-analytical methods offer more sensitivity and reduce analysis time, then few experiments were made to support the above statement. However, literature reports that direct electro-oxidation of metformin at conventional unmodified electrodes is usually limited by the electrode surface with high over-potentials. It has been discovered that the Cu-based metal-organic framework (MOF) is utilized as an efficient electrode modifier for metformin detection (Hadi et al, 2016).

Comparing the use of bare electrodes and modified electrodes. It became evident that the activity towards metformin is very low when an electrode is not modified. Modifying a glassy carbon electrode with Copper-based metal-organic frameworks Cu-BTC or nanotubes provides an improved electron transfer rate at the modified electrode. The high affinity of metal-organic framework (MOF) towards metformin molecules is due to an increased number of active adsorption sites and electrocatalytic reaction centres facilitating the strong chelating action of metformin with  $\text{Cu}^{2+}$  ions. Analysis of metformin performed by cyclic voltammetry produced a wide linear range of 0.50–25.00  $\mu$ M with a detection limit of 0.12  $\mu$ M.

### 2.3 Polymers

A polymer is a large molecule, or macromolecule, composed of many repeated subunits. They are possibly made of more than five monomers and some of which may contain hundreds or thousands of monomers in each chain. Polymers, both natural and synthetic, are synthesised through the process of polymerization of many small molecules, known as monomers. Polymerization is the process of covalently bonding the smaller monomers into forming the polymer. Amongst natural and synthetic polymers, natural polymers were recently discovered to gain momentum for their commercial application due to their thermal and environmental stability (Yussuf et al, 2018); thus, in this work, an organic polymer will be discussed furthermore. Conducting polymers (CPs) are organic materials that have optical, magnetic, and electrical properties. Generally, conductive polymers are conductive due to the existence of a conjugated electron or alternating single bond and double bond system in its chemical structure (Ansari, 2006). Typical conducting polymers

include polyacetylene (PA), polyaniline (PANI), polypyrrole (PPy), polythiophene (PTH), poly(para-phenylene) (PPP), poly(phenylenevinylene) (PPV), polyfuran (PF) (Xiaofeng Lu,2011). Polymers have been previously reported to be stable at room temperature. Polymers are applied differently in industry and polypyrrole was discovered to have technological applications in energy conversion, electrochromic displays, and solar energy.

To prepare conducting polymers several procedures can be followed. Amongst many methods, only two methods have been extensively used for the formation of conducting polymers and that is, chemical and electrochemical polymerization of the monomer. Accordingly, the properties of the conductive polymers vary for both chemical and electrochemical polymerization methods for an example, different conductivity of the same polymer can be produced. Chemical synthesis of the polymer is regarded as the most efficient method for preparing large amounts of conductive polymers while the electrochemical method was presented to be simple in terms of preparing the polymers as self-supporting and free-standing films (Ansari, 2006). Electrochemical polymerization on a metal electrode results in good quality film, while chemical polymerization yields fine conducting powders (Kaur et al, 2015). The main difference between the two methods of synthesis is, the electrochemical technique produces very thin CP films, whereas the chemical procedure produces very thick films or can give CPs in the form of a powder. The most preferred method is the electrochemical technique since thin films of a conductive polymer will be produced successfully.

In this work, polypyrrole will be utilized for the immobilization of metformin and to increase the conductivity of the metal electrode which will be glassy carbon electrode in this case. Polypyrrole is the organic polymer formed by the electrochemical polymerization of pyrrole monomer (Rahaman, 2018). Polypyrrole is regarded as a suitable polymer due to its high conductivity. In Yussuf's paper, polypyrrole was discovered to be gaining momentum for quite many commercial applications and that is due to its excellent thermal stability, good electrical conductivity, relative ease of synthesis and environmental stability (Yussuf et al, 2018). Polypyrrole has been actively used in many potential applications such as electronic devices, sensors, batteries micro actuators and anti-electrostatic coatings. In this work, PPy will be incorporated with copper nanoparticles and form a composite. The polymer is prepared by electropolymerizing pyrrole monomer through



cyclic voltammetry to obtain polypyrrole (PPy) (Figure 3). Electrochemical synthesis of polypyrrole provides a simple and rapid way of controlling the thickness of the polymer film growth since polymer thickness needs serious consideration in the preparation of nanocomposite. The schematic diagram below shows the mechanism of pyrrole polymerization to polypyrrole. The oxidative polymerisation of pyrrole to polypyrrole proceeds to a radical cation by a single-electron oxidation of pyrrole, which then pairs with another radical cation to form the 2,2-bipyrrole. Thereafter, the process is repeated to form longer chains.

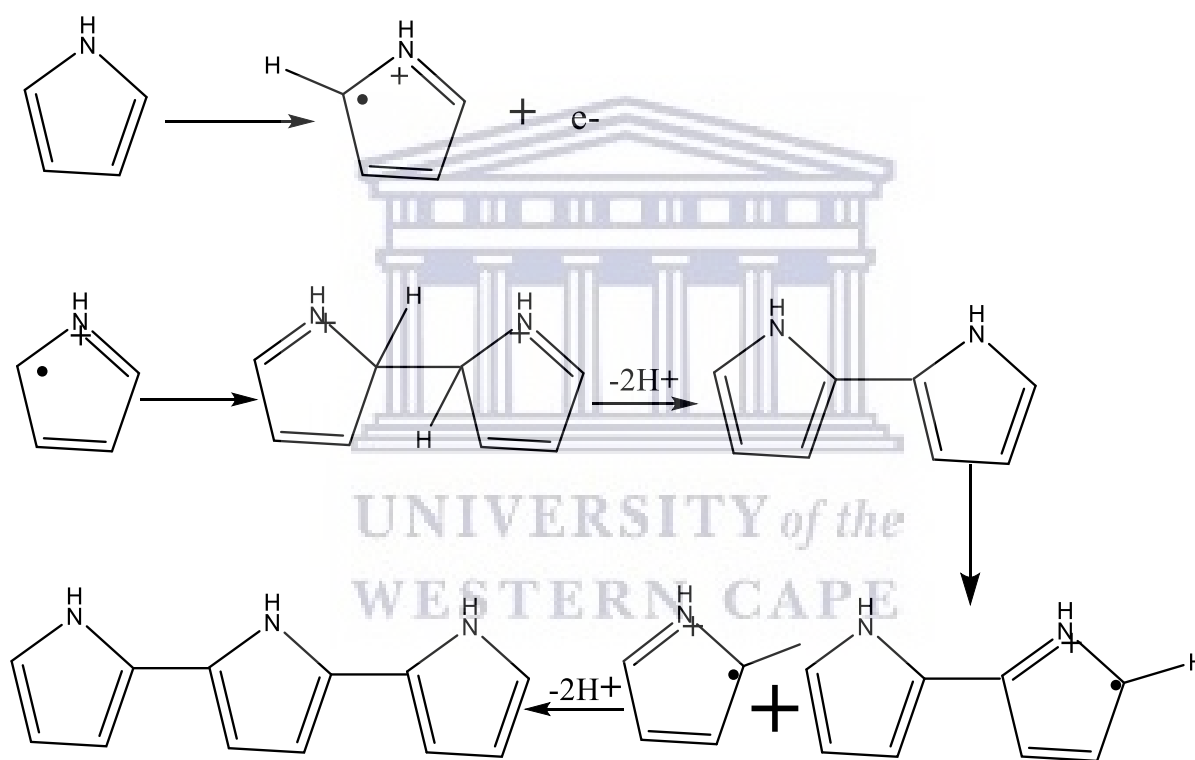


Figure 4: Electrochemical synthesis of polypyrrole from pyrrole monomer.

## 2.4 Polymer Nanocomposite

Polymer nanocomposites (PNCs) can be characterized as a mixture of two or more materials, where the matrix is a polymer and the dispersed phase has at least one dimension smaller than 100 nm (Müller et al, 2017). Recently, the addition of low contents of these nanofillers into the polymer

has been observed to lead to improvements in their mechanical, thermal, barrier and flammability properties, without affecting their processability (de Oliveira et al, 2018). The ideal design of a nanocomposite involves individual nanoparticles homogeneously dispersed in a matrix polymer. The dispersion state of nanoparticles is the major challenge in obtaining the full potential of properties enhancement (Müller et al, 2017). This uniform dispersion of nanofillers can result in a large interfacial area between the nanocomposites constituents (Bitinis et al, 2019). The filler's reinforcing effect is due to several factors, such as properties of the polymer matrix, nature, and type of nanofiller, concentration of polymer and filler, particle size particle, aspect ratio, particle orientation and particle distribution (De Oliveira et al, 2018). Various types of nanoparticles, such as carbon nanotubes, graphene, nanocellulose have been used to obtain nanocomposites with different polymers. In this study, copper nanoparticles will be used to prepare polymer-copper nanocomposite.

A study by (Shahrokhian, 2012), focused on nanocomposites consisting of iron oxide nanocrystals to be intensively due to their potential applications in drug delivery processes, magnetic resonance imaging, detecting, , electrochemical sensors (Wang et al, 2008), biosensors and treating cancer (Shahrokhian et al, 2012). Transition metallic nanoparticle, including copper, has proved to be electrocatalytically active for electrooxidation of some important organic species such as hydrazine, glucose (Jiang, 2012), and acetylcholine. A study by Gholivand, discusses the incorporation of iron nanomaterials with Cu on a carbon paste electrode (CPE) to design a sensor for the detection of metformin (Gholivand, 2013). In Gholivand's paper, Carbon Paste Electrode (CPE) was prepared by mixing analytical grade graphite and paraffin oil in a 70:30 (w/w %) ratio. Thereafter, CPE was modified with Fe and Fe-Cu/TiO composite then the electrochemical behaviour of metformin (MET) was evaluated using cyclic voltammetry (CV) (Gholivand et al, 2014). Electroanalytical response for bare CPE was reported to be very low due to slow electron transfer, whereas the electroanalytical response of the modified electrode was reported to be excellent (Figure 5). Further characterisation was made to evaluate the applicability of the above-proposed sensor in real samples such as synthetic urine and pharmaceutical formulations (Gholivand et al, 2014). The excellent electroanalytical response of CPE modified with Fe/TiO<sub>2</sub> and Fe-Cu/TiO<sub>2</sub> indicates the increased sensitivity of the designed transducer for metformin monitoring which may be due to the presence of copper oxide in the modifier. Gholivand (2014)

reported analytical application of the designed sensor to show recoveries between 97,9 and 102,7%. Correspondingly, the relative standard deviation was revealed to be lesser than 3,5% which indicate the suitable precision of the voltammetric determination of MET using the Fe–Cu/TiO<sub>2</sub>–CPE. In comparison with other reported transducers, the designed sensor was found to have high sensitivity with detection limit of 3 nM

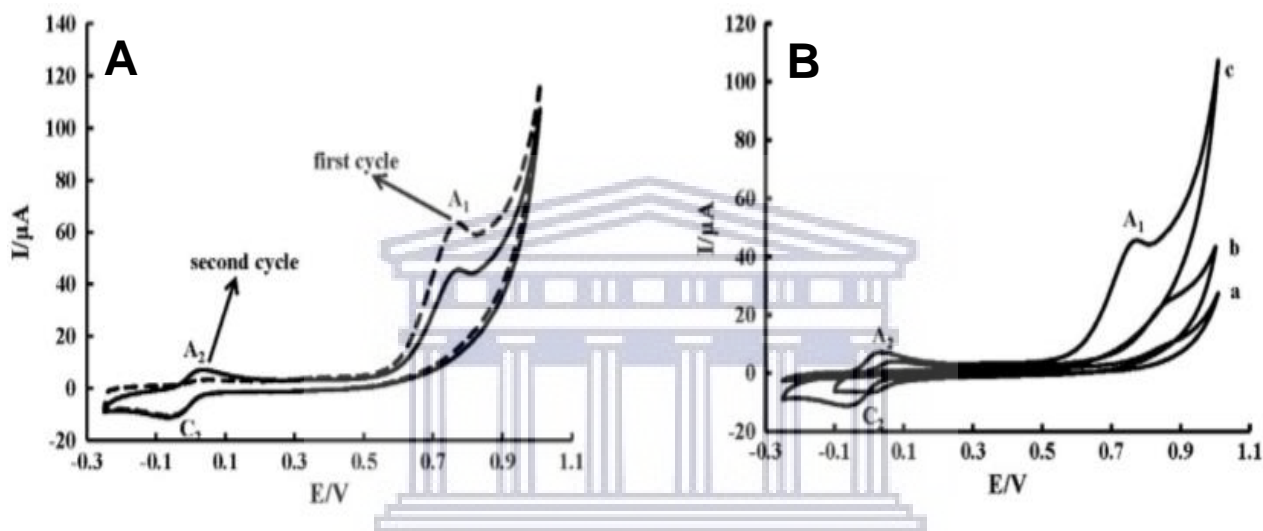


Figure 5: Cyclic Voltammograms corresponding to: (A) 10  $\mu$ M MET at Fe-Cu/TiO<sub>2</sub>-CPE. With the following measurement conditions: pH 12, scan rate= 100mVs<sup>-1</sup> and (B) 10uM MET at (a) CPE, (b) Fe/TiO<sub>2</sub>-CPE and (c) Fe-Cu/TiO<sub>2</sub>-CPE at the same conditions mentioned above (Gholivand et al, 2014).

## 2.5 Biosensors for metformin detection

Biosensors, a hybrid of physical and chemical sensing technique, is among the latest depicted class of the sensor. In principle, biosensors are receptor-transducer based instrument which could be employed for interpreting the biophysical or biochemical property of the medium. Moreover, the most interesting character that separates this kind of sensors from others is organic atoms in the medium. Improvement of biosensors brought the presence of biological/natural recognition component which enables the discovery of a new era of advancement in science (Vigneshvar et al,

2016). Recent discoveries reveal bio detecting as a phenomenon that withholds a set of techniques to produce an accessible detection signal of interaction between biological molecules. Development of biosensors for the detection of an environmental pollutants has received considerable attention in recent years (Hernandez-Vargas et al, 2018). Such sensors provide a great advantage to detect the minimal level of a contaminant in complex matrices, such as wastewater. It has been discovered that biosensors have given effect to current researchers in overcoming the undetectable levels of many harmful agents that would remain undetected, especially in wastewater. Biosensors are also miniaturized systems that enable the development of portable sensors which can monitor effluent on-site (Tsopele et al, 2016). Moreover, due to the specificity, fast response times, low cost, portability, ease of use and a continuous real-time signal of biosensors, distinct advantages in certain cases can be present.

The electrochemical behaviour of metformin on a Cu (II) complex by differential pulse and square wave voltammetry, in a wide pH range, at a glassy carbon electrode modified with a carbon black di-hexadecyl phosphate film (CB DHP/GCE), was investigated. The DNA-electrochemical biosensor is referred to as an electrochemical transducer with DNA immobilized on its surface with an ability of detecting specific drug DNA binding process (Santarino et al, 2014), through electrochemical transduction. Machini's paper reports a successful evaluation for the electrochemical behaviour metformin and electron transfer mechanism using cyclic voltammetry, differential pulse voltammetry and square wave voltammetry in wastewater samples (Machini et al, 2019). Electroanalysis was performed on a bare glassy carbon electrode (GCE) as well as on a GCE modified with a multilayer of dsDNA in designing a biosensor. The in-situ interaction of metformin with dsDNA in solution (0,1 M Phosphate Buffer with pH=7) using DPV and UV-Vis was evaluated by dsDNA electrochemical biosensor. A study by Machini found that at bare GCE no electrochemical redox processes were observed compared to a modified electrode. The oxidation reaction of metformin was only detected using modified electrodes, and, copper (II) ions as a catalyst in solution (Dehdashtian et al, 2015). The catalytic action of Copper (II) ions towards metformin indicated improved electron kinetics, thus oxidation behaviour of metformin in the presence of 5,0  $\mu\text{M}$  Cu ions was successfully investigated by differential pulse and square wave voltammetry, and limit of detection (LOD) and limit of quantification (LOQ) were obtained to be

0.63  $\mu\text{M}$ , and 2.09  $\mu\text{M}$  respectively with relative standard deviation (RSD) of 7.58%. Low limit of detection obtained for the proposed sensor implies a good sensitivity and selectivity to detect and quantify the antidiabetic drug in aqueous medium.

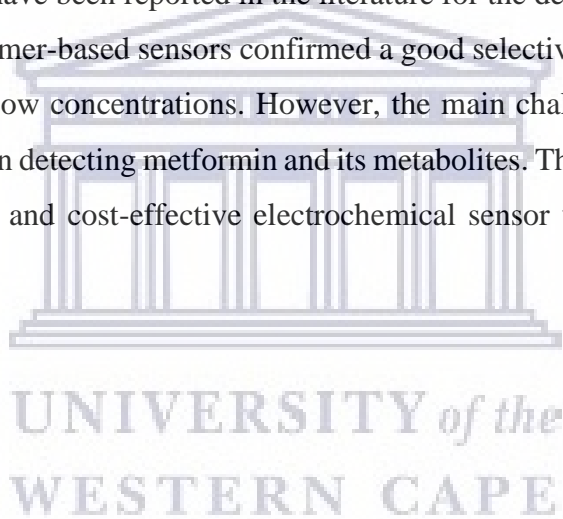
An eco-friendly biosensor which was recently discovered by Wu et al, 2018 is expected to be of assistance for the future design of more complex electrochemical detection systems. A study by Wu, focused on a glucose biosensor which was fabricated by fusing gold nanoparticles (AuNP) and glucose oxidase (GOD) multilayer films onto the polypyrrole (PPy)/reduced graphene oxide (RGO) modified glassy carbon electrode (GCE) through self-assembly and electrodeposition (Wu et al, 2018). A thin film of PPy and graphene oxide on a bare GCE was attained through the process of electrodeposition. Thereafter, AuNPs and GOD were immobilized consecutively onto PPy-RGO/GCE electrode with the electrodeposition of AuNPs and self-assembly of GOD to acquire AuNPs-GOD multilayer films. Additionally, AuNPs were discovered to bind strongly to the biomolecule surface through covalent bonds with the functional groups such as  $-\text{NH}_2$ ,  $\text{SH}$ , and  $-\text{CN}$ . The resulting PPy-RGO-(AuNPs-GOD) n/GCE biosensors were used to characterize and assess their electrocatalytic activity toward glucose using cyclic voltammetry and amperometry. This biosensor showed a good performance for the glucose detection with the detection limit and sensitivity of 5.6  $\mu\text{M}$  and 0.89  $\mu\text{A}/\text{mM}$ , respectively.

### **2.5.1 Copper binding properties towards metformin**

Among a vast number of metals presented in literature, copper was the preferred metal in this study due to its binding properties towards metformin. Previous studies recently demonstrate a metal-binding property of metformin, particularly toward copper, may be one factor in cell responses to this drug (Logie et al, 2012) (Repišćák et al, 2014). However, it remained unclear whether metformin binds to  $\text{Cu}^{\text{I}}$  or  $\text{Cu}^{\text{II}}$ . Recent discoveries report  $\text{Cu}^{\text{II}}$  to have more stable oxidation state in solution. Harthill (2012) found a compelling evidence of direct binding of metformin to metal ions, including extensive crystallographic and spectroscopic analysis, contrasts with the lack of evidence regarding direct binding of metformin to protein targets. Cooperation of biguanides with metals has been known since the 19th century (Logie et al, 2012), a couple of years after their

synthesis and before their antihyperglycemic properties were first revealed. metformin was reported to not only act as a ligand for a variety of divalent transition metal but also indicate the most stable interaction thus far with copper amongst other metals (Uddin et al, 2017). Moreover, copper was discovered to have a high affinity to metformin due to strong chelating action of metformin towards Cu (II) (Hadi et al, 2016). Regardless of an excellent affinity of copper towards MET, when dealing with a large amount of sample where the analyte is likely presented at very low concentration; a sensor with good sensitivity and reproducibility is required. Thus, a conductive polymer is usually incorporated with a metal (copper) based sensor for the early detection of metformin in an aqueous medium. In the past years, several analytical methods have emerged intending to detect anti-diabetic agents in an aqueous medium.

Quite a few sensors which have been reported in the literature for the determination of metformin include biosensors and polymer-based sensors confirmed a good selectivity due to their capability to recognize metformin at low concentrations. However, the main challenge of these sensors is associated with difficulties in detecting metformin and its metabolites. Thus, in this study, the main aim is to develop a simple and cost-effective electrochemical sensor with high sensitivity and selectivity.



## 2.6 Conceptual diagrams

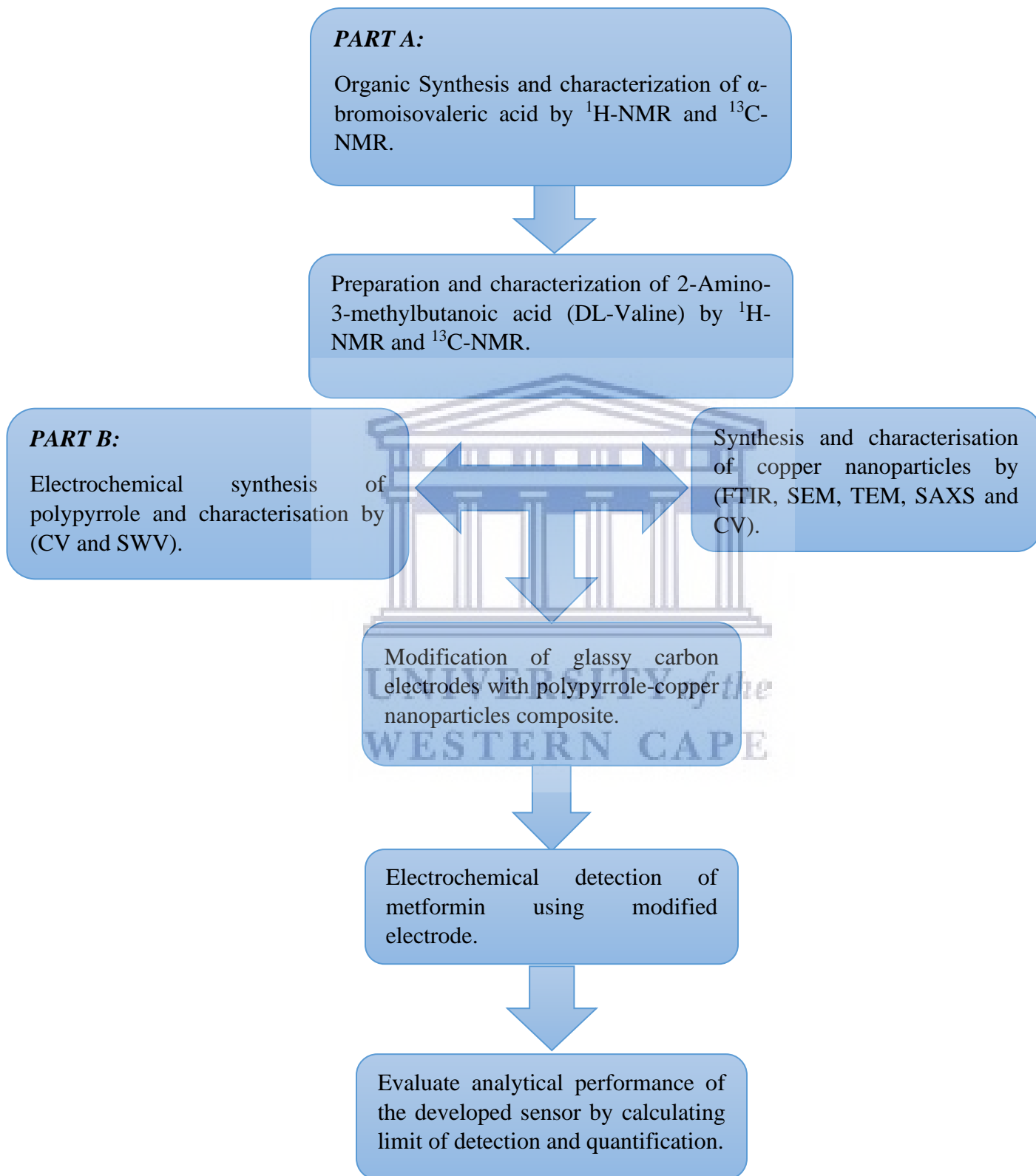


Figure 6: Flow diagram of the thesis for organic synthesis (Part A) and electroanalytical behaviour of metformin on the modified electrode.





# CHAPTER 3

*Synthesis of metformin analogues involves multiple steps and many intermediates. The synthesis and characterization of products and materials required the use of a wide range of spectroscopic and separations equipment and techniques which will be detailed in this chapter. Characterization of the polymer electrode and its modification with Cu nanoparticles, was predominantly achieved by electrochemical and morphology methods.*

## 3.1 Introduction

A high number of nanostructured materials including conducting polymers become extremely essential in sensor and biosensor design. There are several types of sensors that are fabricated using conducting polymers in various transduction modes, the transduction modes are usually categorized into five classes according to the operating rules such as conductometric, potentiometric, amperometric, colorimetric, and gravimetric procedures (Soloduchko et al, 2016). The majority of sensor devices were discovered to employ several polymers with distinct roles, either in sensing mechanism or through immobilizing the species responsible for sensing the analyte component (Gupta et al, 2011). The most widely used polymer-based sensors include a molecularly imprinted sensor, polyindole, polyaniline and polypyrrole. A sensitive and selective electrochemical sensor based on molecularly imprinted polymers incorporated with gold nanoparticles was developed for the trace level for the detection of metformin—an antidiabetic drug in the real sample matrix. The electro-conductivity of the designed sensor was improved by infusing the sol-gel matrix on the surface of the sensor. Spectroscopic, microscopic, and electrochemical techniques were utilized for the characterization of the molecularly imprinted polymer-based electrochemical sensor (Roy et al, 2013). The latest development of different polymer-based sensors with the focus on polypyrrole (PPy) will be discussed further.

Previous studies discovered that the functionalization of polypyrrole with the metal-organic framework has a significant effect on improved sensor performance, such as improved adsorption of organic compounds and detection of low concentration analytes (Šetka et al, 2017). To-date not much has been reported on a polypyrrole-based electrochemical sensor for the detection of metformin. However, recent studies reveal polypyrrole to be used for the fabrication of biosensors for the detection of glucose. A highly sensitive biosensor for the electrochemical determination of glucose was constructed by immobilizing gold nanoparticles (AuNPs) and glucose oxidase (GOD) multilayer films onto the polypyrrole-reduced graphene oxide modified glassy carbon electrode (GCE) through the electrodeposition and self-assembly for the detection of glucose. The electrochemical performance of PPy-RGO-(AuNPs-GOD) n/GCE biosensor was evaluated by electrochemical techniques particularly cyclic voltammetry (Wu et al, 2018). In this work, the electrochemical sensor was designed by immobilizing copper nanoparticles on the polypyrrole thin film at the glassy carbon electrode surface. The sensitivity and selectivity of the polypyrrole-based electrochemical sensor will be further evaluated using various characterisation techniques.

### 3.1.1 Spectroscopic Technique

Spectroscopy is the study of the interaction of electromagnetic radiation with matter. It is an important tool that can acquire information about the molecular structures, composition, and vibration frequencies of a substance (Bellisola et al, 2012). Spectroscopic methods are classified according to the region of the electromagnetic spectrum involved in the measurement. The regions include gamma-ray, X-ray, ultraviolet (UV), visible, infrared (IR), microwave, and radiofrequency (RF). Spectroscopic methods have proved to be the most widely used tools for the elucidation of molecular structure as well as the quantitative and qualitative determination of both inorganic and organic compounds. Spectroscopic data are often represented by an emission spectrum, a plot of the response of interest as a function of wavelength or frequency. In this study, optical radiation (UV-Vis & FTIR) and X-ray (SAXS) were utilized for further characterization of nanomaterials particularly.

### 3.1.1.1 Fourier Transform Infrared spectroscopy (FTIR)

Spectroscopic characterization was performed on Perkin Elmer Spectrum 100, FT. Fourier-transform infrared spectroscopy (FTIR) is a technique used to acquire an infrared spectrum of absorption or emission of a sample investigated. This technique provides qualitative and semi-quantitative information about the sample under investigation. An FTIR spectrometer simultaneously assembles high-spectral-resolution data over a wide spectral range. The infrared radiation reacts with the molecules of the sample and the absorbed radiation generates a band vibration which are characteristics of functional groups. The produced spectrum demonstrating absorption peaks is a molecular fingerprint of the sample. Molecular fingerprints of a sample correspond to frequencies of vibrations between the bonds of the atoms and molecules which make up a material. In this study, FTIR was used to evaluate the chemical bonds and the functional groups of the chemically synthesized copper nanoparticles.

### 3.1.1.2 Small Angled X-ray Scattering (SAXS)

Small-angle X-ray scattering (SAXS) was performed using Sax Space Anton Paar (Austria). Small-angle X-ray scattering (SAXS) was discovered to be a powerful technique that is likely to provide qualitative and quantitative information about the sample of interest. The X-ray radiation interacts with sample molecules resulting in atoms that are present in the sample to scatter the incident radiation into all directions which then provides background radiation that is almost constant at small angles (Schnablegger et al, 2013). The sample consists of small particles that further scatter, and this may be due to the density of the particles and the size which are in the range of the x-ray wavelength. The particle shape is indicated by the features of pair-distance distribution function (PDDF) (Schnablegger et al, 2013). The size distribution of one parameter, such as the particle radius, can be obtained by an inversion of  $P(q, R)$  after the shape is established. This method was found to be non-destructive, accurate, and sample preparation steps are not complicated. This method was discovered to offer reliable estimates of nanoparticle size since the size distribution of nanomaterials analysed by SAXS is assessed over a large number of

nanoparticles as electron microscopy methods analyses particle distribution based on hundreds or thousands of particles (Agbabiaka et al, 2013).

### 3.1.1.3 Nuclear Magnetic Resonance

Nuclear magnetic resonance spectra was performed on Bruker-400 MHz at the University of the Western Cape. Nuclear magnetic resonance spectroscopy (NMR), is a spectroscopic technique for chemical structure determination and local magnetic fields around atomic nuclei. Subsequently, the molecular structure is assigned by the energy spectrum of nuclear spins in a molecule, and by interpreting the symmetry and position of the resonance lines in the spectrum. Several parameters associated with NMR such as chemical shifts assist by providing the information about different chemical environments in a molecule as well as chemical structure determination. Deuterated Chloroform ( $\text{CDCl}_3$ ) is the most preferred solvent for the preparation of the samples for NMR. In NMR the sample is placed in a magnetic field and the NMR signal is formed by exciting the nuclei sample with radio waves into nuclear magnetic resonance, which is detected with sensitive radio receivers. Chemical shifts are expressed in  $\delta$  (ppm) and coupling constants (J) in Hz. In this study, NMR was used to determine the chemical structure of the unknown synthesized compound.  $^1\text{H}$ -NMR and  $^{13}\text{C}$ -NMR were both used to evaluate to the number protons and carbons present in the unique compound.

Nuclear magnetic resonance (NMR) spectroscopy is a quantitative spectroscopic tool since the intensity of a resonance line is directly proportionate to the number of resonant nuclei (Figure 7). Though the method for quantification of MET is already available, more authentic, accurate, and simple method for its intended purpose are utilized. It has been discovered that there are many analytical methods available for quantification of MET nonetheless almost all the methods are based on prolonged chromatographic techniques. Recently NMR finds its application in quantitative analysis in order to determine the impurity of the drug, characterization of the composition of the drug products and in quantitation of drugs in pharmaceutical formulations and biological fluids (Salem et al, 2006). Each approach enables MET determination at different concentration levels.



Figure 7: Nuclear magnetic resonance (NMR) instrument (Bruker-400 MHz).

#### 3.1.1.4 Ultraviolet Spectroscopy

Nicolet evolution 100 UV-Vis instrument was made in use to analyse the amount of light absorbed by a commercial drug (metformin) (Figure 8). Ultraviolet-visible spectroscopy is regarded as an optical spectroscopy where the interaction of light with matter is investigated. UV-Vis spectroscopy is a sensitive method in molecular spectroscopy that uses ultraviolet and visible light in the wavelength range. The technique measures the absorption of light across the ultraviolet and visible light wavelengths through a liquid sample. Samples are dispensed into a cuvette and placed in the path between a UV-Vis light and a detector. According to Beer-Lambert's law, with a constant light path length and known absorption coefficient (dependent upon wavelength), the concentration of a compound evaluated can be determined from the light absorbed by the sample

at that wavelength. The commercial drug of metformin was prepared with distilled water and placed in 10.00 mm quartz cuvettes. The region of the UV-Vis absorption spectra was between 200 nm – 400 nm.

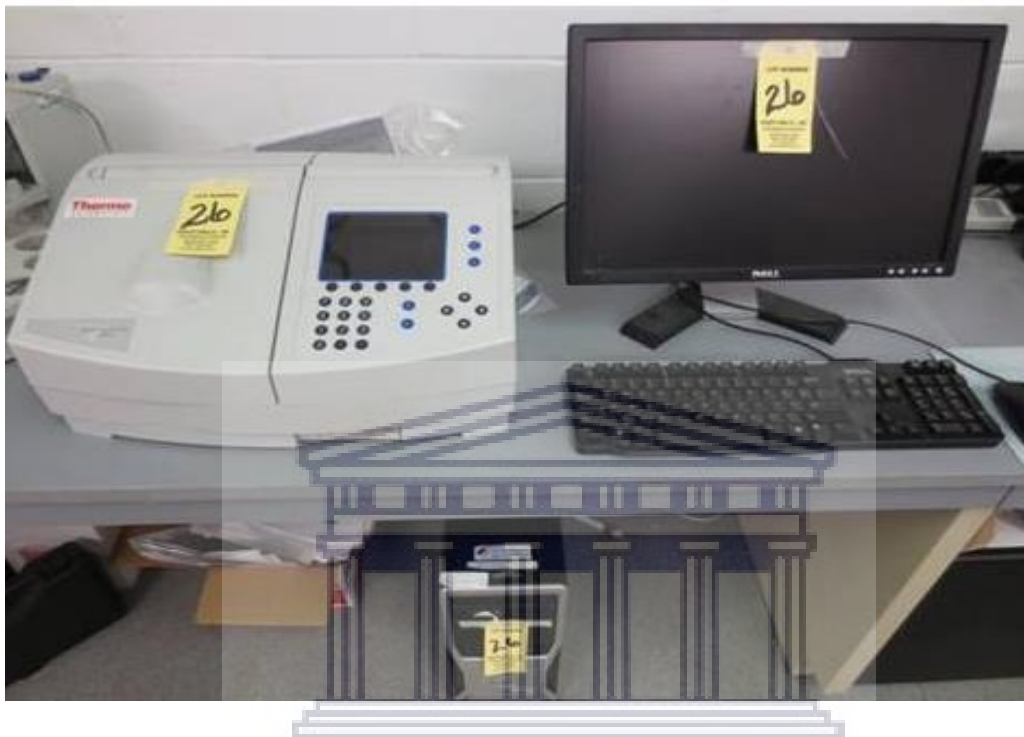


Figure 8: Nicolet evolution 100 UV-Vis instrument.

### 3.1.2 Microscopic Techniques

Microscopy is a category of characterization techniques that probe and map the surface and sub-surface structure of a material. These techniques can use photons, electrons, ions or physical cantilever probes to gather data about a sample's structure on a range of length scales. Some common examples of microscopy instruments include:

#### 3.1.2.1 Scanning Electron Microscope (SEM)

Scanning Electron Microscope (SEM) analysis was conducted on Hitachi S3000N Scanning Electron Microscope and Zeiss Auriga, High resolution (fegsem) field emission gun scanning

electron microscope. A scanning electron microscope (SEM) is a type of electron microscope that produces images of a sample by scanning the surface with a focused beam of electrons (Figure 9). In this technique, electrons interact with atoms of the evaluated sample producing various signals which then give information about the surface topography and composition of the sample. The signals from secondary electrons (SE), back-scattered electrons (BSE), X-rays, specimen current, cathodoluminescence (CL) and transmitted electrons were produced based on the working principle of SEM. These signals are used to generate a high-resolution image providing information about the sample's surface morphology, topography, and composition (Aroon et al, 2010). Literature reports SEM as one of the most powerful instruments in sciences since it interacts physically with the analyte of interest. Different magnification was applied at an acceleration voltage of 5.0 kV. The scanning electron microscopy will be used to study the topography, morphology, and composition of the copper nanoparticles.

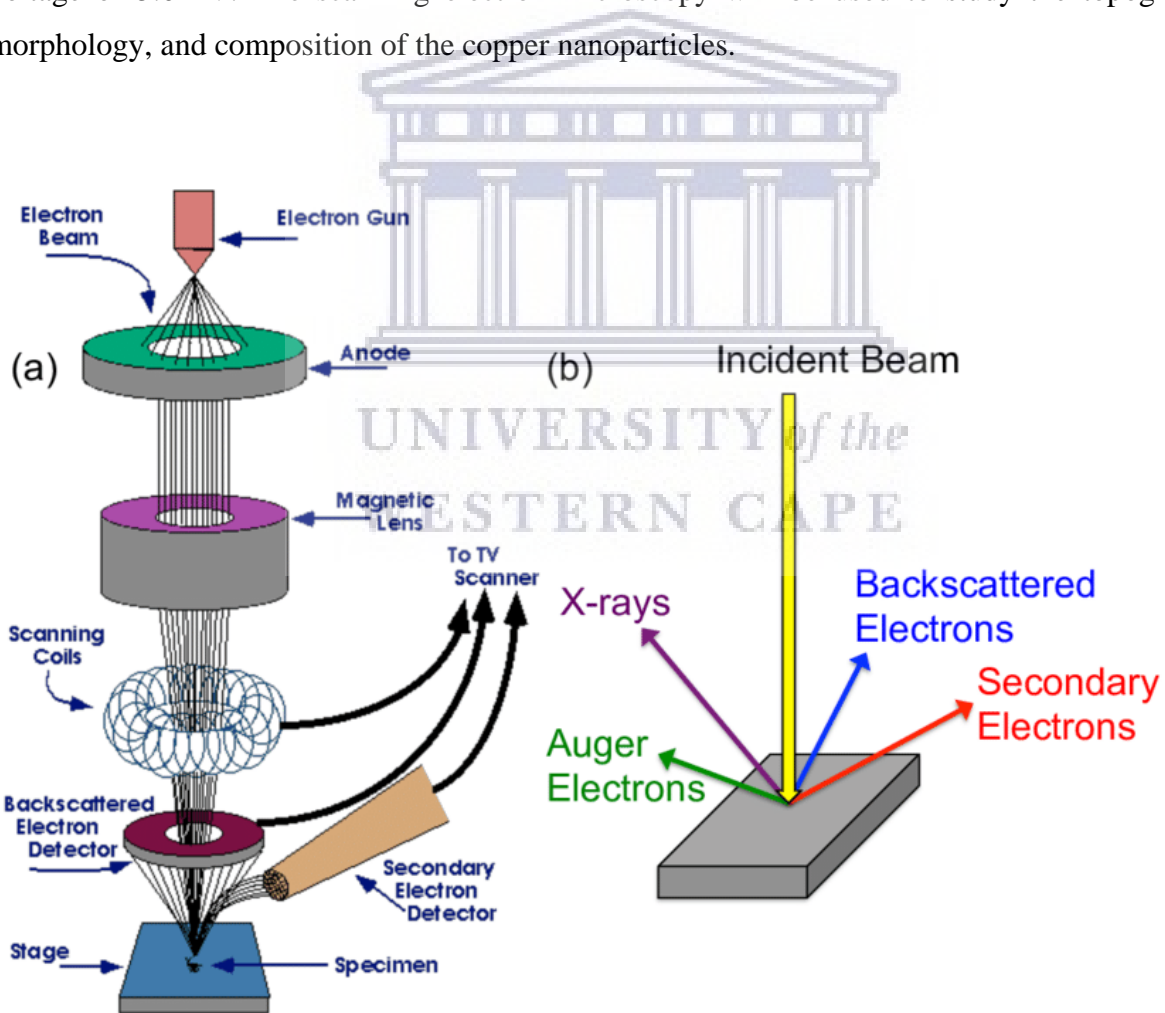


Figure 9: Schematic diagram of scanning electron (SEM).

### 3.1.2.2 Transmission Electron Microscopy (TEM)

Transmission Electron Microscopy (TEM) analysis was performed with a FEI Tecnai G2 F20X-Twin MAT 200 kV Field Emission Transmission Electron Microscope (Eindhoven, Netherlands) with Energy Dispersive X-ray Spectrometry (EDS) and Selected Area Electron Diffraction (SAED) capabilities. Transmission electron microscopy (TEM) is the most widely used technique in which a beam of electrons is transmitted through a specimen to form an image for studying all aspects of phase transformations in the material of interest over the length scale range of 1–100 nm (Mielanczyk et al,2015). An ultrathin specimen was prepared with a thickness of less than 100 nm or a suspension on a grid. This method works by transmitting a beam of electrons through a thin specimen and interacts with the specimen as it passes through. An image with high resolution is formed from the interaction of the electrons with the sample as the beam is transmitted through the specimen. The generated image is then magnified and focused onto an imaging device, such as a fluorescent screen, a layer of photographic film, or a sensor such as a charge-coupled device (CCD). The microscopes of this method are capable of imaging at a significantly higher resolution than light microscopes, owing to the smaller de Broglie wavelength of electrons. Transmission electron microscopes are discovered to be the most powerful electron microscopes which can magnify the nanomaterial effectively by a million times. Transmission electron microscopy is a major analytical method that can be used in the physical, chemical and biological sciences. In this study, TEM will be used to analyze copper nanoparticles.

### 3.1.3 Electrochemical characterization

Electrochemical characterization deals with chemical phenomena related with charge separation, usually in liquid media, such as solutions. The separation of charge is often allied with charge transfer, which can occur homogeneously in solution between different chemical species, or heterogeneously on electrode surfaces. Electrochemical characterization is one of the effective techniques that can be used to study electron transfer properties of the material being analysed (being in solution or solid-state). The work described in this critique encompasses current



measurement, voltammetry, and many voltammetry techniques, such as cyclic voltammetry (CV) and square wave voltammetry (SWV).

### 3.1.3.1 Cyclic Voltammetry

All cyclic voltammetry experiments were performed using PalmSens Ptrace 4.4 electrochemical workstation using a three-electrode cell. Cyclic voltammetry (CV) is a prevailing and popular electrochemical technique commonly employed to investigate the reduction and oxidation processes of molecular species. This technique is also used to determine the potential window of electrodes or devices. Cyclic voltammetry has been used extensively to investigate the redox properties of conductive and semi-conductive material (Espinoza et al, 2019). The measurement of the resulting current when applying a linear potential to an electrode between two potential limits is the main principle of CV. Scan rate is referred to as a rate of change of potential with time. In this technique, a supporting electrolyte is utilized during the experiment to prevent charges and products from migrating. The potential of a working electrode is scanned linearly and the current from the applied potential is measured by potentiostat. The resulting current potential plot is known as the cyclic voltammogram (Figure 10). In this study, CV was further used to evaluate redox reactions of polypyrrole (PPy), copper nanoparticles (CuNP) and polymer-based nanocomposite (PPy/CuNP) to acquire information about the chemical behaviour of the designed electrochemical sensor for the detection of the analyte.

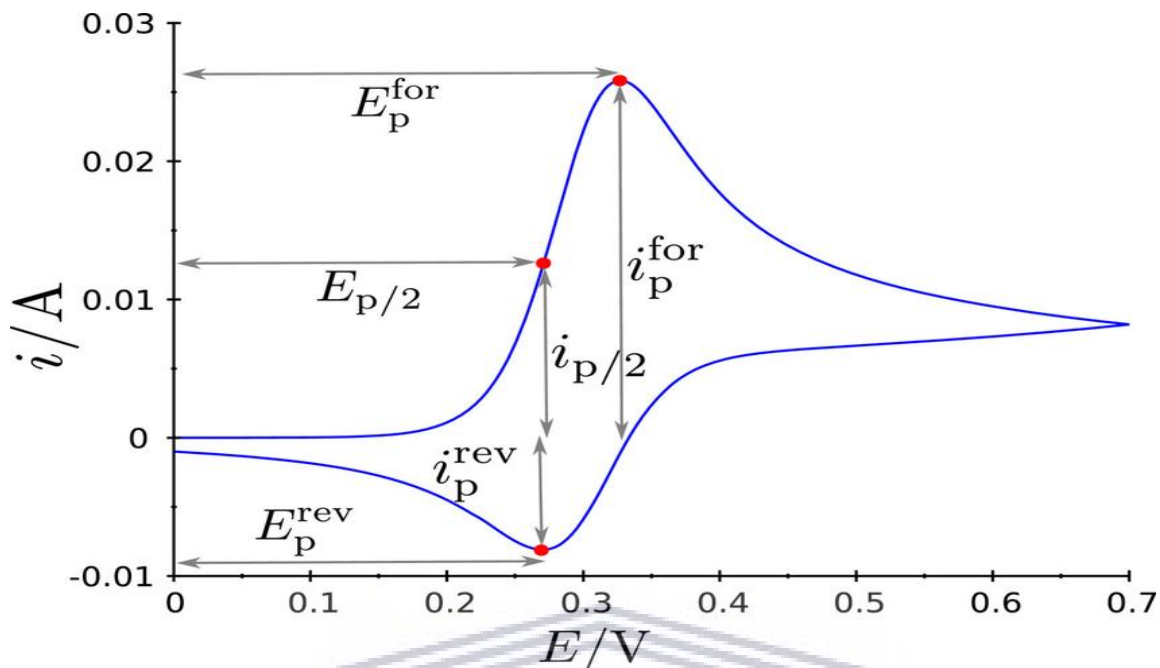


Figure 10: A typical diagram of cyclic voltammogram.

The electrochemical parameters on the cyclic voltammogram are likely used for analysis purposes. The peak potential ( $E_{pa}$  and  $E_{pc}$ ) and peak current ( $I_{pa}$  and  $I_{pc}$ ) provide significant information about the analyte evaluated. The cyclic voltammogram also provide information about electron transfer kinetics, electrochemical reversibility, irreversibility or quasi-reversibility and diffusion coefficient of the system. The effect of scan rate at peak current ( $I_p$ ) in cyclic voltammetry is described by the Randles-Sevcik equation (equation 1). Randles-Sevcik also provide information about the diffusion of analyte in solution.

Randles-Sevcik equation:

$$I_p = 2.69 \times 10^5 \times n^{3/2} \times A \times D^{1/2} \times C \times V^{1/2} \dots \text{Equation 1}$$

Where:

$I_p$  is the forward peak current (A)

$n$  is the number of electrons transferred in the redox reaction.

$A$  is the area of the electrode in  $\text{cm}^2$

$D_0$  is the diffusion coefficient in  $\text{cm}^2.\text{s}^{-1}$

$C_0$  is the concentration in  $\text{mol}/\text{cm}^3$

$\nu$  = scan rate in V/s

The peak to peak separation ( $\Delta E_p$ ) in an electrochemically reversible process is given by the separation between the anodic and cathodic peak potentials.

$$\Delta E = E_{pa} - E_{pc}$$

$$\Delta E = \frac{59}{n}$$

### 3.1.3.2 Square Wave Voltammetry

Square Wave Voltammetry (SWV) is a potential electrochemical technique among the various pulse techniques for analytical applications, the study of electrode mechanisms and their kinetics. This technique can be used for quantitative analysis as well as studying the mechanism, kinetics, and thermodynamics of chemical reactions. In a square wave voltammetry experiment, the quantification of the redox properties of the analyte is measured at the working electrode surface where the potential varies linearly with time with the constant contribution of the reference electrode. The current at a working electrode is measured while the potential among the working electrode and the reference electrode is swept linearly in time. All the SWV experiments were carried out at a PalmSens Ptrace 4.4 workstation on a three-electrode system. The main advantage of SWV over CV is its high sensitivity. In this study, Square wave voltammetry will be used to confirm peaks observed in the CV which will then offer reliable analytical parameters that include sensitivity, LOD, and LOQ of the electrochemical sensor.

### 3.1.3.3 Capillary electrophoresis

Recently, the determinations of drugs in biological fluids by capillary electrophoresis (CE) in fused-silica capillaries have been developed (Robbert et al, 2018) as an attractive alternative to HPLC. However, no capillary electrophoresis (CE) assay for metformin in plasma has yet been reported. The key advantages of CE over HPLC are substantially lower reagent and low time consumption, improved mass-sensitive detection limit and high separation efficiency (Salim et al, 2018). Capillary electrophoresis is preferred for quantification of metformin due to its cost- and time-effectiveness and short analysis time. The analysis of metformin was conducted in aqueous solution of a borate buffer (pH9). Compared to HPLC, the retention time for metformin in capillary electrophoresis was observed to be less than 5 min for the quantification of metformin. Recoveries studies were calculated to be in a range of 99-100.2% in Athiporn Doomkaew (2015) review paper and that suggested good selectivity and accuracy of the method. Furthermore, capillary electrophoresis was discovered to be sensitive than liquid chromatography with low limit as being detection in a range of 2, 2 - 4 mg/mL. The low limit of detection shows high sensitivity, efficiency, and accuracy of this method for the quantification of metformin in pharmaceutical products (Mohamed et al, 2019). Nonetheless, this approach entails expensive instrumentation and is limited to certain compounds which fluorescence at the few excitation wavelength provided.

The materials prepared for the sensor transducer included polypyrrole and Cu nanoparticles. These materials were characterized by spectroscopy, microscopy, and electrochemistry. Spectroscopy methods such as Fourier-transform infrared spectroscopy (FTIR) was used to evaluate chemical bonds and functional groups of copper nanoparticles, Small-angle X-ray scattering (SAXS) will be useful in determining the size of the nanoparticles. Nuclear magnetic resonance spectroscopy (NMR) will be used to determine the chemical structure of the unknown synthesized compound in chapter 4. Ultraviolet-visible spectroscopy (UV-Vis) was used for quantitative analysis of metformin, it was also used to evaluate the optical properties of copper nanoparticles. Microscopic methods such as scanning electron microscopy (SEM) and transform electron microscopy (TEM) will be used to study the topography, morphology, and composition of the copper nanoparticles.

# CHAPTER 4

*This synthesis of metformin analogues is a multistep process for which the starting materials was not readily available, in this chapter we detail the synthesis of starting material and the stepwise methodology adopted for metformin synthesis including purification and elucidation methods of all materials prepared. Due to cost and time considerations, the full synthetic route could not be explored during this work. Electroanalytical determination was done using commercial metformin formulations.*

## 4.1 Chemical Reagents

Isovaleric acid, polyphosphoric acid, Bromine, dichloromethane (DCM), magnesium sulphate (MgSO<sub>4</sub>), methanol (MeOH), ethyl acetate (EtOAc), ethanol (EtOH), hexane (Hex), and deuterated chloroform (CDCl<sub>3</sub>) were purchased from Sigma Aldrich (Merck) (South Africa).

## 4.2 Chromatography

Chromatography is a laboratory technique that enables separation, identification, and purification of the components of a mixture for qualitative and quantitative analysis. Separation in chromatography works by passing the mixture in solution or suspension through a medium in which the components move at different rates. Chromatographic procedures have produced a great improvement and gained a broad acceptance as a major analytical tool for qualitative and quantitative analysis of metformin in plasma medium (Merey, 2018). The chromatographic techniques that have been reviewed thus far in literature for the determination of metformin include GC-MS and HPLC. To-date, not much have been reported on detection of metformin by GC-MS. Nonetheless, a study by Goedecke et al, 2013 performed a quantitative analysis of metformin by GC-MS on surface water at low concentration (Goedecke et al,2013). GC-MS does not only provide good sensitivity and specificity, it also offers additional information from mass spectral data, which is effective in confirming the identity of the drug. However, GC-MS equipment is cost effective compared to HPLC, with a complicated sample preparation procedure before analysis.

Throughout the literature reports it was observed that HPLC was the most commonly used method amongst other chromatographic techniques. The HPLC methods specificity is outstanding and at the same time adequate accuracy is also achievable.

Metformin was among the three anti-diabetic drugs which were detected by HPLC in Chhetri's paper. Analysing metformin using HPLC was due to some significant advantages such as analysing large volumes of sample. Literature reports the quantification of metformin in human plasma using HPLC at different mobile phases (Chhetri et al, 2013). Discoveries show that mobile phases are evaluated to find the most suitable condition for the quantification process. However, accuracy and precision can only be achieved if wide-ranging systems suitability tests are performed before the HPLC analysis, which then lead to long chromatographic run times. The main disadvantage of HPLC is that it suffers the safe disposal of the solvents used in HPLC analysis. Moreover, metformin is a strong polar molecule thus, it is difficult to analyse it using chromatography. In this study the only chromatographic techniques which will be used include column chromatography (to purify synthesised product) and thin layer chromatography (separation).

#### **4.2.1 Column Chromatography (CC)**

Chromatography is referred to as a physical separation process in which the components to be separated are dispersed between two phases, stationary phase, and mobile phase (Figure 11). The main purpose of chromatography is to separate the components of a mixture for later use hence it is regarded as a form of purification (Patel, 2018). Chromatography was discovered to rely on the principle where molecules in mixture applied onto the surface or into the solid stationary phase (stable phase) is separating while moving with the aid of a mobile phase (Coskun, 2016). This separation technique consists of some molecular characteristics which are associated with adsorption, partition, and differences among their molecular weights. In view of these distinctions, some components of the mixture remain longer in the stationary phase, and were observed to move gradually in the chromatography framework, while other components of the mixture passed rapidly into mobile phase due to high retention time (Coskun, 2016). Based on this approach, three components form the basis of the chromatography technique. Stationary phase is a phase likely

composed of a solid phase or a layer of a liquid adsorbed on the surface solid support. Mobile phase is likely comprised of liquid or a gaseous component. The last component is the separated molecules after the separation and purification process.

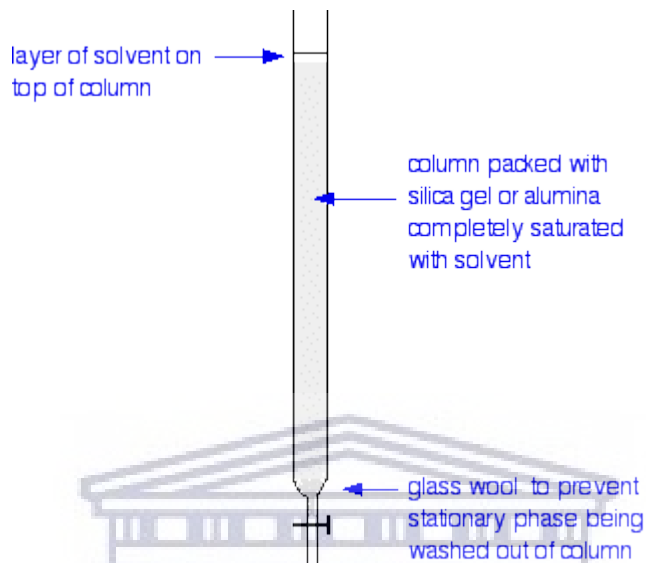


Figure 11: A typical Column Chromatography.

In this study, the solid phase was Silica gel 60 and Sephadex LH-20, the mobile phase was hexane and ethyl acetate. Silica gel 60 (0.040-0.063mm) 230-400 mesh particle size (Merck) and Sephadex LH-20 (Sigma Aldrich) were packed in glass columns (10-25mm diameter) to prepare for column chromatography analysis. Size-exclusion chromatography was carried out using Sephadex® LH-20 (Pharmacia), eluting with ethanol. Thereafter, column chromatography was used to purify the synthesized compound depending on its polarity or hydrophobicity as well as to isolate single chemical compound from a mixture of compound synthesized following organic synthetic route.

#### 4.2.2 Thin Layer Chromatography (TLC)

Thin-layer chromatography (TLC) is a chromatographic technique used to separate the components of a mixture (non-volatile mixtures) using a thin stationary phase supported by an inert backing (Bele et al, 2010). Thin layer chromatography is carried out on a sheet of glass, plastic, or aluminium foil coated with a thin layer of adsorbent material, typically silica gel,

aluminum oxide (Figure 12). This layer of adsorbent is known as the stationary phase (Cid-Hernández et al, 2018). In this type of chromatography, the sample is likely applied on the plate, thereafter a solvent mixture (mobile phase) is drawn up the plate through capillary action. The solvent is drawn up through the particles on the plate through the capillary action, and as the solvent moves over the mixture each compound will either remain with the solid phase or dissolve in the solvent and move up the plate (Bele et al, 2010). The physical properties (solubility or molecular structure) of the evaluated compound determines whether the compound moves up the plate. The most soluble compounds are likely eluted up the TLC plate while the less soluble compounds with high affinity are less eluted (Kagan et al, 2014).

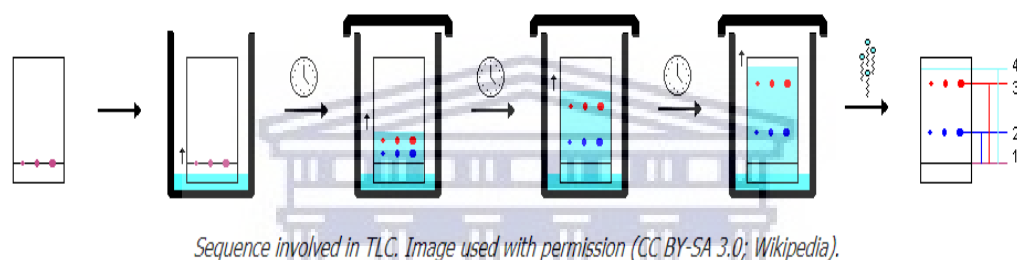


Figure 12: A typical Thin Layer Chromatography (TLC).

For thin-layer chromatographic analysis of the synthesized compound, pre-coated TLC plates of silica gel 60 F254 [Merck (Darmstadt; Germany)] were used. In this study TLC was used to identify active compounds after the separation process from column chromatography. It also allows the optimization of the solvent system for a given separation problem. The thin layer chromatography requires only small quantities of the compound (~ng) and is faster compared to column chromatography. To visualize the spots or bands after developing the TLC plates in a different solvent system, UV-Vis lamp of  $\lambda 254/\lambda 360 \text{ nm}$  was used.

### 4.3 Nuclear Magnetic Resonance (NMR)

To prepare samples for nuclear magnetic resonance (NMR), Deuterated chloroform ( $\text{CDCl}_3$ ) was used. Nuclear magnetic resonance (NMR) spectra were recorded at  $25^\circ\text{C}$  on a Bruker Avance III



HD 400 MHz NMR spectrometer (Germany) using a 5 mm BBO probe. The standard 1D and 2D NMR pulse sequences were used to acquire 1D and 2D data, respectively. The  $^1\text{H}$  ( $\delta H$ ) and  $^{13}\text{C}$  ( $\delta C$ ) chemical shifts were measured comparatively to  $\text{CDCl}_3$  signals in parts per million (ppm). In this work NMR will be used to determine the chemical structure of the unknown synthesized compound. Both  $^1\text{H}$ -NMR and  $^{13}\text{C}$ -NMR were used to evaluate the number of protons and carbons present in the unique compound.

#### 4.4 Synthesis of metformin and its analogues

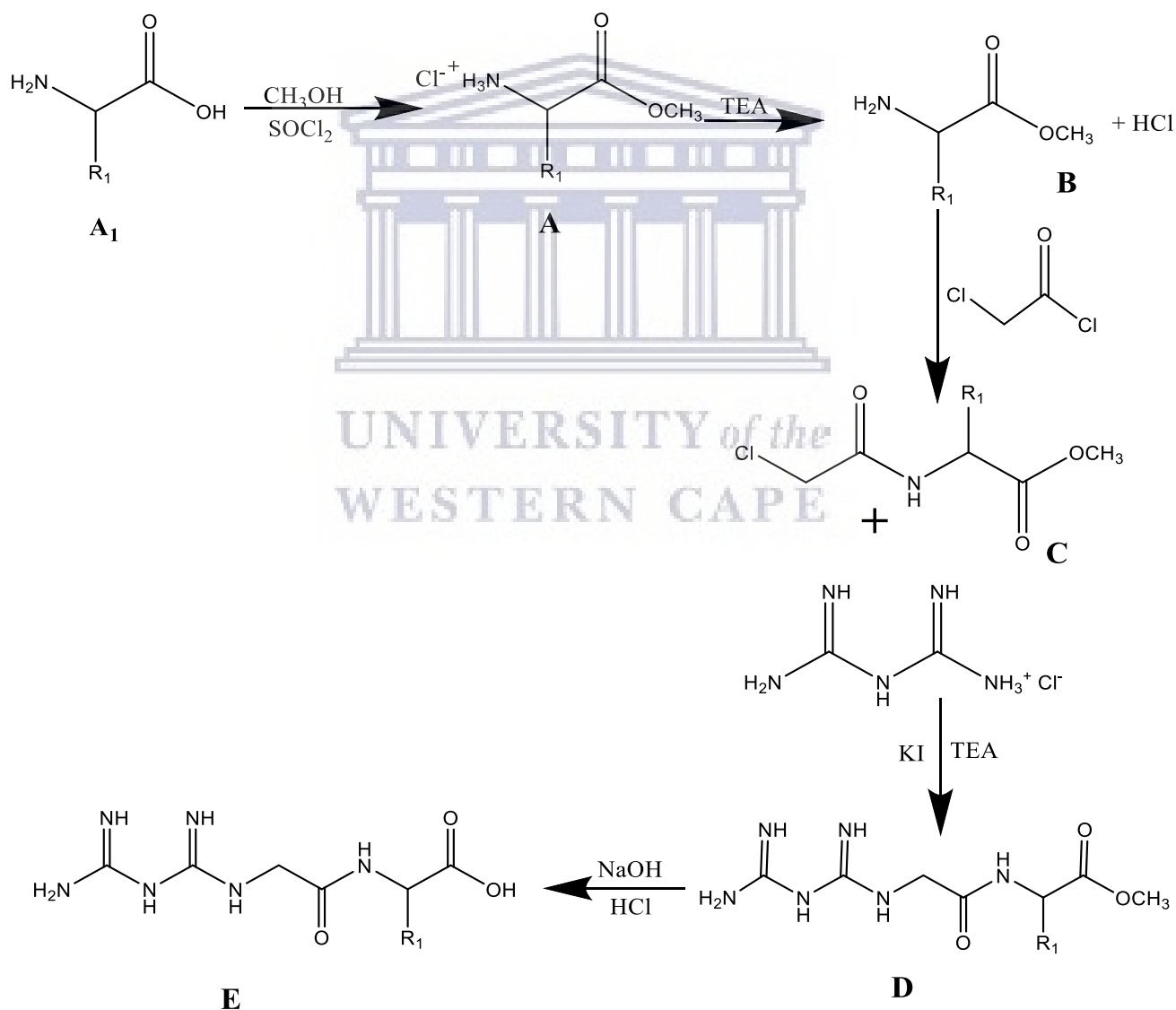
Previously reported studies demonstrate the synthesis of metformin by various procedures such as Schiff base, microwave, and chemical reaction. The final product of metformin is likely purified by crystallization process. Almost all these procedures produce an excellent yield of metformin in its purest form (Huttunen et al, 2009). Metformin was produced due to its excellent effect on glucose lowering ability and the low risk of hyperglycaemia in individuals suffering from type 2 diabetes mellitus. However, it has been recently discovered that metformin has a hydrophilic nature which results in its inability to passively diffuse through cell membranes. Interestingly, the incomplete absorption of metformin from the gastrointestinal tract is due to its relative low bioavailability, resulting in it being excreted unchanged in the urine (Cetin et al, 2015). Thus, prodrugs were designed by incorporating sulfenamide with nitrogen atom. Previously reported studies indicate the synthesized metformin prodrugs to have a 10% improvement in bioavailability compared to metformin (Huttunen et al, 2009). However, the designed derivatives were discovered to disrupt endothelial cell function and were pharmacologically inactive (Markowicz-piasecka, 2019). In this study the main purpose is to improve bioavailability of metformin by incorporating three amino acids (Table 1) through  $\text{R}_1$  following an organic synthetic route (**Scheme 1**). Previously reported studies indicate metformin analogues with improved bioavailability to be safer on lower doses and clinically accepted (Rojas et al, 2013). The above illustrated mechanism (**Scheme 1**) presents the full synthetic route for metformin analogues. However, the availability for the starting material (A) was limited hence synthesizing it was of interest. **Scheme 2** was proposed to synthesize 2-amino-3-methylbutanoic acid **A1** in certain conditions.

Table 1: Amino acids side chains

| Amino Acids | Structure |
|-------------|-----------|
| Valine      |           |
| Leucine     |           |
| Isoleucine  |           |

The multistep reaction for the synthesis of metformin analogues was conducted using four types reactions such as esterification, substitution, elimination, and amine nucleophilic substitution reaction. Esterification reaction is referred to as the chemical process of forming esters from carboxylic acids (Rathod et al, 2014). Esters are compounds of the chemical structure R-COOR', R and R' are either alkyl or aryl groups. Substitution reaction (also known as single displacement reaction) is referred to as a chemical reaction during which one functional group in a chemical compound is substituted by another functional group (Dey, 2015). In chemistry, substitution reactions are of prime importance. Substitution reactions in chemistry are classified either as electrophilic or nucleophilic depending upon the reagent involved. In this work electrophilic substitution reaction was likely used in Scheme 2, for the preparation of  $\alpha$ -bromoisovaleric acid **G** where bromine (electron leaving specie) was first substituted. Thereafter, bromine was eliminated following a one-step reaction. An elimination reaction is a type of organic reaction in which two substituents are removed from a molecule in either a one or two-step mechanism (Ouellette et al, 2018), The E2 reaction is known as the one-step mechanism whereas the E1 reaction is the two-step mechanism. The numbers refer not to the number of steps in the mechanism, but rather to the kinetics of the reaction: E2 is bimolecular (second order) while E1 is unimolecular (first-order). Subsequently, the bromine was substituted with an amino group through amine nucleophilic

substitution reaction. Electrophilic ammoniation is a chemical process involving the formation of a carbon–nitrogen bond through the reaction of a nucleophilic carbanion with an electrophilic source of nitrogen. Electrophilic ammoniation reactions can be classified as either additions or substitutions (Kromann et al, 2018). Although the resulting product is not always an amine, these reactions are unified by the formation of a carbon–nitrogen bond and the use of an electrophilic aminating agent. The final product was purified through the process of crystallization. Purification is the physical or chemical process of removing contaminants from a compound. The above-mentioned types of reactions are applied to the mechanisms below.



**Scheme 1:** Proposed synthetic access of metformin and its analogue E.

The detailed step for the proposed synthetic route of metformin analogues as follows: -

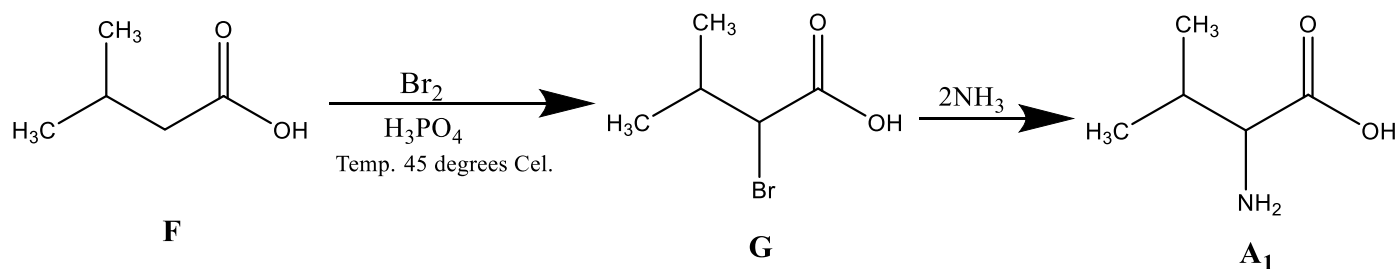
**Step A:** Compound **A**<sub>1</sub> is treated with methanol (CH<sub>3</sub>OH) and thionyl chloride (SOCl<sub>2</sub>) and undergoes esterification reaction to form a methyl ester hydrochloride (**A**).

**Step B:** Dehalogenation reaction occurs in methyl ester hydrochloride **A** in the presence of a base catalyst, triethylamine (TEA) (Li et al, 2008) to form amino acid methyl ester **B** and hydrochloric acid.

**Step C:** The addition reaction of metformin with amino acid ester-chloroacetyl chloride **C** is demonstrated in **Scheme 1**. In this step, the amine group attacks the C-atom of the acid halide and generate a tetrahedral intermediate, where O (oxygen) is negatively charged and N (nitrogen) is positively charged then Cl (chlorine) becomes a good leaving group resulting in metformin-aminomethyl ester **D**.

**Step D:** The metformin-aminomethyl ester **D**, is treated with sodium hydroxide (NaOH) and hydrochloric acid (HCl) forming metformin-amino acid **E**.

Compound **A**<sub>1</sub> in **Scheme 1** was not readily available, therefore a three-step scheme (**Scheme 2**) was proposed for its preparation. The initial step in the synthesis of  $\alpha$ -bromoisovaleric acid **G** was to prepare 2-amino-3-methylbutanoic acid **A**<sub>1</sub>, using the substitution reaction. The  $\alpha$ -bromoisovaleric acid is prepared through the bromination reaction at alpha-carbon of the isovaleric acid compound **F**. A yield of 92.1% was obtained from recrystallization of the yellow-orange  $\alpha$ -bromoisovaleric acid **G**.



**Scheme 2:** Synthetic route for 2-Amino-3-methylbutanoic acid **A<sub>1</sub>**.

#### 4.4.1 Column Chromatography of alpha-bromoisovaleric acid

Chromatography is a spectroscopic technique widely used for separation of impurities which depends on the differential interaction of molecules between a stationary phase and a mobile phase (Chakravarti, 2016). In this study, column chromatography was used to purify and separate components of the synthesized mixture for qualitative and quantitative analysis (Coskun, 2016). Consequently, a flash column liquid chromatography which is referred to as a quick and (usually) easy way to separate complex mixtures of synthesized compound was utilized (Figure 13). The mobile phase is hexane and ethyl acetate, and the stationary phase is silica gel. The crude compound of 2-Bromo-3-methylbutanoic acid (9.2 g) (Figure 14) was applied to a silica gel column and eluted with Hex: EtOAc gradient mixtures of increasing polarity as shown in Table 1. Fractionation of solutes occurs as a result of differential migration through a closed tube of stationary phase, and a mobile phase which can be monitored while the separation is in progress.

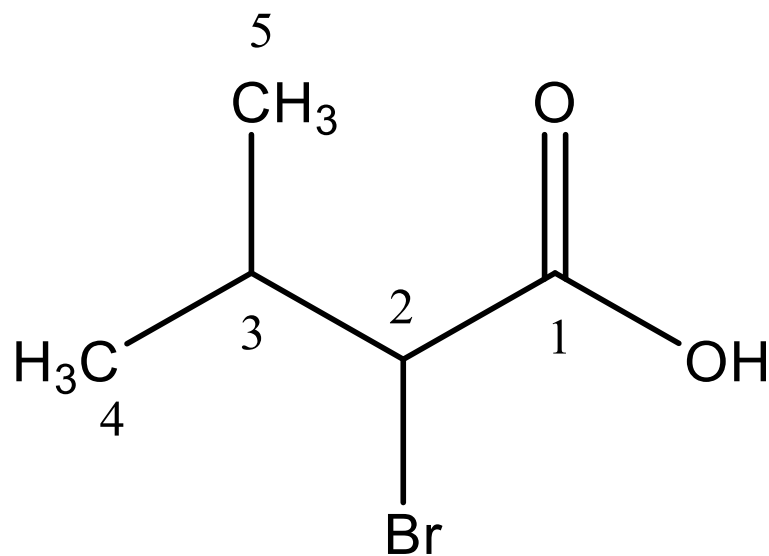


Figure 13:  $\alpha$ - bromoisovaleric acid

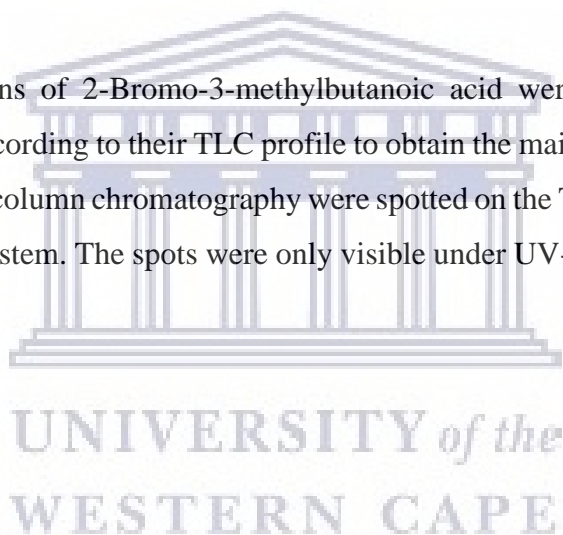


Figure 14: Flash Column for the crude product ( $\alpha$ -bromoisovaleric acid) with the solvent system of 9:1 (Hex: EtOAc).

Table 2: Fractionation of 2-Bromo-3-methylbutanoic acid (9.0g)

| Solvent System    | Volume (L) | Fractions   |
|-------------------|------------|---|
| <i>Hex: EtOAc</i> |            |   |
| 90:10             | 1          | 1-20  |
| 80:20             | 2          | 20-24, 93-128                                     |
| 70:30             | 1          | Reaction mixture (RM) and starting material (SM). |
| 60:40             | 1          | 25-40   |
| 50:50             | 2          | 129-187   |
| 0:100             | 1          | 188-200   |

Approximately 200 fractions of 2-Bromo-3-methylbutanoic acid were collected. Comparable fractions were combined according to their TLC profile to obtain the main fractions (Table 2). The fractions obtained from the column chromatography were spotted on the TLC plates and developed on a Hex: EtOAc solvent system. The spots were only visible under UV-Vis light at a wavelength of 254 nm.



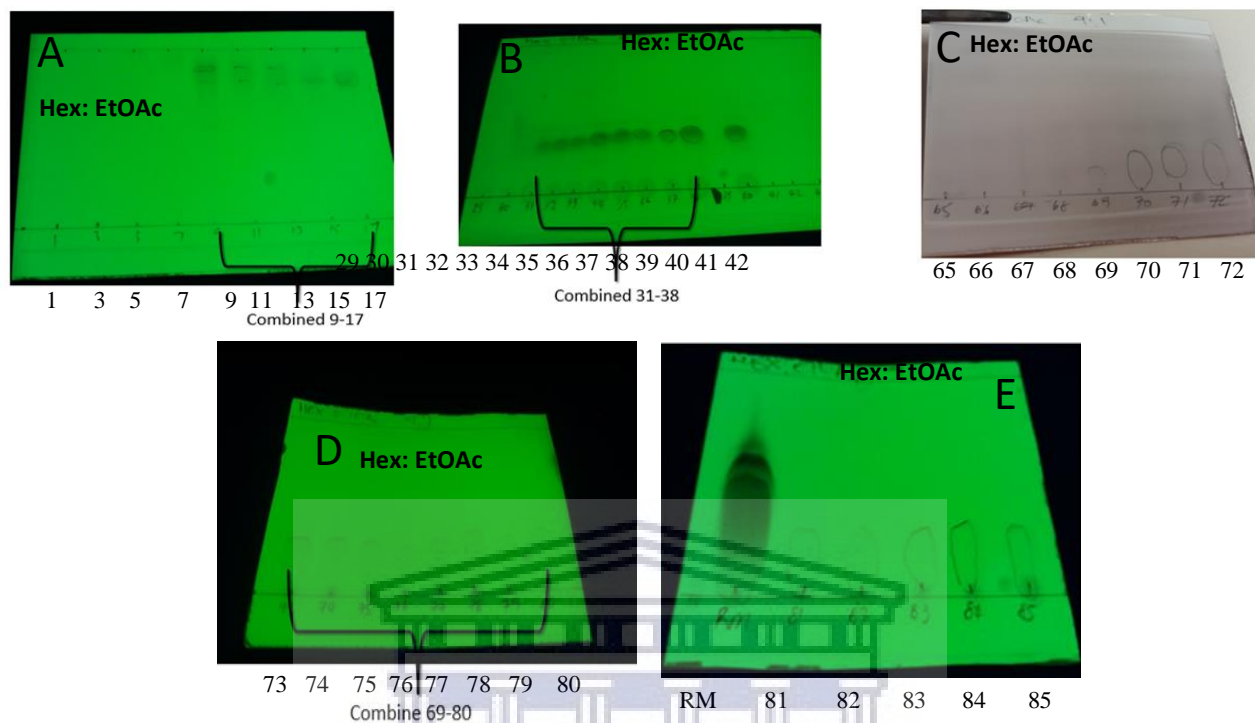


Figure 15: Thin layer chromatograms of fractions obtained from column chromatogram of alpha-bromoisovaleric acid.

**Adsorbent:** Silica gel

**Solvent System:** **A** [Hex: EtOAc (9:1)]; **B** [Hex: EtOAc (6:4)]; **C** [Hex: EtOAc (8:2)]; **D** [Hex: EtOAc (9:1)]; [Hex: EtOAc(8:2)]

Fractions with similar spots were pooled together for further characterization. Fractions from 86 to 200 were not evaluated on TLC plates due to their inactivity under UV-Vis.



Table 3: Combination of main fractions of  $\alpha$ -bromoisovaleric acid.

| Combined fractions | Mass (g) |
|--------------------|----------|
| 1-7                | 1.126    |
| 9-17               | 3.5445   |
| 29-30              | 0.6296   |
| 31-38              | 0.2145   |
| 39-42              | 0.0912   |
| 43-64              | -        |
| 65-68              | 0.3977   |
| 69-80              | 2.8950   |
| 81-85              | 0.0385   |
| 86-200             | -        |
| Total              | 8.937    |

The total mass of the sub-fractions were calculated to be 8.937 g with a percentage yield of 89.37 %. One-dimensional NMR experiments are essential in determining the resonance frequency of each  $^1\text{H}$  or  $^{13}\text{C}$  nucleus in the molecule, hence,  $^1\text{H}$  and  $^{13}\text{C}$  NMR experiments were both employed highly in interpreting the structure of the synthesized compound in the current study (Pineiro et al, 2012). The combined fractions from the column chromatography were subjected to NMR spectroscopy to determine the molecular structure and purity of the obtained active compound. Consequently, NMR confirmed the first two fractions to be pure compounds of alpha-bromoisovaleric acid (Figure 13). Additionally, the chemical shifts acquired provided a significant information about the nature and number of protons and carbons in the compound of interest. The previously reported data was utilized to substantiate the recorded chemical shifts (Pineiro et al, 2012).

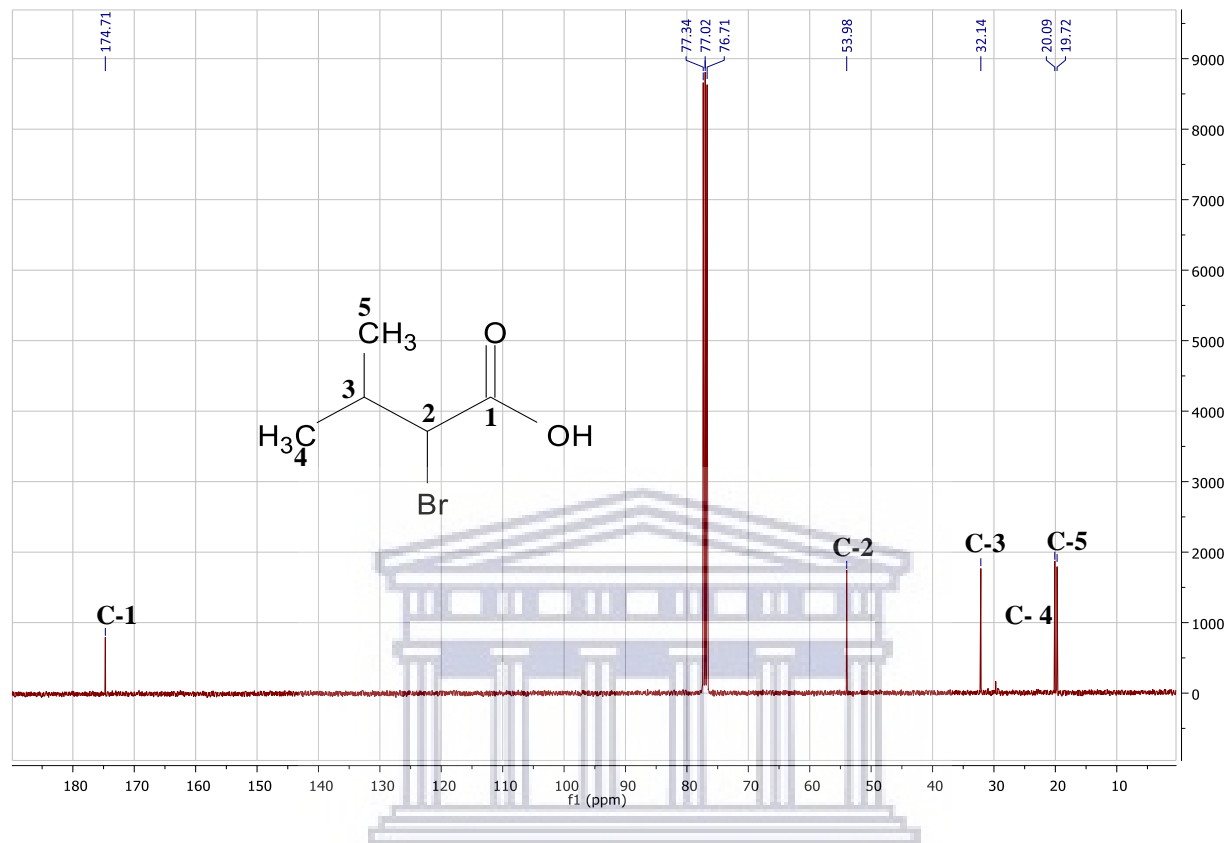


Figure 16: <sup>13</sup>C NMR of α-bromoisovaleric acid G in CDCl<sub>3</sub>.

The formation of α-bromoisovaleric acid G was confirmed by <sup>13</sup>C-NMR and <sup>1</sup>H-NMR. The examination of α-bromoisovaleric acid G by <sup>13</sup>C-NMR indicated the presence of five carbons [ $\delta_C$ = 174.74 (C-1), 53.93 (C-2), 32.4 (C-3), 20.09 (C-4), 19.72 (C-5)]. The <sup>13</sup>C spectrum confirms the presence of five carbon nuclei. Carbon-1 signal was observed at a higher chemical shift of 174.74 ppm and that is due to the presence of a carbonyl group (C=O). The chemical shift of C-2 was observed at 53.98 ppm and that is attributed to carbon being attached to a halide (C-Br). Carbon-3 was observed to have a chemical shift of 32.14 ppm, while C-4 and C-5 were observed at 20.09 ppm and 19.72 ppm, respectively. The tertiary carbon (C-3) is likely to have higher chemical shift than primary carbons (C-4 and C-5). The other carbon resonances did not de-shield as anticipated since nitrogen is more electronegative than bromine. Further analysis was conducted to confirm the formation of 2-amino-3-methylbutanoic acid A<sub>1</sub>.

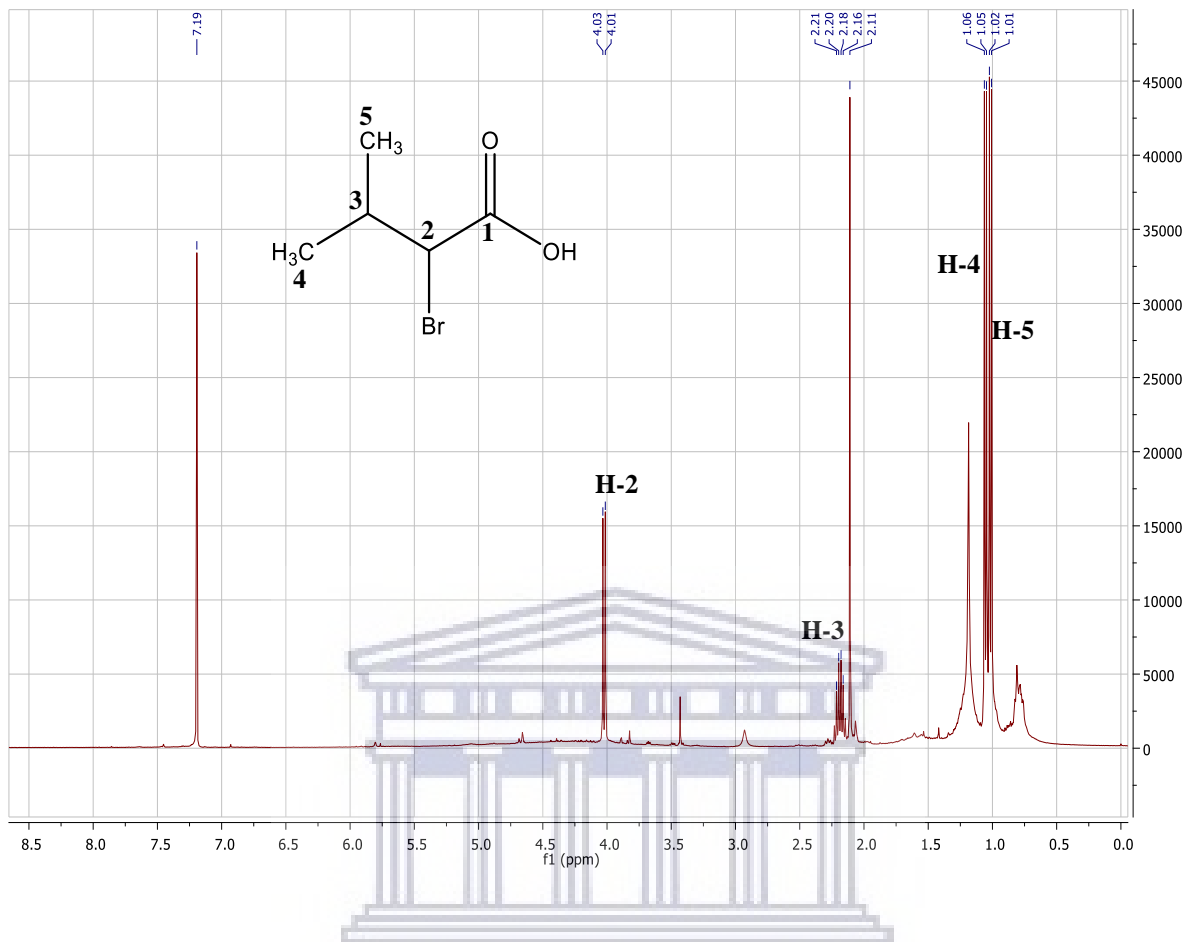


Figure 17: <sup>1</sup>H NMR of α-bromoisovaleric acid G in CDCl<sub>3</sub>.

The <sup>1</sup>H NMR spectrum analysis (Figure 17), reveals 5 signals. Two doublets result from coupling of the 4-H proton (1.12 ppm) and 5-H proton (1.12 ppm) nuclei with each. The observed multiplet spectra at 3-H proton (2.25 ppm) is attributed to two methyl protons attached to a tertiary carbon atom. The proximity of bromine to the 2-H proton leads to de-shielding of the 2-H (4.09) proton compared to the 3-H (2.25 ppm) proton. The de-shielded spectra (H-1) which appear at 7.25 ppm are attributed to the solvent system which deuterated chloroform (CDCl<sub>3</sub>). Deuterated chloroform is a protic deuterated solvent and OH protons are likely to exchange with the deuterium, thus OH proton peak was not observed in the spectrum.

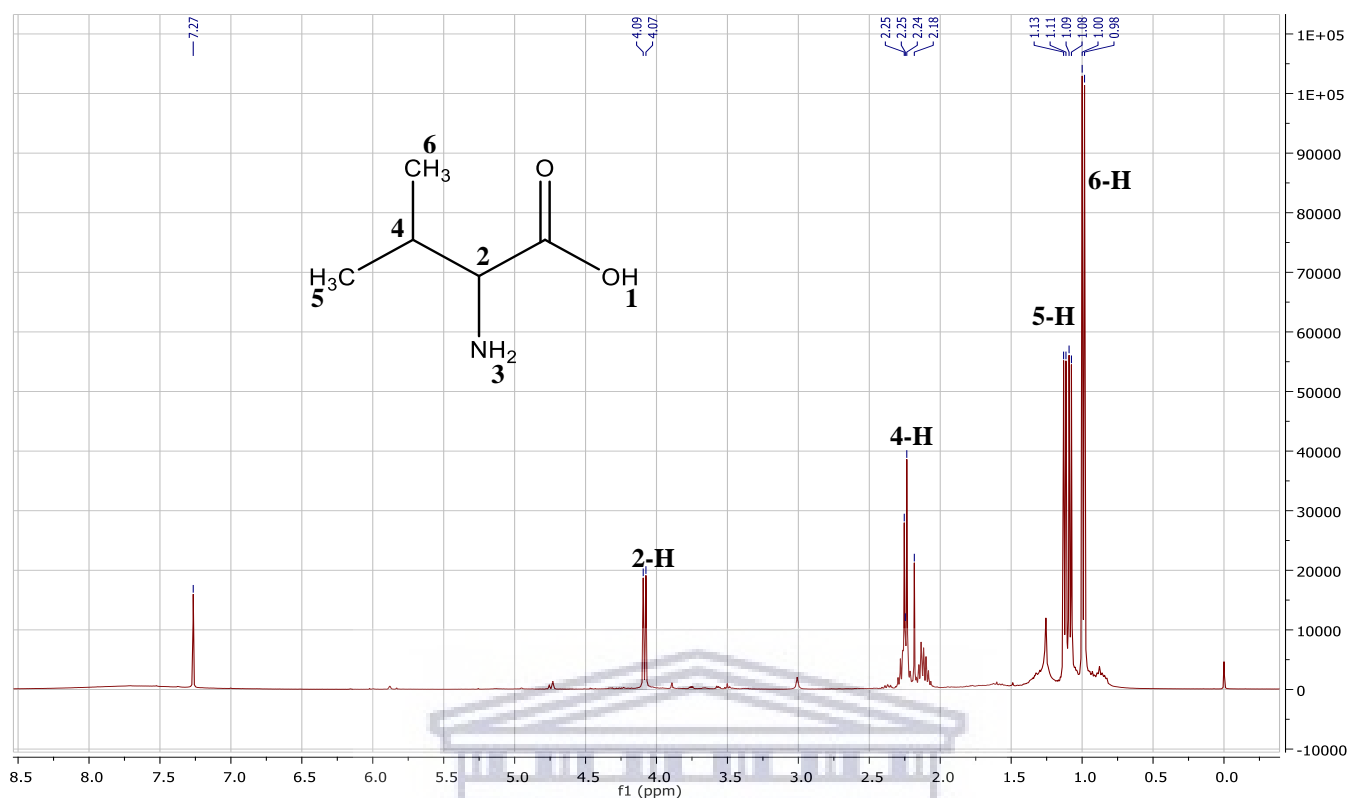


Figure 18: <sup>1</sup>H NMR of 2-amino-3-methylbutanoic acid **G** in CDCl<sub>3</sub>.

Similarly, the <sup>1</sup>H NMR data for the 2-amino-3-methylbutanoic acid **A<sub>1</sub>** permits the stereochemistry to be recognized. Compared to the proton NMR of **G**, 5-H proton (1.12 ppm) proton in **A<sub>1</sub>** indicated a less intense signal than 6-H proton (1.10 ppm), whereas in **G** both protons are intense and that may be due to the presence of NH<sub>2</sub>. The spectral data of 2-amino-3-methylbutanoic acid **A<sub>1</sub>** agrees with the previously reported study (Kohda et al, 1987). The OH proton was expected to be observed at 12.39 ppm; however, the proton was not observed and that may be due to the use of protic deuterated solvent (CDCl<sub>3</sub>).

The chemical modification of metformin by incorporating amino acids through the R<sub>1</sub> into forming metformin analogues was attempted following a proposed mechanism in **Scheme 1**. The α - brominevaleryl was prepared by bromination at α-position in one pot reaction with a percentage yield of 92.1%. The chromatographic techniques such as column chromatography (CC), thin layer chromatography (TLC) were used to purify the synthesised product and nuclear magnetic resonance (NMR) was for structural elucidation. The obtained product was characterized using

chromatographic techniques such as column chromatography (CC) for purification of the compound, thin layer chromatography (TLC) for separation and nuclear magnetic resonance (NMR) for structural elucidation. The percentage yield of  $\alpha$ -brominevaleryl **G** after chromatographic studies was obtained to be 89.37 %. The ammoniation of  $\alpha$ -brominevaleryl as illustrated in **Scheme 2** (B) resulted in small yields of DL-norvaline. Both proton and carbon nuclear magnetic resonance (NMR) suggested the elucidated structure to be of DL-norvaline (Qian et al, 2009). The DL-norvaline produced is a good starting point for the design and synthesis of novel analogues of metformin. Consequently, the small yields produced from its preparation made it impossible to complete the synthesis of metformin following **Scheme 1**. The experimental procedure for the preparation of novel analogues of metformin was observed to be a laborious expensive exercise and time consuming. Notwithstanding the incomplete organic synthesis of metformin derivatives, the second aim of this study was pursued, which is to investigate the electrochemical behaviour of metformin and its synthetic intermediates in an aqueous medium. Hence, the electrochemical behaviour of metformin was evaluated using a commercial drug. Previously reported studies show metformin to have similar structural characteristics with its analogues (Mahdi et al, 2017). The redox reaction of metformin on a modified platform indicated oxidation of amino groups on an anodic peak and reduction of N-carbonyl-guanidine on cathodic peak. The amino groups observed on anodic peak are comparable with amino groups in 2-amino-3-methylbutanoic acid. Thus, 2-amino-3-methylbutanoic acid is regarded as the good starting point for the synthesis of metformin analogues.

# CHAPTER 5

*This chapter presents the preparation of electrolyte and metformin solutions it also provides with the preparation of copper nanomaterials and electrochemical synthesis of a polymer. Moreover, characterization of metformin solution, polymer, and copper nanoparticles this includes microscopic, spectroscopic, and electrochemical characterization techniques.*

## 5.1 Materials

Glucophage 500mg tablets, Hydrochloric acid (32%) (HCl), Copper salt (Copper sulphate pentahydrate ( $\text{CuSO}_4 \cdot 5\text{H}_2\text{O}$ ) (98%), Sodium Borohydride ( $\text{NaBH}_4$ ), Sodium hydroxide (NaOH), polyethylene glycol (6000) (PEG) were purchased from Sigma Aldrich and Kimix. All the chemicals mentioned above were of analytical grade and were not purified before use. In preparation of all solutions, deionized water purified by a Milli-TQM system (Millipore) was made in use as reagent water. All the chemicals were analytical grade and used as purchased without further purification. Copper (II) sulphate pentahydrate salt,  $\text{CuSO}_4 \cdot 5\text{H}_2\text{O}$ , of 98% purity (Merck), was dissolved in high purity water. Polyethene glycol 6000 (PEG 6000—Merck) was used as the capping agent. Sodium borohydride ( $\text{NaBH}_4$ -Reagent Plus) 99% was used as reducing agent.

## 5.2 Methods

### 5.2.1 Preparation of HCl solution

To prepare 0.1 M Hydrochloric acid (HCl) solution, 4,5 mL of HCl (32%) was diluted with deionized water in a 500mL volumetric flask.

### 5.2.2 Preparation of metformin solution

Five tablets of Glucophage 500 mg were weighed and the average mass per tablet was determined, then these tablets were powdered. The powdered tablets were accurately weighed and transferred

into a 100 mL volumetric flask which contains 70 mL of distilled water. The prepared sample solution was sonicated for about 30 min and the volume of distilled water was made to 100 mL. The active compound of metformin in solution was discovered to have impurities and insoluble excipients which are separated through the process of filtration before the experiments were carried out. Aliquots of the drug solution were introduced into the electrolytic cell and the experiments were conducted.

### 5.2.3 Electropolymerization of pyrrole

The pyrrole monomer was triple distilled before use. Subsequently, electrochemical polymerization of pyrrole was carried out in a three-electrode system with pyrrole monomer and 0.1 M HCl as the supporting electrolyte.

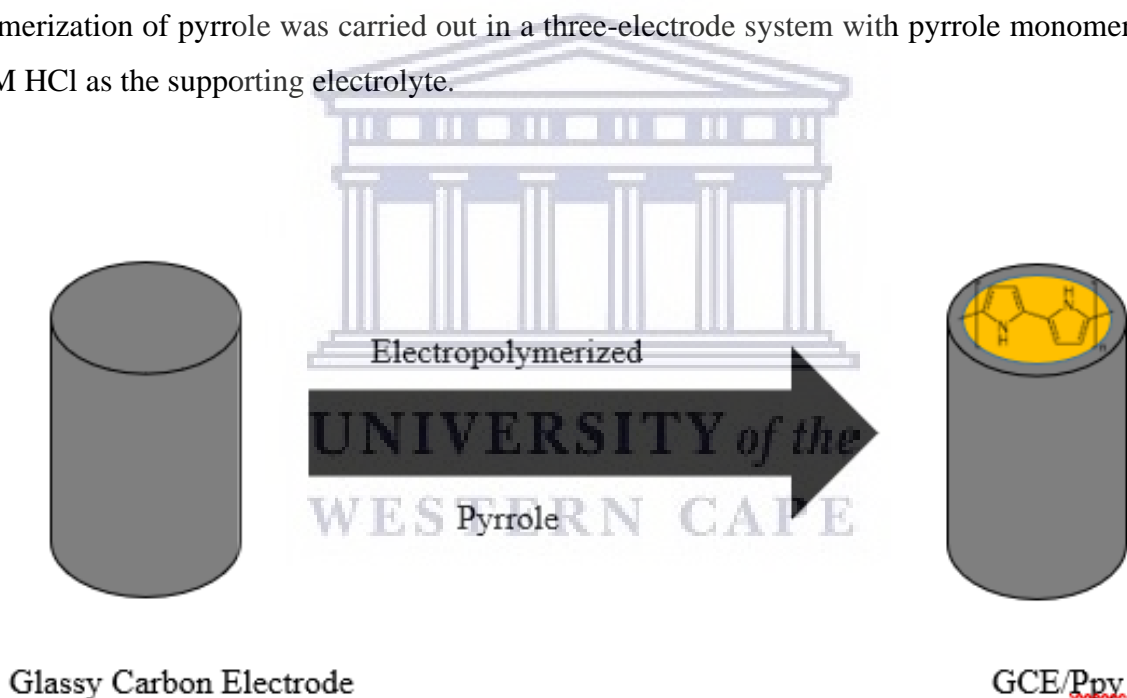


Figure 19: Electrochemical synthesis of polypyrrole (PPy) thin film.

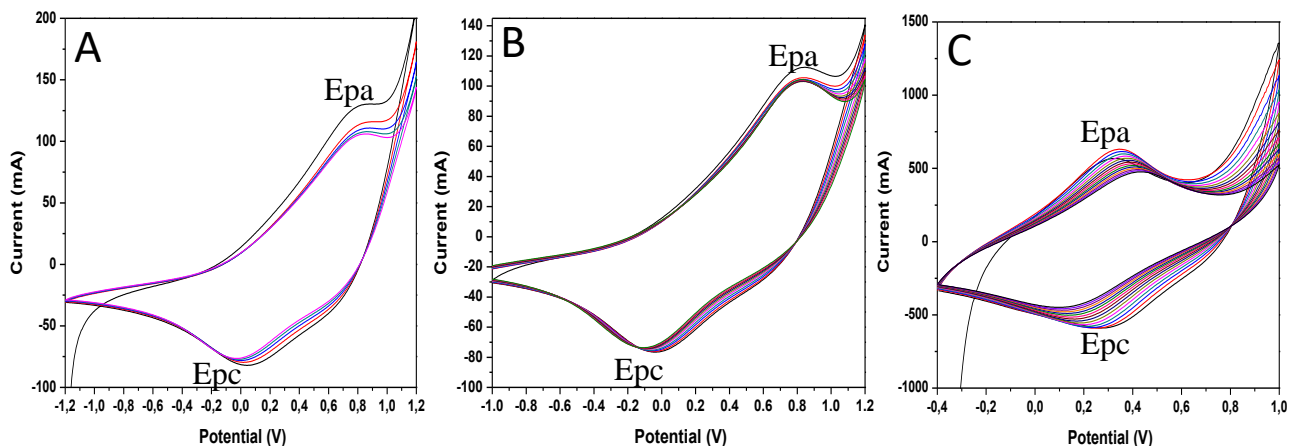


Figure 20: Electro polymerization of polypyrrole at glassy electrode carbon electrode glassy (GCE) for (A) 5 Cycles, (B) 10 cycles and (C) 15 cycles in a 0,1M HCl at 50 mV/s.

The above diagram demonstrate three different types of polymer films were prepared by changing the number of cycles from 5 to 10 and 15 for each film produced (Figure 20). In graph A&B, polymerisation was performed in the potential range of -1.0 to 1.2 V at 50 mV/s, as illustrated on Figure 20. However, the polymerisation in graph C was performed in the potential range of -0.4 to 1.0 V, since Epa and Epc peaks were well defined in this range compared to the range used in graph A&B. As the number of cyclic voltammetric cycles increases the voltammogram polymerisation current increases and that confirmed a conductive nature of the polymer. Figure 20 (B & C) shows that the peak current  $I_p$  of the anodic peak decreases significantly upon continued cycling as the film become thicker. An increase in current response as the number of cycle increases, confirmed the conductive nature of the polymer. Reported studies agree with cyclic voltammogram of polypyrrole indicated in figure 20 with Epa and Epc attributed to doping and un-doping processes of the thin film of polymer (Bozzini, et al, 2017). As the number of cyclic voltammetric cycles increases the voltammogram (Figure 20, A) polymerisation current increased as well and that confirmed a conductive nature of the polymer.



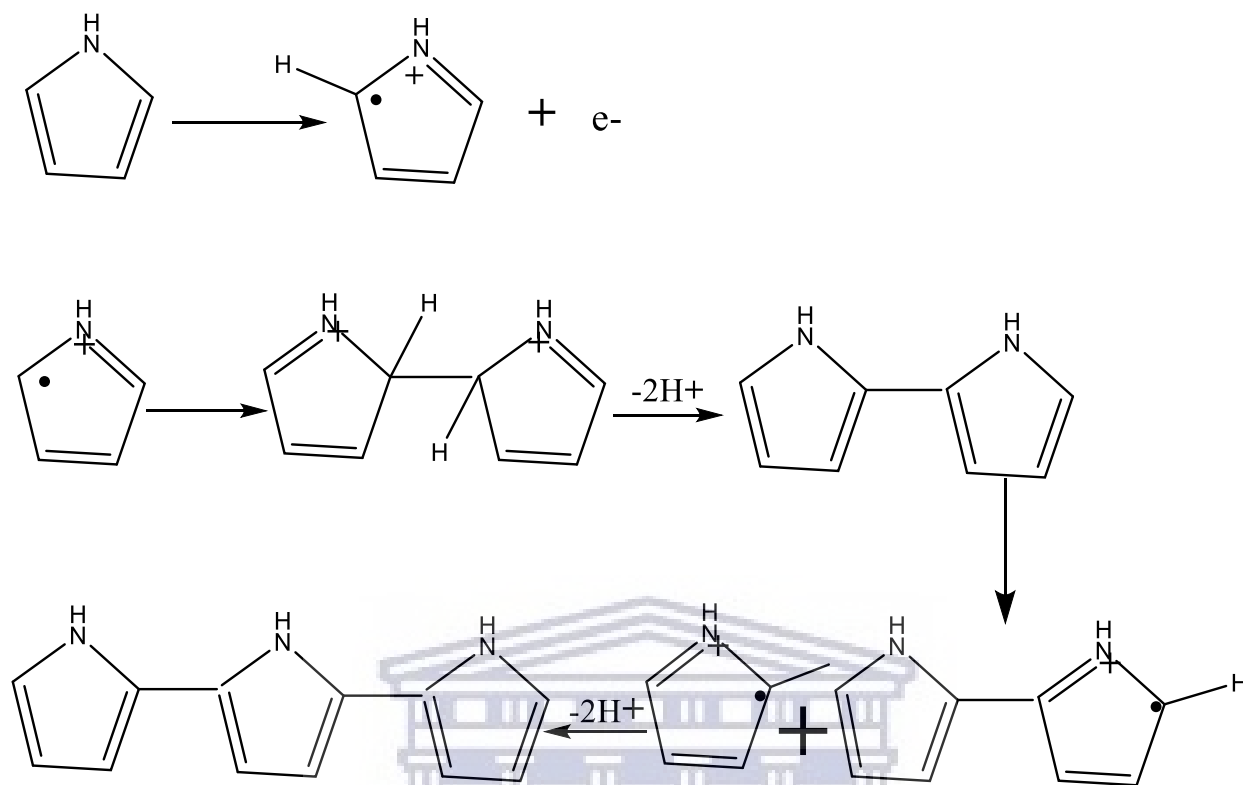


Figure 21: Electrochemical synthesis of polypyrrole from pyrrole monomer.

The pyrrole monomer on the first oxidative sweep oxidizes by losing an electron forming a radical cation of the pyrrole (Figure 21). The radical undergoes electronic rearrangement during the reverse sweep. Throughout the subsequent cycles more radicals are produced, and they interact with each other forming a dimer radical cation. The further reaction of the formed dimer radical cations with monomer molecule produces the desired polymer and that is indicated by the polymer growth. To control the thickness and morphology of the film the type of solvent, type of electrode material, applied potential, polymerization time and the number of cycles must be monitored. The number of cycles influence the stability of the polymer film as well as the thickness of the film. The film thickness must be carefully controlled to maximize the redox ability of the polymer film and in this work the film thickness was obtained after 10 cycles was used to modify the electrode surface in a reproducible manner.

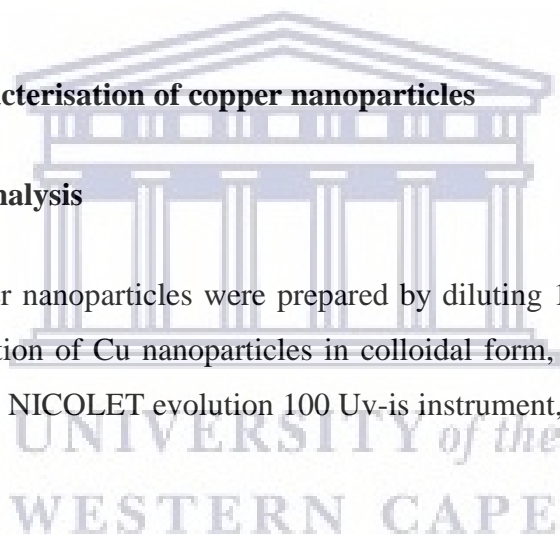
#### ***5.2.4 Synthesis of Copper nanoparticles***

Preparation scheme for copper nanoparticles starts with dissolving copper (II) sulphate pentahydrate salt,  $\text{CuSO}_4 \cdot 5\text{H}_2\text{O}$  (0.01 M, 0.25 g), in deionized water to obtain a blue solution. Polyethylene glycol (PEG) 6000 (0.04 M, 18 g) was dissolved in water and added to the aqueous solution containing the copper salt while vigorously stirring. Polyethene glycol in the synthesis of nanomaterial works by limiting the agglomeration of nuclei from forming particle size out of nanometric scale. In this step, the solution changed from blue to white. In the third step, sodium borohydride which was used as reducing agent (0.001 M, 0.004g) was added to the synthesis solution. The stirring was sustained for 1 hour 30 minutes at room temperature. Spectrochemical and microscopic characterizations were used to confirm the synthesised copper nanomaterial.

### **5.3 Spectrochemical characterisation of copper nanoparticles**

#### **5.3.1 Ultraviolet-Visible analysis**

For Uv-Vis analysis, copper nanoparticles were prepared by diluting 10  $\mu\text{L}$  of the sample with distilled water. The absorption of Cu nanoparticles in colloidal form, as soon as possible after synthesis was analysed on a NICOLET evolution 100 Uv-is instrument, in a scanning mode from 400 to 800 nm.



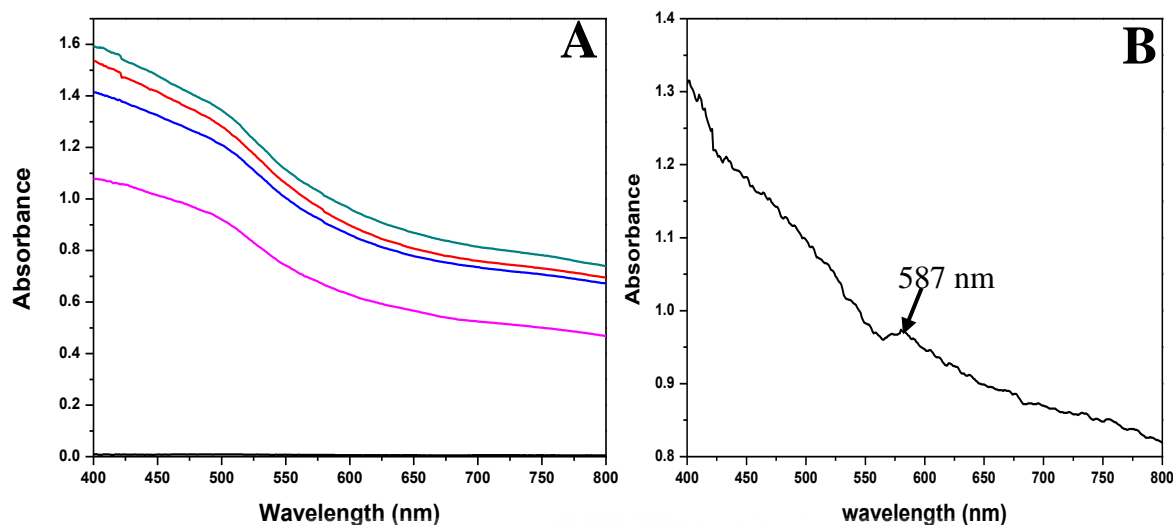


Figure 22:UV-Visible spectra of copper nanoparticles synthesised by chemical reduction method (A) immediately after synthesis (B) 24 hours after synthesis.

The colloidal dispersion of nanoparticles displays an absorption band in the UV–Vis region. This is because of the excitation of Plasmon resonance or interband transition and is a distinctive property of a metallic nature of nanoparticles (Suramwar et al, 2011). Figure 22 shows the absorption spectrum of the synthesized copper nanoparticles. Figure 22, A shows the absorption spectra of copper nanomaterial after synthesis while Figure 22, B correspond to the absorption spectra of copper nanoparticles, 24 hours after the synthesis. In this work, the distinctive absorption peak of the synthesized copper nanoparticles with the size of 51 nm was observed at 587 nm (Figure 22 B). In the studies conducted by Sierra-Ávila and Suramwar, the absorption peak of copper nanoparticles was observed at 566 nm and 590 nm respectively, and that is in agreement with the work in this study. Moreover, Sierra-Ávila revealed the shape of the nanoparticles to be spherical which also agrees with work in this study (which is confirmed by SAXS) (Sierra-Ávila et al, 2015). The size of copper nanoparticles was further confirmed by microscopic techniques. The chemical composition of nanoparticles was evaluated by fourier transformation infrared.

### 5.3.2 Fourier Transform Infrared

All synthesised copper nanoparticles samples were characterised by fourier transform infrared (FTIR) by injecting the solution into FTIR cell holder and were recorded on a spectrum II Perkin-Elmer Fourier-transform Infrared (FTIR) Spectrometer (Perkin-Elmer, Boston, Massachusetts) was used to study the structure of synthesized materials between  $500\text{ cm}^{-1}$  and  $4000\text{ cm}^{-1}$ .

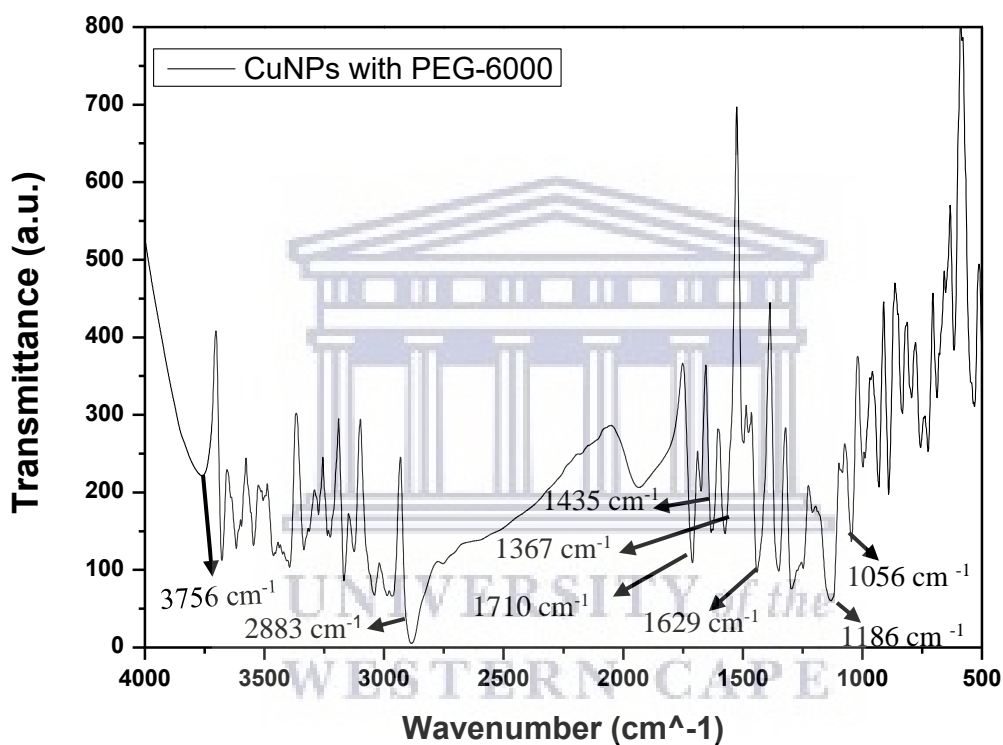


Figure 23: FTIR Spectrum of copper nanoparticles.

The FTIR spectrum of copper nanoparticles in the range from  $500$  to  $4000\text{ cm}^{-1}$  is shown in figure 23. The FTIR analysis was used to determine the functional organic groups in the surface of the nanoparticles synthesised (Burlibasa et al, 2020). Several absorption peaks were observed as presented on the above spectra. The absorption at distinct frequencies is related to various modes of interatomic bond vibration (stretching or bending) and degrees of hydrogen bonding. Throughout the analysis of Cu nanomaterial, the broad and strong band were observed at  $3752.00$

cm<sup>-1</sup> which were attributed to O–H (hydroxyl) stretching vibrations on the surface of the nanomaterials (Moniri et al, 2017). Hydroxyl group were observed to be the most intense and easily recognizable brands in the spectra of CuNP's. The precise position of the hydroxyl group depends on the strength of hydrogen bonds. In general, the width of the band is due to the degree of hydrogen bonding with neighbouring OH groups and alteration of intermolecular interaction strength present in the sample. The assignment of peaks for the FTIR spectrum of copper nanoparticles is illustrated in the Table 5.

Table 5: Fourier Transform Infrared peak assignment for copper nanoparticles.

| Assignment       | Frequency (cm <sup>-1</sup> ) |
|------------------|-------------------------------|
| C-O Stretching   | 1039                          |
| C-O-H stretching | 1186                          |
| C-H Bending      | 1367                          |
| C-H Bending      | 1447                          |
| O-H Bending      | 1574                          |
| C-H Stretching   | 2892                          |
| O-H stretching   | 3756                          |

The interaction of synthesised copper nanoparticles obtained with PEG was confirmed by the FTIR spectra in Figure 23. Fourier transform infrared analysis was used to determine the functional groups in the surface of the nanoparticles synthesised. The two bands at 1039 cm<sup>-1</sup> and 1186 cm<sup>-1</sup> are attributed to C-O and C-O-H stretching at the surface of copper nanoparticle in PEG. The aliphatic C-H bending at 1367 cm<sup>-1</sup> and 1447 cm<sup>-1</sup> were due to C-H vibrations. The absorption peak observed at 2883 cm<sup>-1</sup> is attributed to the C-H stretching. The broad and strong band at a frequency of 3756 cm<sup>-1</sup> is attributed to O–H (hydroxyl) stretching vibrations on the surface of copper nanoparticles. The absorption peaks on the spectra on Figure 23 indicated a successful synthesis of copper nanoparticle, however, further characterization was made to confirm the size of the nanoparticles.

## 5.4 Microscopic characterisation of copper nanoparticles

### 5.4.1 Scanning Electron Microscopy (SEM) analysis

Copper nanoparticles were drop coated on the surface of a glassy electrode a day before the experiment. The SEM analysis was performed on a Phenom-world desktop SEM, thermo fisher scientific phenom world coupled with Energy Dispersive X-ray analyser.



Figure 24: SEM image of copper nanoparticles.

The surface morphology of the nanomaterial was studied by SEM and a cluster CuNP with a large surface area was observed. The agglomeration of nanoparticles shown in Figure 24 could be nanoparticles experiencing induced magnetism, which more often than not results in agglomerations. The chemical composition of copper nanoparticles was further investigated by EDS.

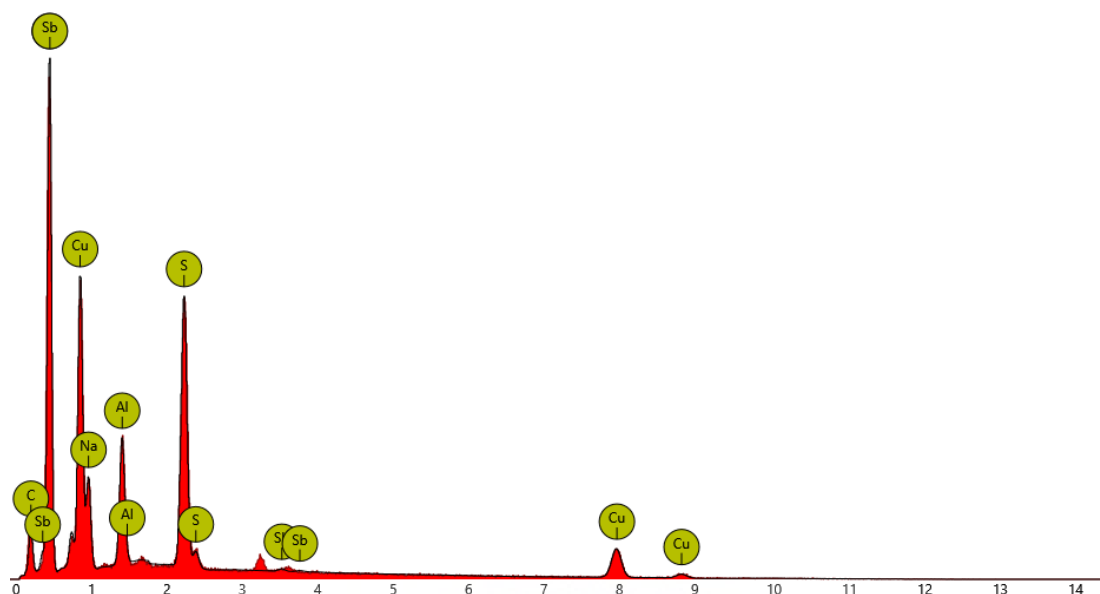


Figure 25:EDS of copper nanoparticles.

Figure 25 show the EDS spectrum of copper nanoparticles prepared with a sodium borohydride. The EDS spectra figure 20 shows the presence of a metallic copper along with a trace amounts of other elements such as S, Sb, Al, and C which are attributed to contamination. The presence of Na can be attributed to the presence of sodium borohydride in the nanoparticles. Copper nanoparticles were further characterised by transmission electron microscopy (TEM) to confirm the size and evaluate the shape of the nanomaterials.

Table 6: Percentage (%) of elements present in copper nanoparticles.

| Element Number | Element Symbol | Element Name | Atomic Concentration | Weight Concentration |
|----------------|----------------|--------------|----------------------|----------------------|
| 29             | Cu             | Copper       | 6.45                 | 20.06                |
| 6              | C              | Carbon       | 23.10                | 13.59                |
| 16             | S              | Sulfur       | 8.10                 | 12.72                |
| 11             | Na             | Sodium       | 5.31                 | 5.98                 |
| 13             | Al             | Aluminium    | 4.33                 | 5.72                 |
| 51             | Sb             | Antimony     | 0.12                 | 0.71                 |

### 5.4.2 Transmission Electron Microscopy (TEM)

Copper nanoparticles solution was characterised by transmission electron microscopy (TEM). Transmission electron microscopy (TEM) is a high-resolution tool which is able to produce images at the nanoscale. TEM analysis was performed with a FEI Tecnai G2 F20X-Twin MAT 200 kV Field Emission Transmission Electron Microscope (Eindhoven, Netherlands) with Energy Dispersive X-ray Spectrometry (EDS) and Selected Area Electron Diffraction (SAED) capabilities.

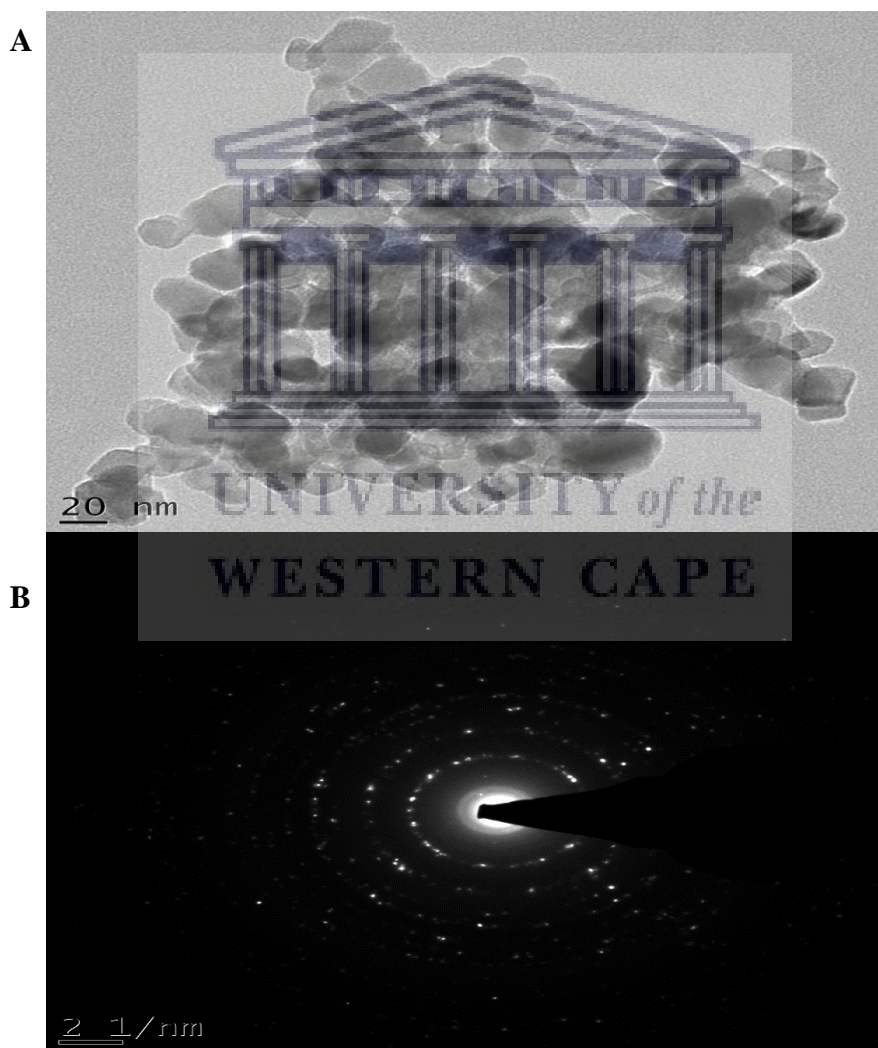


Figure 26: TEM (A) and SAED (B) images for copper nanoparticles.



The size and shape of colloidal Cu nanoparticles were confirmed through TEM analysis. Figure 26 (A) illustrates the TEM image of Cu colloidal NPs on the scale of 20 nm. These nanoparticles are spherical in configuration (Figure 26(A)). The TEM image indicated clusters of copper nanoparticles with large surface area and that may be due to the strong Van de Waals forces as well as large surface of the copper nuclei (Lin et al, 2014). The homogeneous nucleation from initial nano-sized clusters having a monocrystalline structure also contribute the agglomeration of nanoparticles (Dang, et al, 2011). The SAED pattern (Figure 26, B) shows diffraction rings which provides information about the crystallinity of the sample being analysed (Suresh, et al, 2016). The bright spots observed confirmed the copper nanoparticles to be crystalline. Copper nanoparticles will be further characterised to confirm the size and shape of the nanoparticles. Small-angle X-ray scattering (SAXS) is normally used to evaluate colloidal systems in their native, solution environments, which can be challenging using TEM.

### 5.4.3 SAX Space

Small-angle X-ray scattering (SAXS) is a powerful technique to detect nanoscale structures. SAXS was performed using Sax Space Anton Paar (Austria). The analysed sample was in a solution form. The sample was placed on a  $\mu$ -cell then the distribution curves of copper nanoparticles were obtained as indicated below.

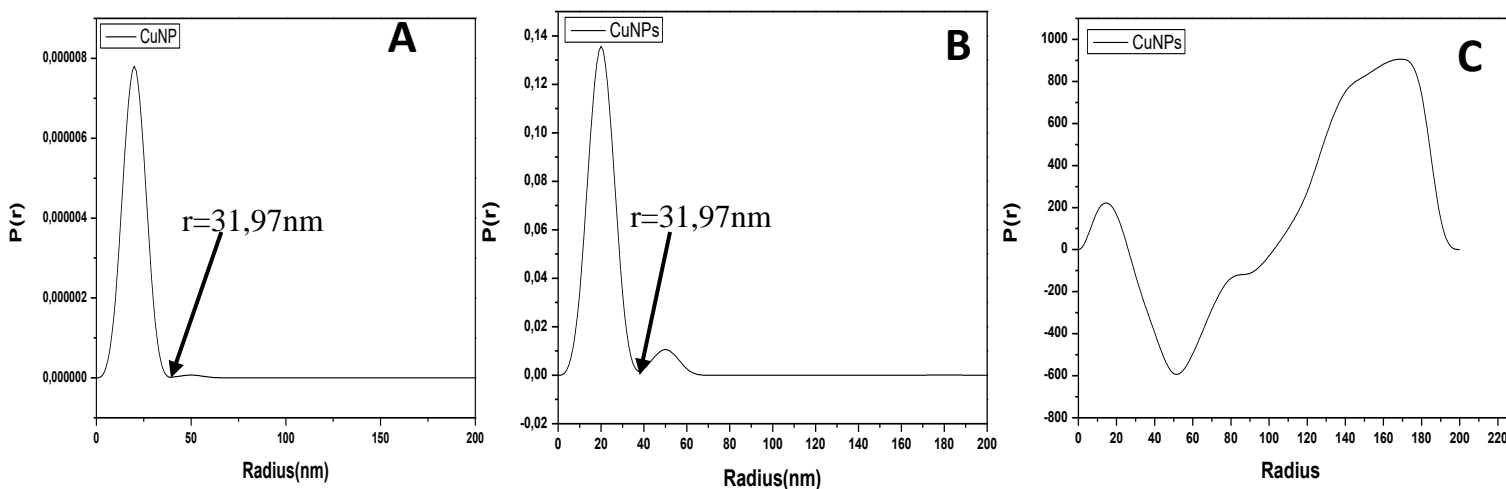


Figure 27: Distribution curves of copper nanoparticles (A, B) distribution by number (C) PDDF.

Small-angle X-ray-scattering was employed to determine the size and shape of the nanoparticles as well as distribution thereof. Figure 27 A and B illustrated above are the distribution by number graphs, which then provide information about the radius and number of copper nanoparticles. Figure 27 C is the pair distance distribution function (PDDF) graph which gives information about the shape and diameter of copper nanoparticles. The distribution by number graphs indicate the polydispersity of nanoparticles by illustrating radii of 37,91 nm and 60 nm on figure 27 B. The PDDF graph indicate two bell shape curves which means the particles are spherical in shape. Generally, the second curve on a PDDF graph indicate the agglomeration of nanoparticles. The PDDF also shows that the nanoparticles have a diameter of 51 nm as the diameter of a particle is observed at the point at which  $p(r)$  goes to zero (Nyman et al, 2015). In Suresh's paper, copper nanoparticles were synthesised by green chemical reduction method using an extract as a stabilizer. In Suresh's paper, the size, shape and distribution of copper nanoparticles were evaluated by TEM and SAXS. In their work, the shape of the nanoparticles was spherical which agrees with the work in this study (Suresh et al, 2016). The particle size of copper nanoparticles was obtained to be 19 nm which is smaller than the particle size attained from this work and that may be due to different reducing agents utilized. In Suresh's paper, two reducing agents, Hydrazine Hydrate and L-Ascorbic acid were made in use. In this work only one reducing agent (sodium borohydride) was used and that may be the reason why the nanoparticles are bigger than 19 nm.

### **5.5 Electrochemical characterisation**

PalmSens 3.0 electrochemical workstation (Bioanalytical Systems, USA) was utilized to conduct cyclic voltammetry (CV) experiments. In measuring electrochemical behaviour of electrode material, three-electrode configurations were often used. This includes a working electrode (WE) where the polymer material was deposited electrochemically, reference electrode (RE) utilized was Ag/AgCl and a platinum wire counter electrode submerged in 3ml of HCl electrolyte. All the experiments were purged with Argon gas and blanketed with Argon atmosphere during measurements. The temperature at which the experiments were conducted was room temperature (RT), 25<sup>0</sup>C.

### 5.5.1 Concentration profile of metformin

The working electrode (Glassy carbon electrode) was cleaned with 0.1  $\mu\text{m}$ , 0.3  $\mu\text{m}$  and 0.05  $\mu\text{m}$  fine alumina powder respectively and sonicated in ethanol for 10 minutes and the electrode was rinsed with distilled water before use. The HCl electrolyte was purged with an Argon gas before electrochemical analysis. A clean glassy carbon electrode was placed in an electrolyte (0.1 M, HCl) and metformin solution was added in increments of 10  $\mu\text{L}$  to create concentration profile, each cycle corresponded to an increment of metformin. The cyclic voltammogram in Figure 23, revealed an increase in current response as the concentration of metformin increased from 0.01 mM to 0.11 mM. Electrochemical characterization was performed by cycling the potential between -0.4 and 1.0V at a scan rate of 50 mV/s. All the electrochemical experiments were performed on a PalmSens Ptrace workstation and PalmSens Trace software.

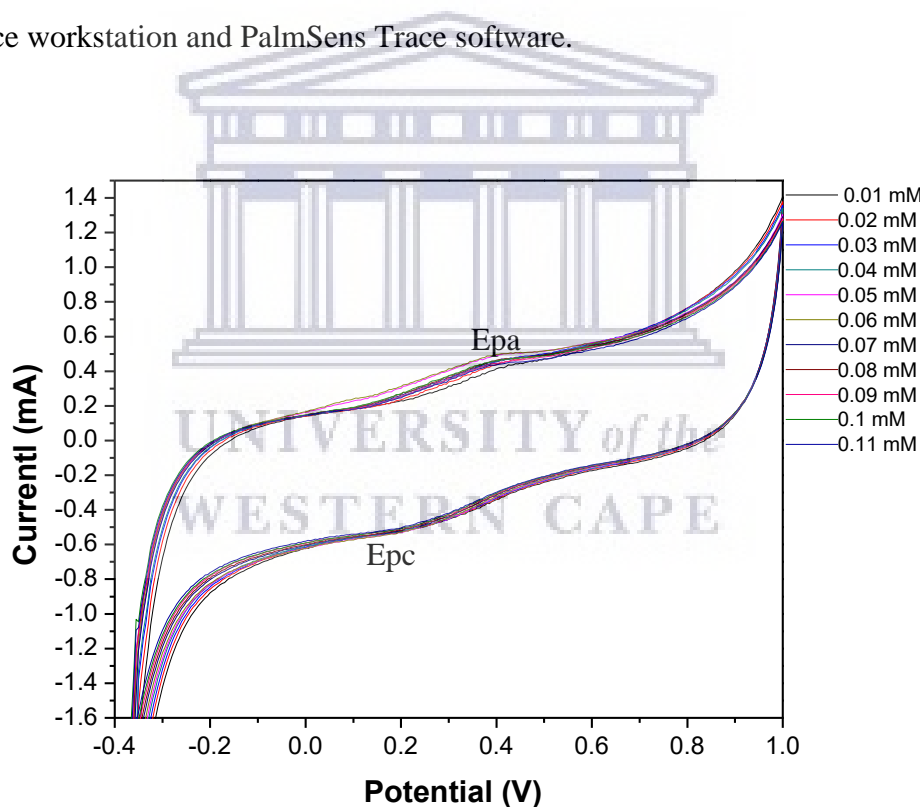


Figure 28: Concentration dependent cyclic voltammogram of metformin at GCE in 0,1 M HCl at 50 mV/s.

In figure 28, the current response of metformin at different concentrations was measured by cyclic voltammetry at GCE in 0.1 M HCl at 50 mV/s. The peak current responded positively to increasing

concentrations of metformin in the range of 0.01 – 0.11 mM and a calibration curve was developed from this concentration trend for the quantitative evaluation of metformin. To monitor the current response as a function of metformin concentration, the peak identified at 0.43 V (vs Ag/AgCl) will be consistently used as an indicator to modified and unmodified electrodes.

### 5.5.2 Characterisation of metformin on GCE

The concentration profile of metformin standard solution was evaluated, and a redox couple was observed even though the peaks are not well defined. The redox couple is due to hydrolysis of metformin in a supporting electrolyte.

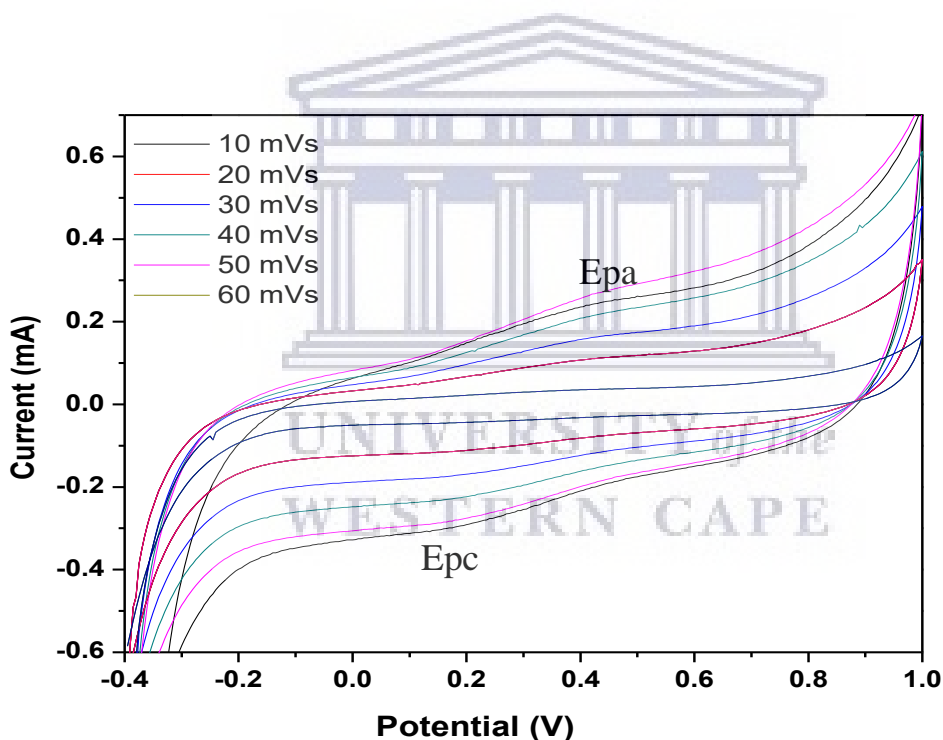


Figure 29: Multi-scan voltammogram of metformin at bare GC electrode in 0,1M HCl at 10 to 60 mV/s.

The electrochemical behaviour of metformin on a glassy carbon electrode indicated a poor response since the observed peaks are not well defined (Figure 29). The redox peaks were identified as Epa and Epc, respectively. The peak currents were observed to increase as the scan

rate increase and that indicated a good diffusion-controlled electron mobility. The increase in current response as a function of scan rate may be due to the hydrolysis of N-hydroxy guanidine (Hadi, et al 2016). The cyclic voltammogram demonstrated on figure 29 agrees with previously reported studies (Hadi, et al 2016) with low activity of the GC electrode towards MET. Therefore, Electropolymerization of pyrrole on glassy carbon electrode was adopted to enhance electroactivity of GCE.

Table 7: Effect of different scan rates for redox processes of metformin in 0,1M HCl at glassy carbon electrode at 10 to 60mV/s.

| Scan rate (mV/s).    | The square root of scan rate $v^{1/2}$ (mV/s) | Anodic peak potential Epa V | Cathodic peak potential Epc V | Formal Potential $E^0$ | Peak potential separation $\Delta E^0$ | Anodic peak current Ipa mA | Cathodic peak current Ipc mA | $\frac{Ipc}{Ipa}$ |
|----------------------|---|-----------------------------|-------------------------------|------------------------|--|----------------------------|------------------------------|-------------------|
| 10 mVs <sup>-1</sup> | 3.16  | 0.3390                      | 0.2630                        | 0.301                  | 0.076                                  | 0.0383                     | -0.0391                      | -0,9795           |
| 20 mVs <sup>-1</sup> | 4.47  | 0.3628                      | 0.2431                        | 0.3029                 | 0.1197                                 | 0.0976                     | -0.1030                      | -1,0553           |
| 30 mVs <sup>-1</sup> | 5.48  | 0.4027                      | 0.2151                        | 0.3089                 | 0.1876                                 | 0.1569                     | -0.1670                      | -1,0644           |
| 40 mVs <sup>-1</sup> | 6.32  | 0.4266                      | 0.1830                        | 0.3048                 | 0.2436                                 | 0.2119                     | -0.2262                      | -1,0675           |
| 50 mVs <sup>-1</sup> | 7.07  | 0.4388                      | 0.1631                        | 0.3009                 | 0.2757                                 | 0.2527                     | -0.2855                      | -1,1298           |
| 60 mVs <sup>-1</sup> | 7.75  | 0.4753                      | 0.1470                        | 0.3111                 | 0.3283                                 | 0.2847                     | -0.2990                      | -1,0502           |

The calculated values of the peak potential separation ( $\Delta E_p$ ) in Table 7, were obtained as a function of scan rate. The peak potential separation ( $\Delta E_p$ ) at faster and slower scan rate was found to be 0.3283 V and 0.076 V, respectively. The formal potential ( $E^0$ ) obtained for bare GCE is 0.3 V. The peak potential separation is centred on 0.2051 V which indicated quasi-irreversible behaviour of MET. A straight line was obtained, with a high correlation coefficient which confirmed diffusion-controlled behaviour at the interface according to the Randles Sevcik equation (Figure 30).

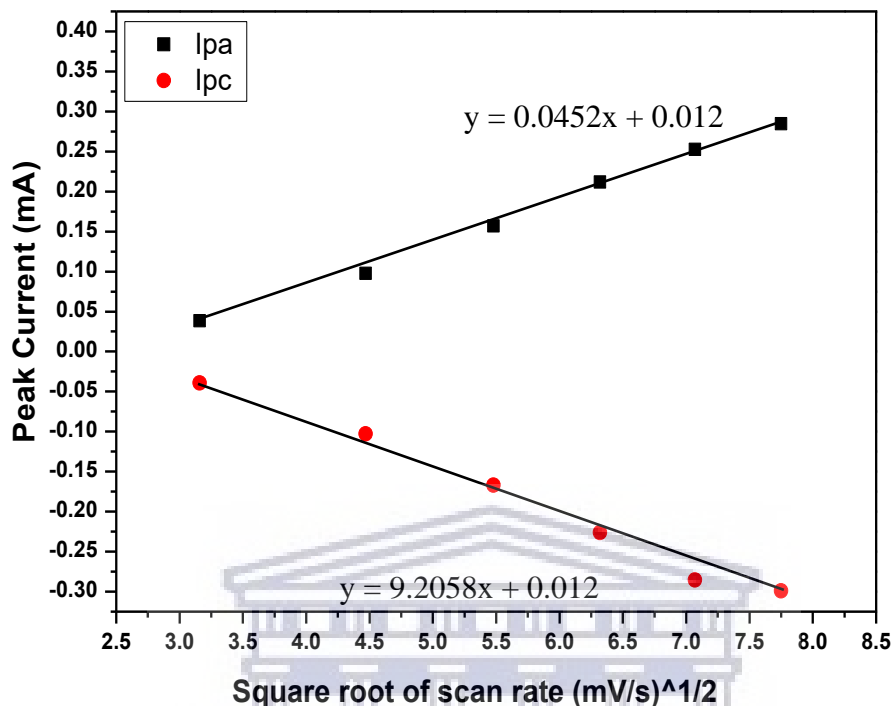


Figure 30: Randles Sevcik plot for the detection of metformin at a bare GCE at 10 - 60 mV/s in 0.1 M HCl.

The rate at which electrons are transferred within the bare electrode was assessed from the slope of the Randles Sevcik plot by the Randles Sevcik (equation 1). The diffusion coefficient ( $D_o$ ) was calculated to be  $1.4157 \times 10^{-3} \text{ cm}^2\text{s}^{-1}$  and  $0.2035 \text{ cm}^2\text{s}^{-1}$  for Epa and Epc, respectively. The glassy carbon electrode was modified with polypyrrole to increase the electroactivity of the electrode surface.

### 5.5.3 Characterisation of PPy-GCE

A standard three-electrode cell system was utilized in the cyclic voltammetry measurements with a glassy carbon electrode (GCE) as a working electrode. The auxiliary electrode was platinum wire and Ag/AgCl as a reference electrode. The thin layer of polypyrrole was synthesised electrochemically on the surface of GCE to increase the conductivity of glassy carbon electrode.

the electrosynthesis of was carried out in an aqueous solution of 0.1 M hydrochloric acid as the supporting electrolyte at 10 different scans. The peak potential of polypyrrole was observed at 0.71 V at 50 mV/s as indicated below (Figure 31).

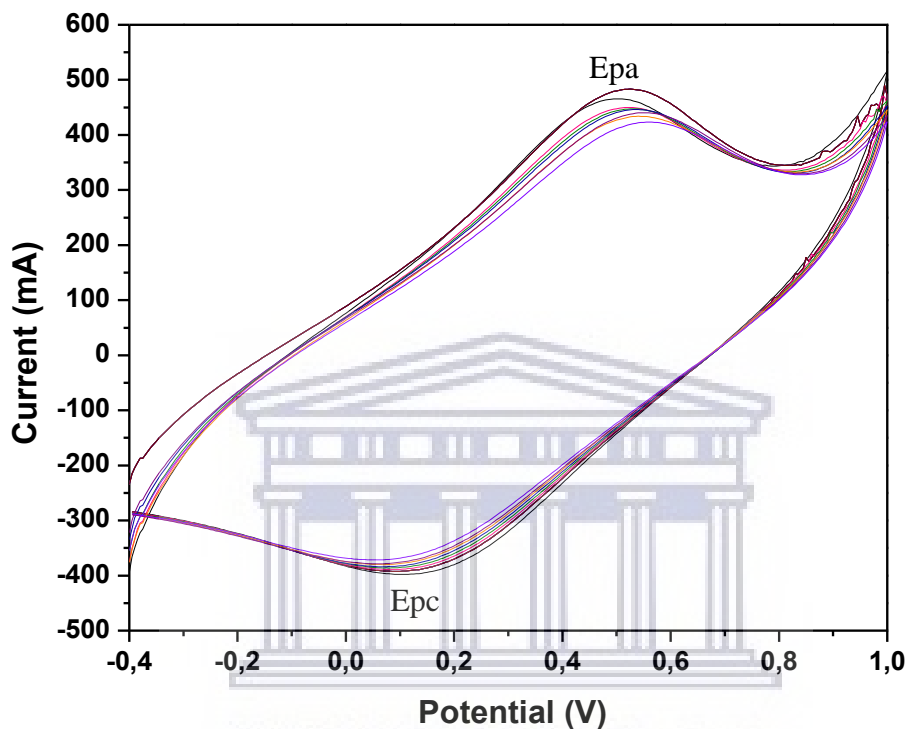


Figure 31: Cyclic voltammogram showing polymer growth during 10 cycles of polymerization of pyrrole at GCE in 0,1M HCl, at 10-100 mV/s.

The oxidation peak Epa, observed at 0.55 V vs AgCl, was attributed to the p-doping of PPy thin film (Figure 31). The increase in peak current with each successive cycle, was attributed to doping of PPy (Epa) and de-doping (Epc). The p-doping of polypyrrole include two simultaneous processes which are diffusion of the counter-ion into of the polypyrrole film to maintain charge neutrality, and the transfer of electrons from polypyrrole (Ngema et al, 2018). Previously reported studies suggested that there are two p-doping sites in pure PPy (Chen et al, 2007).

Table 8: Effect of different scan rate for redox processes of metformin in 0,1M HCl at PPy/GCE.

| Scan rate<br>$v$ (mV/s). | The square<br>root of scan<br>rate $v^{1/2}$<br>(mV/s) | Anodic<br>peak<br>potential<br>$E_{pa}$ V | Cathodi<br>c peak<br>potential<br>$E_{pc}$ V | Formal<br>Potential | Peak<br>potential<br>separation<br>$\Delta E^0$ | Anodic<br>peak<br>current $I_{pa}$<br>mA | Cathodic<br>peak<br>current $I_{pc}$<br>mA | $\frac{I_{pc}}{I_{pa}}$ |
|--------------------------|--|---|--|---------------------|---|--|--|-------------------------|
| 10                       | 3,16   | 0.2191                                    | 0,2508                                       | 0.2349              | 0,0317  | -47,5150                                 | 22,6652                                    | -0,4770                 |
| 20                       | 4,47   | 0.2350                                    | 0,2468                                       | 0.2409              | 0,0118  | -89,5685                                 | 57,6188                                    | -0,6433                 |
| 30                       | 5,48   | 0.2508                                    | 0,2228                                       | 0.2368              | 0,028   | -121,2452                                | 103,2222                                   | -0,8514                 |
| 40                       | 6,32   | 0,2788                                    | 0,2070                                       | 0.2429              | 0,0718  | -152,6488                                | 141,9989                                   | -0,9302                 |
| 50                       | 7,07   | 0,3268                                    | 0,1911                                       | 0.2589              | 0,1357  | -177,2256                                | 184,0524                                   | -1,0385                 |
| 60                       | 7,75   | 0,3507                                    | 0,1750                                       | 0.2628              | 0,1757  | -208,9022                                | 222,5560                                   | -1,0654                 |
| 70                       | 8.37   | 0.3908                                    | 0,1550                                       | 0.2729              | 0.2358  | -226,3790                                | 268,1595                                   | -1,1846                 |
| 80                       | 8,94   | 0.4027                                    | 0.1510                                       | 0.2768              | 0,2517  | -250,9558                                | 303,3861                                   | -1,2089                 |
| 90                       | 9,49   | 0,4347                                    | 0,1510                                       | 0.2928              | 0,2837  | -275,5325                                | 355,8165                                   | -1,2914                 |
| 100                      | 10   | 0,4708                                    | 0,1319                                       | 0.3015              | 0,3389  | -293,0092                                | 404,9699                                   | -1,4698                 |

The peak currents were plotted as a function of the square root of scan rate to assess the diffusion behaviour of PPy thin film on glassy carbon electrode as indicated in (Figure 32). A straight line with high correlation was attained and that confirmed the diffusion-controlled behaviour of the conductive polymer according to the Randles Sevcik equation.



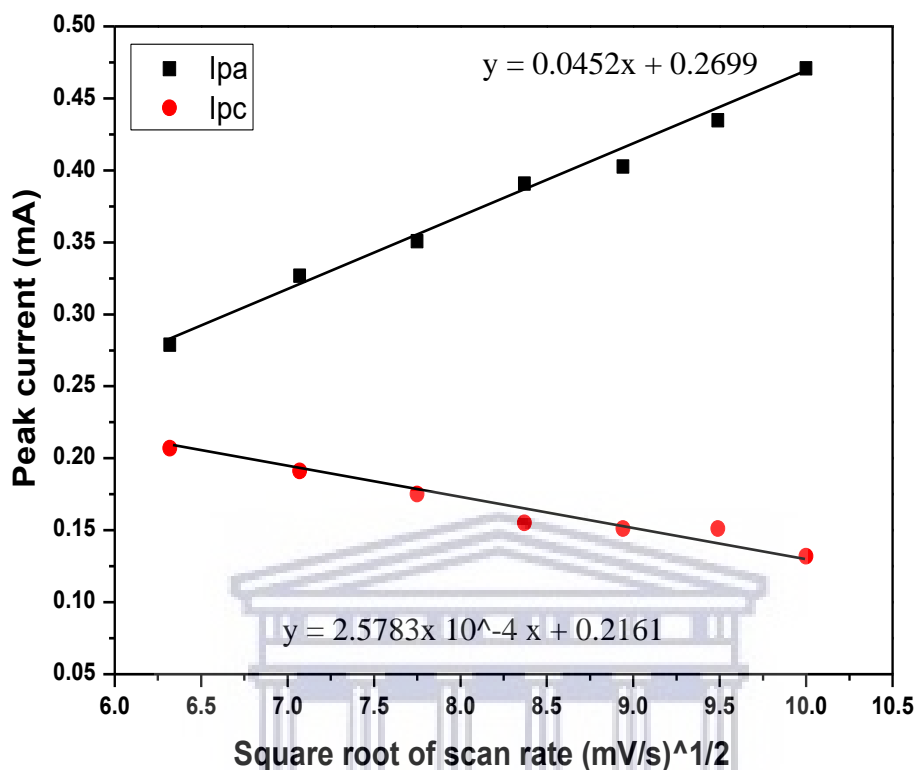


Figure 32: Randles Sevcik plot for the detection of metformin at GCE/PPy at 10 - 100 mV/s in 0.1 M HCl.

The rate at which electrons are transferred within the polymer layer was assessed from the slope of the Randles Sevcik plot by the Randles Sevcik equation (equation 1). The diffusion coefficient for E<sub>pa</sub> and E<sub>pc</sub> of PPy were calculated to be  $3.7845 \times 10^{-3} \text{ cm}^2/\text{s}$  and  $1.9756 \times 10^{-4} \text{ cm}^2/\text{s}$  respectively. The diffusion coefficient ( $D_0$ ) for oxidation was obtained to be slightly higher compared to that of reduction. The formal potential ( $E^0$ ) for the polymer platform was 0.26 V (vs Ag/AgCl).

#### 5.5.4 Electrodeposition of copper nanoparticles on PPy-GCE

The synthesised copper nanoparticles were characterised on a bare glassy carbon electrode in comparison with the standard solution of commercial copper. 300  $\mu\text{L}$  of the standard solution of commercial copper was added to 3 ml of HCl and it was characterised by CV 0.1 M HCl at a scan rate of 50 mV/s. The cyclic voltammograms of copper nanoparticles (red) and standard solution of commercial copper are indicated below.

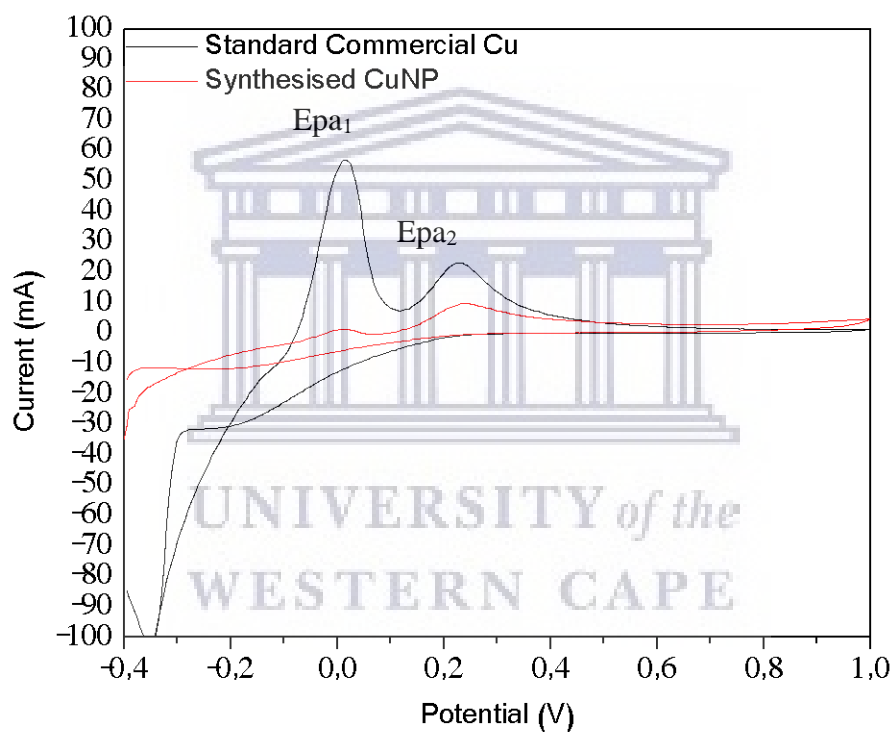
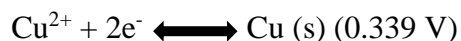


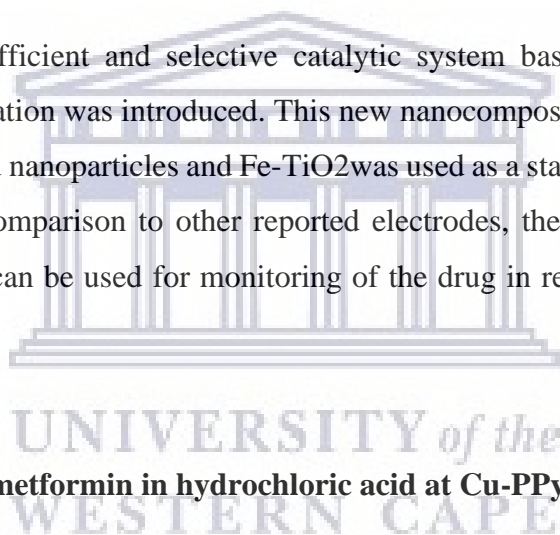
Figure33:Cyclic voltammogram corresponding to commercial copper and synthesised copper nanoparticles Cu NP in 0.1 M HCl at a bare GCE, 50 mV/s scan rate.

The cyclic voltammogram above display anodic peaks (Epa<sub>1</sub> and Epa<sub>2</sub>) at 0.02 V and 0.23 V (vs Ag/AgCl) respectively for a standard copper solution. The commercial copper solution shows two oxidation peaks a potential of 0.01 V (Epa<sub>1</sub>) and 0.23 V (Epa<sub>2</sub>), on the other hand copper nanoparticles indicated two peak potentials at 0.02 V and 0.24 V (Figure 28). The oxidation peaks

for commercial copper (black) and synthesised copper nanoparticles (red) did not agree with the standard reduction potential of 0.339 V for  $\text{Cu}^{2+}$ . However, the oxidation peaks for a standard copper solution and copper nanoparticles agreed with reported studies in the literature (Rana, et al, 2014). The electrochemical behaviour of copper nanoparticles displayed a low current response while standard copper solution displayed higher peak currents, that may be due surface area of glassy carbon electrode and concentration of the interface. Out of all the nanomaterial for other metals, copper was the most preferred due to its high affinity and catalytic action towards the oxidation of MET.



In the present study, an efficient and selective catalytic system based on a Fe-Cu/TiO<sub>2</sub>/CP electrode for the MET oxidation was introduced. This new nanocomposite material which has the salient properties of both Cu nanoparticles and Fe-TiO<sub>2</sub> was used as a stable and sensitive modifier for CPE construction. In comparison to other reported electrodes, the proposed sensor has the lowest detection limit and can be used for monitoring of the drug in real samples with different matrices.



### 5.5.5 Characterisation of metformin in hydrochloric acid at Cu-PPy/GCE

The novel CuNP-PPy/GCE was prepared by electrodepositing copper nanoparticles on bare glassy carbon electrode (GCE) modified with polypyrrole at a scan rate of 50 mV/s. The cyclic voltammogram showed two well-defined anodic peaks of a commercial standard solution of copper (black) and synthesised copper nanoparticles. However, the current response of synthesised copper is lower than a standard copper solution that may be due to agglomeration of CuNP which will then lead to polydispersity (Figure 34).

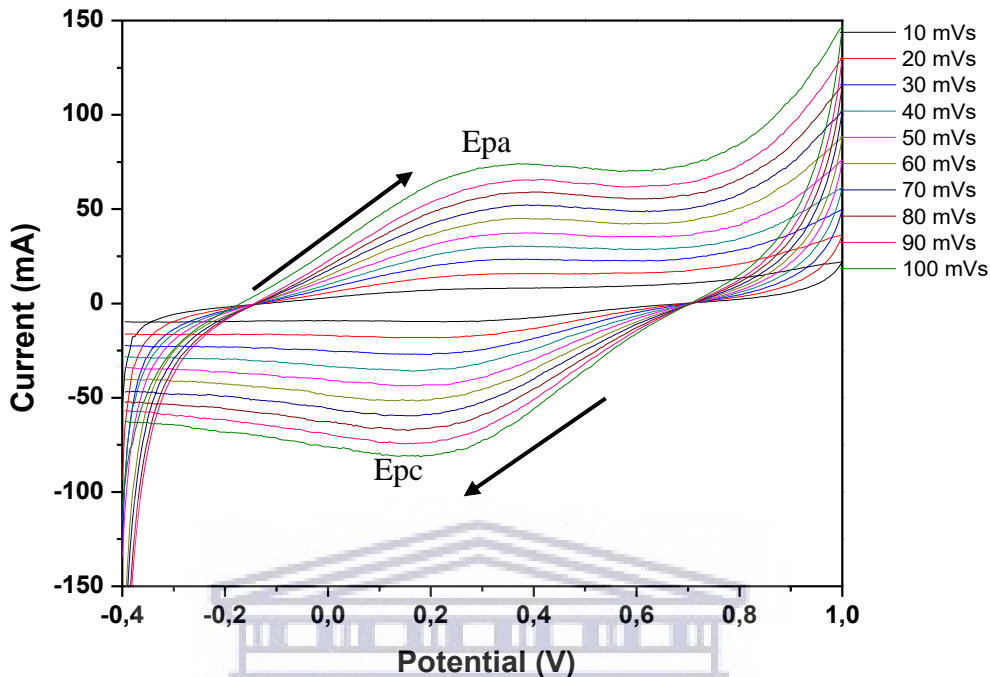


Figure 34: Multi-scan voltammogram of metformin in 0,1M HCl at Cu-PPy/GCE, 10-100 mV/s.

The scan rate effect on CuNP-PPy/GCE was evaluated in Figure 34. The Cu-metal nanoparticles (Cu-NPs) were incorporated with PPy thin film at the surface of GCE by cycling the potential from -0.4 to 1.0 V in 0,1M HCl solution at a scan rate of 10-100 mV/s (Figure 34). The cyclic voltammogram of Cu nanoparticles modified polypyrrole film electrode showed redox couple which is reversible. The incorporation of copper nanoparticles with polypyrrole to form CuNP-PPy nanocomposite was revealed by the oxidation and reduction peak at a potential of 0.38 V and 1.50 V respectively, which agreed with previously reported studies (Ulubay et al, 2010). Upon characterisation of CuNP-PPy/GCE, oxidation and subsequent reduction peak indicated an increase in current response as the scan rates increase. However, high current background (Figure 34) may be due to the higher density of carbonyl groups generated on the PPy film after the electrochemical over-oxidation process.

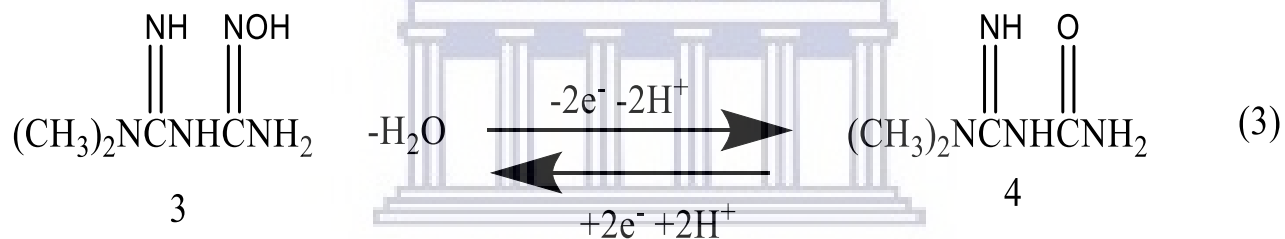
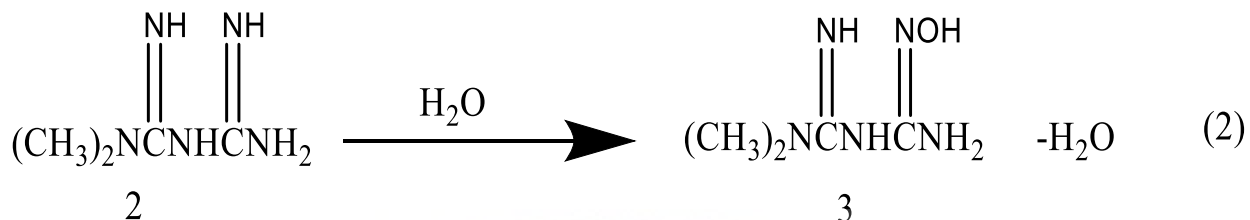
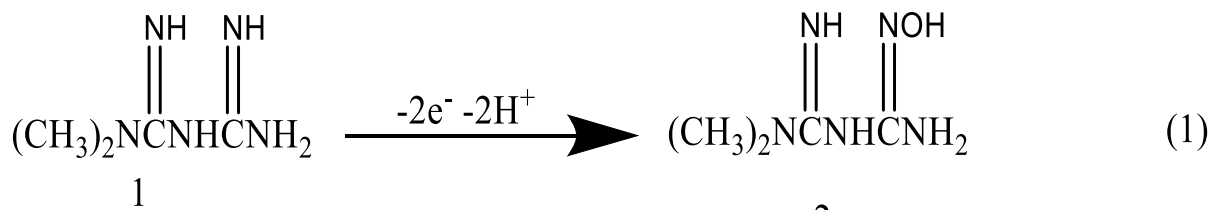


Figure 35: Suggested oxidation mechanism of metformin.

UNIVERSITY of the  
WESTERN CAPE

Table 9: Effect of different scan rates for redox processes of metformin in 0,1m HCl at CuNP-PPy/GCE.

| Scan rate $v$ (mV/s) | The square root of scan rate $v^{1/2}$ (mV/s) | Anodic peak potential $E_{pa}$ V | Cathodic peak potential $E_{pc}$ V | Formal Potential | Anodic peak current $I_{pa}$ mA | Cathodic peak current $I_{pc}$ mA | Peak potential separation $\Delta E^0$ | $\frac{I_{pc}}{I_{pa}}$ |
|----------------------|---|----------------------------------|------------------------------------|------------------|---------------------------------|-----------------------------------|--|-------------------------|
| 10                   | 3,16  | 0,1830                           | 0,3109                             | 0.2469           | 5,7346                          | -7,9465                           | 0,1279                                 | -1,3857                 |
| 20                   | 4,47  | 0,2191                           | 0,2950                             | 0.2570           | 14,1726                         | -17,4495                          | 0,0759                                 | -1,2312                 |
| 30                   | 5,48  | 0,2269                           | 0,2829                             | 0.2549           | 21,5456                         | -24,7406                          | 0,056                                  | -1,1483                 |
| 40                   | 6,32  | 0,2431                           | 0,2590                             | 0.2510           | 28,9186                         | -32,1160                          | 0,0159                                 | -1,1106                 |
| 50                   | 7,07  | 0,2711                           | 0,2390                             | 0.2550           | 36,2916                         | -41,6166                          | 0,0321                                 | -1,1467                 |
| 60                   | 7,75  | 0,3227                           | 0,2228                             | 0.2727           | 42,5997                         | -50,0546                          | 0,0999                                 | -1,1750                 |
| 70                   | 8.37  | 0,3389                           | 0,2070                             | 0.2729           | 51,0377                         | -57,4276                          | 0,1319                                 | -1,1252                 |
| 80                   | 8,94  | 0,3588                           | 0,1911                             | 0.2749           | 59,3938                         | -64,8007                          | 0,1677                                 | -1,0910                 |
| 90                   | 9,49  | 0,3669                           | 0,1750                             | 0.2709           | 66,7668                         | -73,1567                          | 0,1919                                 | -1,0957                 |
| 100                  | 10  | 0,3828                           | 0,1590                             | 0.2709           | 75,2048                         | -81,5948                          | 0,2238                                 | -1,0850                 |

The table above (Table 9) indicates calculated values of peak potential separation ( $\Delta E^0$ ) for CuNP-PPy nanocomposite in 0.1 M HCl. A straight line with high correlation was attained and that confirmed the diffusion-controlled behaviour of CuNP-PPy/GCE. The rate of electron mobility within the layer of a nanocomposite CuNP-PPy was assessed by Randles Sevcik equation. The diffusion coefficients of the modified PPy and CuNP-PPy were calculated by Randles Sevcik equation 1.

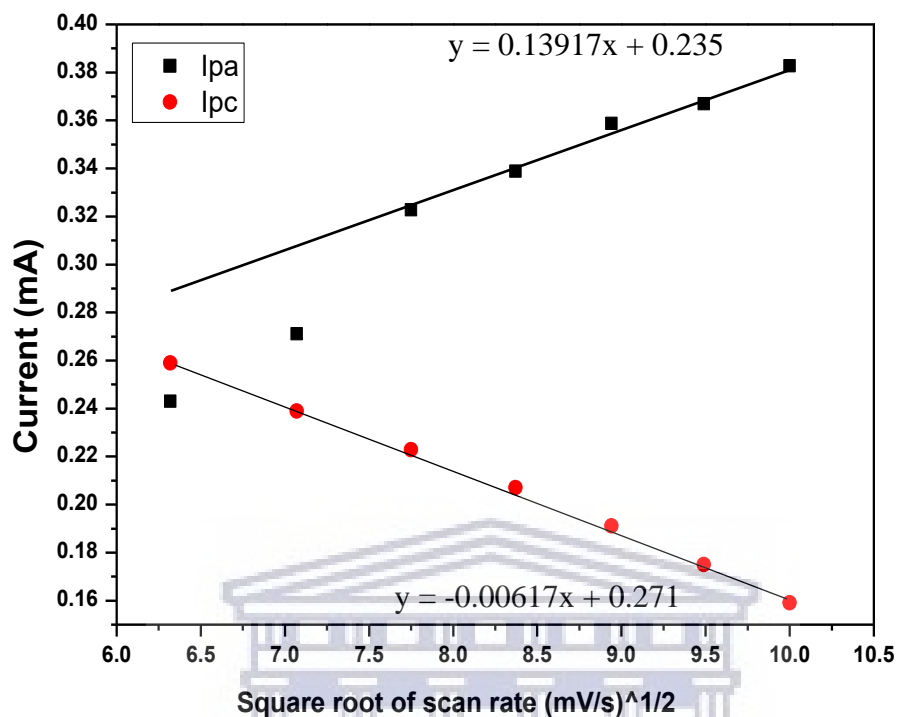


Figure 36: Randles Sevcik plot for the detection of metformin at GCE/PPy-CuNP at 10 - 100 mV/s in 0.1 M HCl.

Figure 36 is the Randles Sevcik plot for metformin on nanocomposite material (CuNP-PPy) at different scan rates. The peak potential separation for the redox couple of 0.1279 V and 0.3828 V were higher than peak separation for PPy 0.0317 V and 0.3389 V, that may be due to enhanced electron transfer in CuNP-PPy platform. The formal potential obtained for the polymer (PPy) and nanocomposite (CuNP-PPy/GCE) was found to be 0.56 V and 0.80 V, respectively. Furthermore, the diffusion coefficient was found to be smaller for reduction ( $5.0185 \times 10^{-5} \text{ cm}^2/\text{s}$ ) compared to oxidation ( $1.1319 \times 10^{-3} \text{ cm}^2/\text{s}$ ) with formal potential of 0.80 V (vs Ag/AgCl). The  $D_0$  for the reduction was discovered to be higher compared to the diffusion coefficient of oxidation and that indicated reduced state as a favoured kinetics system. The diffusion coefficient for CuNP-PPy ( $5.0185 \times 10^{-5} \text{ cm}^2/\text{s}$ ) is smaller than previously reported studies of ( $7.6 \times 10^{-6} \text{ cm}^2/\text{s}$ ) for Fe-Cu/TiO<sub>2</sub> nanostructure (Gholivand, et al, 2014). That might be due to different supporting

electrolyte ( $K_4[Fe(CN)_6]$ ) used in their studies as well as different surface area since different types of the nanocomposite were used.



UNIVERSITY *of the*  
WESTERN CAPE



# CHAPTER 6

*This chapter presents the quantitative analysis of metformin on modified and unmodified glassy carbon electrode by ultraviolet-visible spectroscopy (UV-Vis), cyclic voltammetry (CV) and scan rate voltammetry (SWV).*

## 6.1 UV-Vis of metformin

### 6.1.1 Sample preparation

Standard solutions of 0.06 M of metformin were prepared by diluting 50  $\mu\text{L}$  of metformin in a 10 ml of distil water and diluted further to different concentrations. Analysis of the prepared solutions with different concentrations will be performed on a NICOLET evolution 100 Uv-vis instrument.

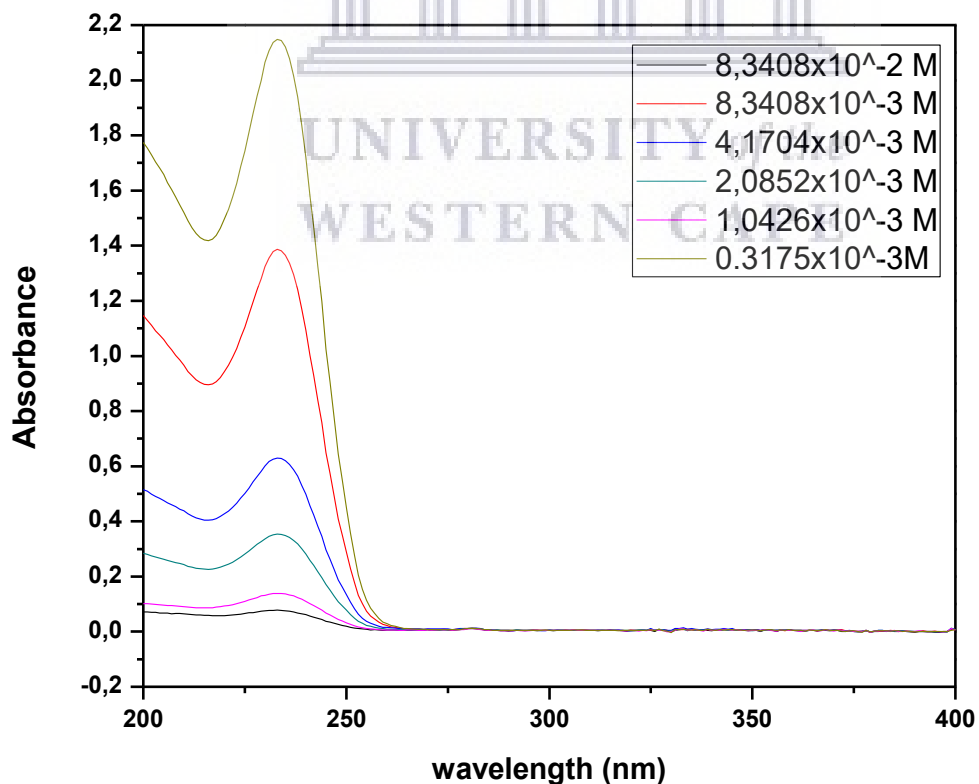


Figure 37:UV-Vis absorption spectra of metformin at  $\lambda=232\text{nm}$ .

Figure 37 shows the absorption spectra of metformin solution in distilled water. The absorbance spectra were recorded between the wavelength range of 200 – 400 nm. UV-Vis spectra of MET indicate one peak with a wavelength of 232 nm at maximal light absorbance.

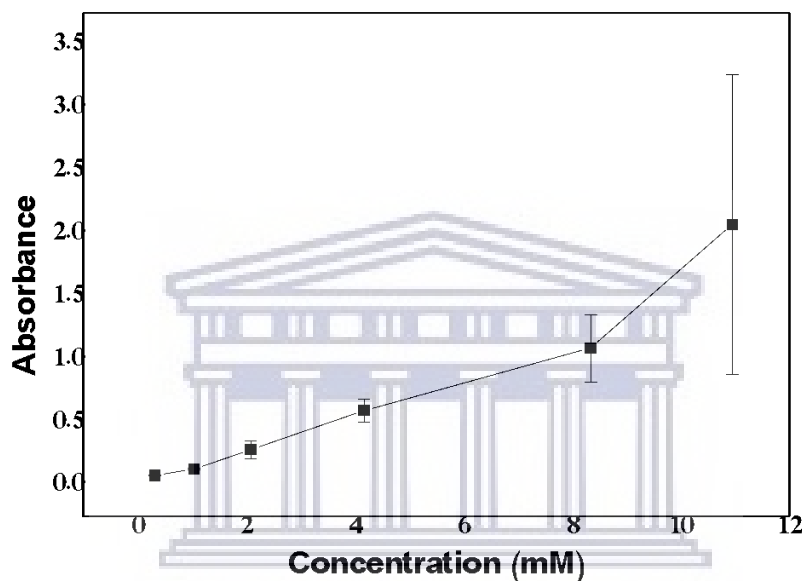


Figure38:Calibration curve for the detection of metformin (83,408 – 0.3175 mM) by UV-Vis, at maximum wavelength of 232 nm.

The schematic diagram above indicates a good linear response of metformin at low concentrations as well as a plateau being reached at high concentrations. Limit of detection (LOD) and limit of quantification (LOQ) was calculated using the following equation:

$$\text{LOD} = 3 \times \frac{SD}{\text{Slope}} \dots \text{Equation 2}$$

$$\text{LOQ} = 10 \times \frac{SD}{\text{Slope}} \dots \text{Equation 3}$$

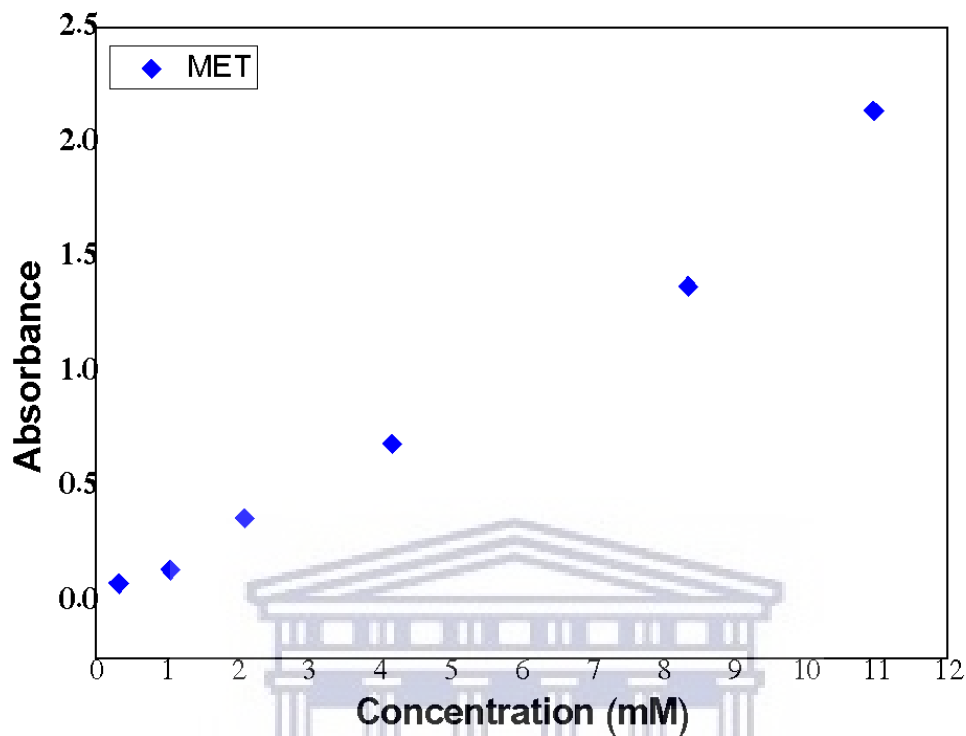


Figure 39: Full calibration curve of UV-Vis for different concentrations of metformin at maximum wavelength of 232 nm.

The calculated concentration in the range of (0.3175 mM- 8.341 mM) was made in use to construct the calibration curve in Figure 38. In this concentration range, Beer's law is obeyed. The determination coefficient value was calculated ( $r^2 = 0.9828$ ,  $y = 0.1880x - 0.0462$ ). Limit of detection was calculated to form the linear range of  $5.2660 \times 10^{-3} M$  and the limit of quantification (LOQ) were 0.016 M (Figure 39). The UV/vis method sensitivity for the detection of metformin in a solution using standard solutions was found to be 0.1880 mA/M.

## 6.2 Electrochemical detection of metformin

The standard solutions of metformin were prepared prior the experiments as indicated above. The standard solution of metformin was added in increments of 10  $\mu L$  in an electrochemical cell. The

electrochemical detection of metformin was then studied using cyclic voltammetry and square wave voltammetry (SWV) at a bare electrode as well as at a modified electrode in 0.1 M HCl within the potential window of -0.4 V to 1.0 V, scan rate of 50 mV/s.

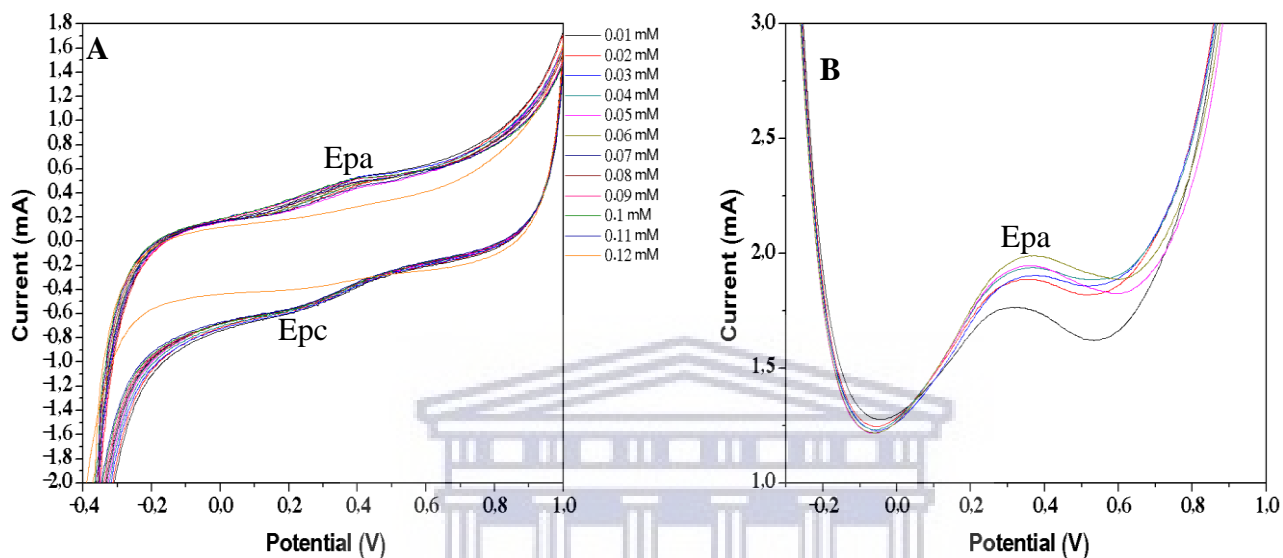


Figure 40: Concentration-dependent cyclic voltammogram (A) and square wave voltammogram (B) of metformin at a bare GCE in 0,1 M HCl, scan rate of 50 mV/s.

The electrochemical behaviour of metformin was measured by cyclic voltammetry (CV) at GCE/MET in 0,1M HCl at a scan rate of 50 mV/s. The cyclic voltammogram demonstrated above indicates an increase in current response with every increase of metformin (Figure 40). Figure 40 shows that as the concentration of metformin increases no peaks of metformin are observed and that means the activity of the electrode towards metformin is very low are a bare electrode. The oxidative square wave voltammetry of metformin at a bare glassy carbon electrode confirmed the increasing current with concentration behaviour observed with cyclic voltammetry with improved resolution of the oxidation peak at 0.41V (vs Ag/AgCl).

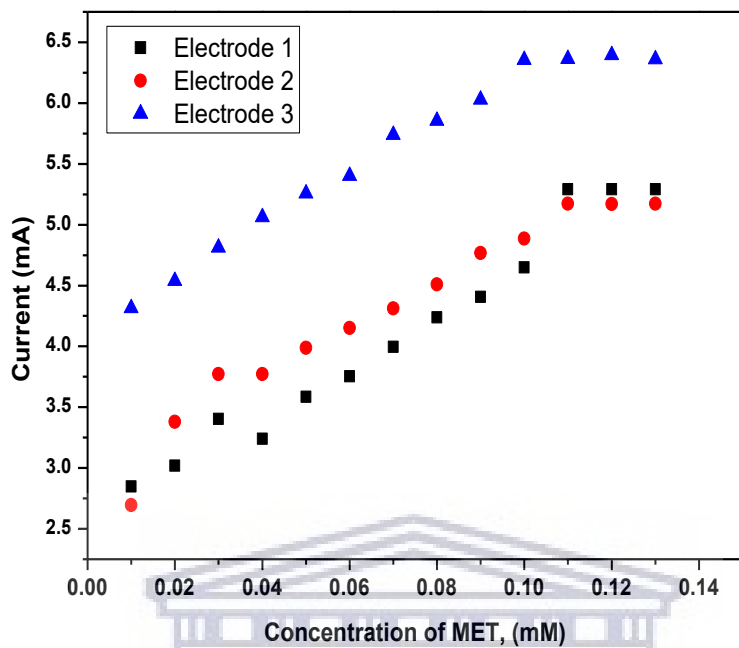


Figure 41: Calibration curve for the detection of metformin (0.01 - 0.13 mM) at bare GC electrodes, at a potential between -0.4 to 1.0 V (Ag/AgCl), 50 mV/s in 0.1 M HCl.

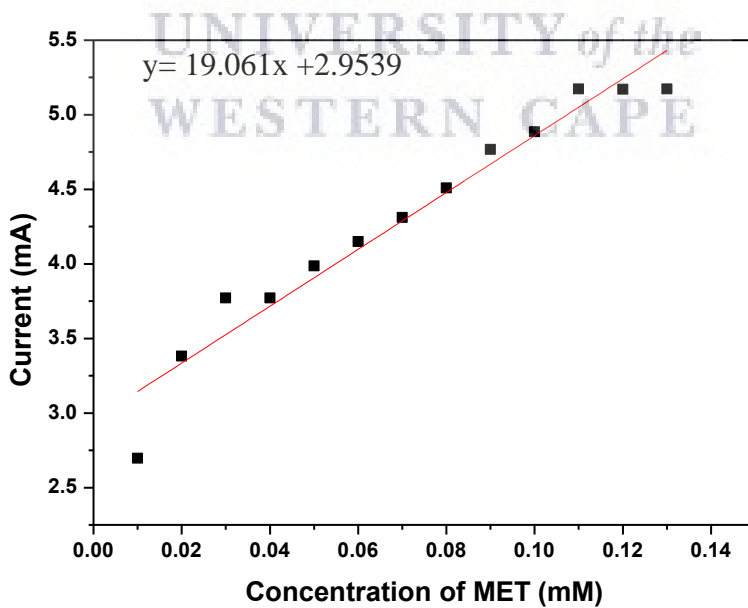


Figure 42: Linear plot of the current response of metformin within the concentration range of 0.01-0.13 mM at GCE in HCl, scan rate of 50 mV/s.

The calibration curve of the bare electrode at different concentrations of metformin in Figure 41 showed a linear relationship in the range (0.01 mM- 0.11 mM) between peak current and metformin concentration (Figure 42). Figure 41 confirms the experiment to be repeated three times at three different electrodes, meaning there are 3 limits of detections (LOD) calculated from the experiments conducted. The limit of detection is a measure of the smallest concentration of an analyte an electrochemical sensor can detect. The calculated limit of detections were  $6,36 \times 10^{-3}$  M,  $6,4726 \times 10^{-3}$  M,  $7,0 \times 10^{-3}$  M respectively with a relative standard deviation of 7.1418 %. Additionally, the average limit of detection was calculated to be  $6,6109 \times 10^{-3}$  M with a sensitivity of 19,06 mA/M. The analytical performance of metformin on a bare GCE was poorly observed with low sensitivity similar to the sensor reported by Hadi, et al, 2016. Thus, modifying the electrode was of interest, in order to increase sensitivity and selectivity.

Table 10: Comparison of the analytical performance of the GCE/MET.

| Electrode  | Sensitivity (M) | LOD (mM) | LOQ (M) | R-Square |
|------------|-----------------|----------|---------|----------|
| GCE- Met 1 | 21,7230         | 6,3610   | 0,0192  | 0,9613   |
| GCE-Met 2  | 19,0680         | 6,4726   | 0,0196  | 0,9416   |
| GCE-Met 3  | 18,4793         | 7,0000   | 0,0202  | 0,9574   |

UNIVERSITY of the  
WESTERN CAPE

### 6.3 Electrochemical detection of metformin on PPy/GCE

The electroanalytical response of metformin was studied using cyclic voltammetry (CV) as well as the square wave voltammetry (SWV) with the electrode modified with polypyrrole in 0.1 M HCl at 50 mV/s.

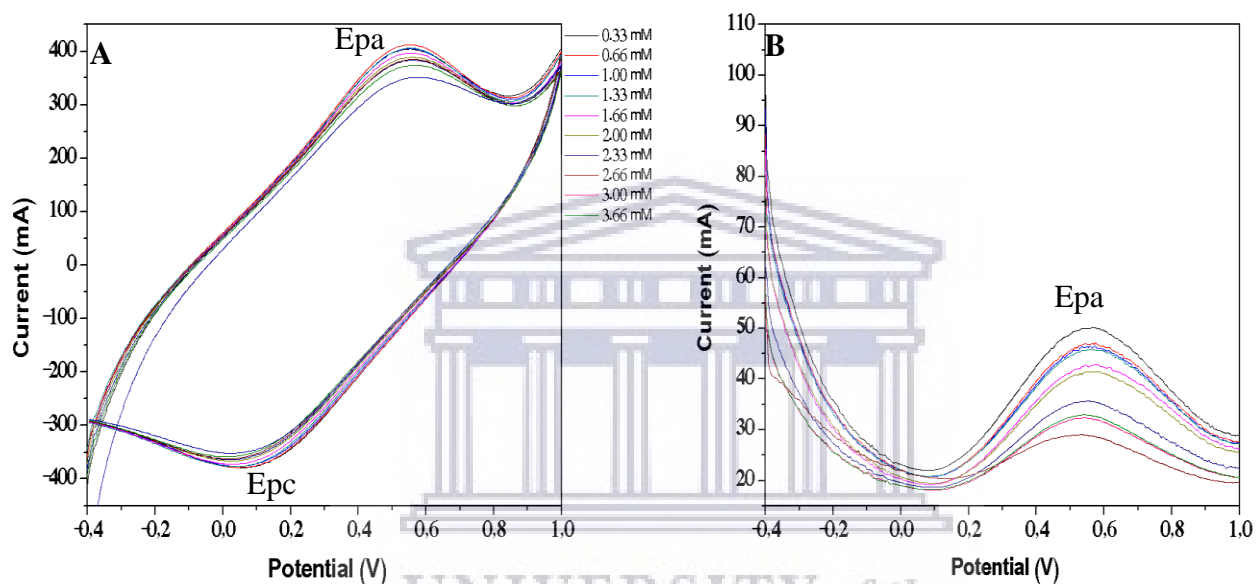


Figure 43: Concentration dependent cyclic voltammogram (A) of metformin on PPy/ GCE in 0,1 M HCl at 50 mV/s.

Figure 43 shows the detection of metformin on polypyrrole modified electrode in HCl electrolyte. The analytical performance of the sensor was investigated with CV (A) and SWV (B). The above figures indicate the current response to increase as the concentration of metformin increases. Upon the addition of 10  $\mu$ L of metformin in the cell, oxidation and subsequent reduction peaks appeared at 0.55 V and 0.06 V respectively, indicating a quasi-reversible electrode process which is probably due to the diffusion barrier of the polymeric film. Comparing the concentration profile of metformin at bare electrode and at PPy modified electrode, the peak potential of the modified electrode shifted to the right and started to increase with the increasing concentration of metformin.

In Ulubay's paper, similar redox peaks were obtained at lower potentials of 0.24 (oxidation) and 0.16 V (reduction). The peak characteristics of the above diagram clearly indicate an electrocatalytic oxidation of metformin at PPy modified electrode. Comparing the electrochemical behaviour of metformin on a bare electrode and on a polypyrrole modified electrode, the polypyrrole modified electrode indicated an active surface area by increasing the analytical determination sensitivity of metformin. Metformin was further characterised by SWV. The oxidative square wave voltammetry of metformin at PPy modified glassy carbon electrode confirmed the increasing current as a function of metformin concentration behaviour with improved resolution of the oxidation peak at 0.55 V (vs Ag/AgCl).

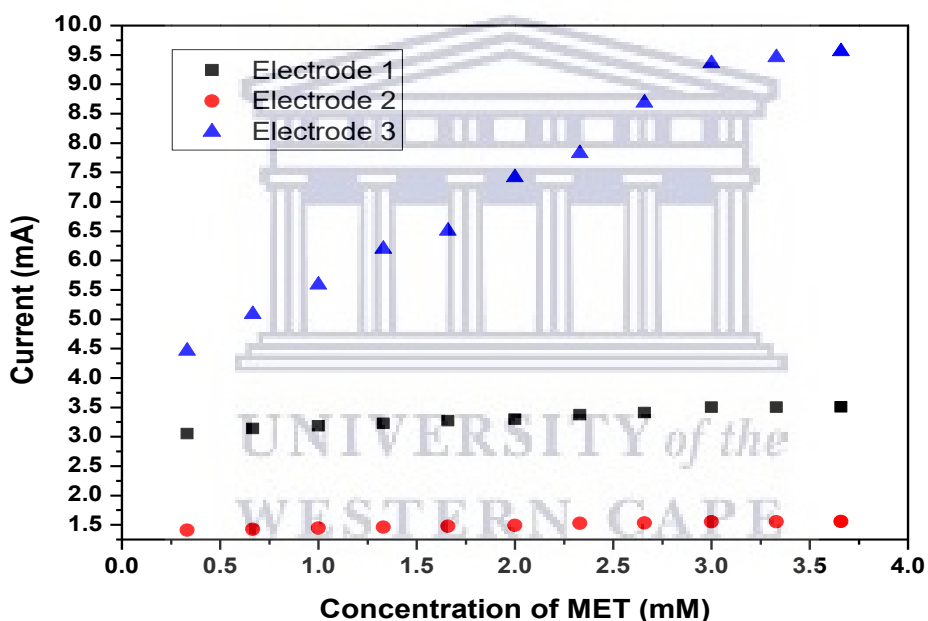


Figure 44: Calibration curve for the detection of metformin (0.33 – 3.66 mM) at PPy/GCE electrodes, at a potential range of -0.4 to 1.0 V (Ag/AgCl), 50 mV/s in 0.1 M HCl.



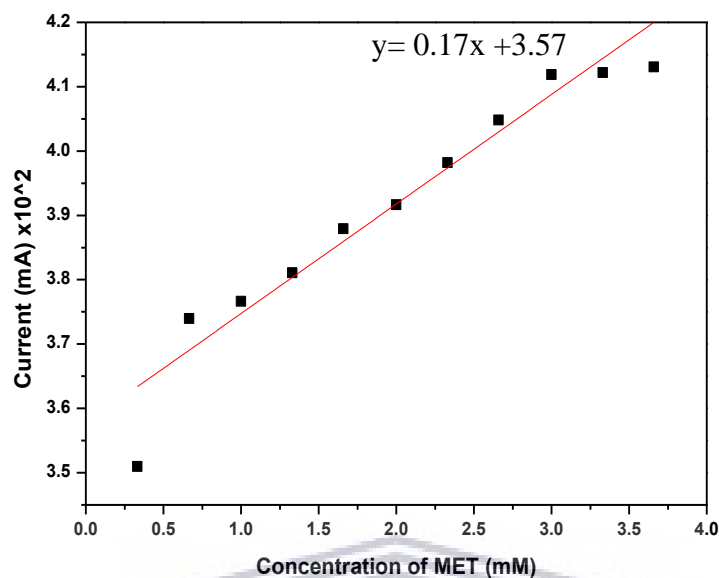


Figure 45: Linear plot of the current response of metformin within the concentration range of 0.33-3.66 Mm at PPy/GCE in HCl, scan rate of 50 mV/s.

The calibration curve of PPy/GCE electrodes correspond to the current response of metformin at different concentrations (0.01 mM- 0.11 mM). Electrode 3 indicated a high current background compared to the other two electrodes and that could be influenced by electrode surface as well as faradaic processes. Electrode 1 was indicated to have a better linearity compared to other electrodes. The experiments were repeated three times; hence three limits of detections were calculated from the experiments conducted. The limit of detection was calculated using equation 2. The calculated limit of detections was  $2.0431 \times 10^{-2}$  M,  $7.1466 \times 10^{-2}$  M,  $1.7279 \times 10^{-2}$  M respectively with a relative standard deviation of 7.1418 %. The average limit of detection was calculated to be  $3.6392 \times 10^{-2}$  M with a sensitivity of 0.17 mA/M. The detection limit was obtained to be higher than the one in the previously reported studies (Ulubay et al, 2010).

## 6.4 Electrochemical detection of metformin on CuNP-PPy/GCE

The electrochemical study of MET standard solution in 0,1 M HCl at CuNP-PPy/GCE was performed using cyclic voltammetry and square wave (Figure 41) at 50 mV/s.

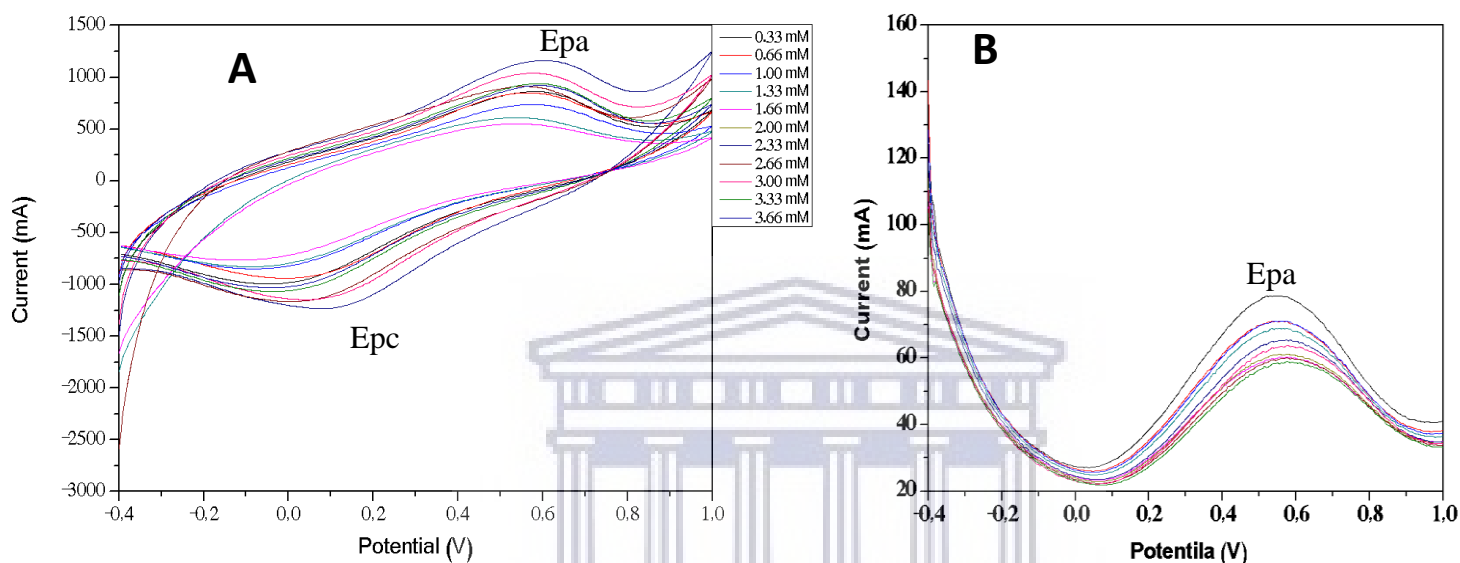


Figure 46: Cyclic voltammogram (A) and oxidative square wave voltammogram (B) of concentration dependent metformin analysis at Cu-PPy/ GCE composite in 0,1 M HCl at 50 mV/s.

The analytical performance of CuNP-PPy chemical sensor was evaluated with CV (Figure 46, A) and SWV (Figure 46, B). To date, not much has been reported on metformin electrochemistry on this platform. Nonetheless, CuNP-PPy chemical sensor was comparable to the reported studies. The redox couple of Epa at 0.61 V (Ag/AgCl) and Epc at 0.1 V oxidation of the amino group (NH) and reduction of N-carbonyl-guanidine. The cyclic voltammogram (A) indicates an enhancement and shift of oxidative peak from low potentials to high potential compared to the bare GC electrode. However, increasing metformin concentrations presented that the CuNP-PPy thin films peaks indicated a decreasing trend. A more sensitive electrochemical technique (SWV) was applied and well define peaks indicating current response as a function of metformin concentration at a modified electrode is demonstrated at Figure 46 B. Improvement of peak potential is due to

strong chelating of  $\text{Cu}^{2+}$  which is present in CuNP towards metformin (Hadi, et al, 2016). The modified electrode showed a high electron transfer rate which indicated improve sensitivity.

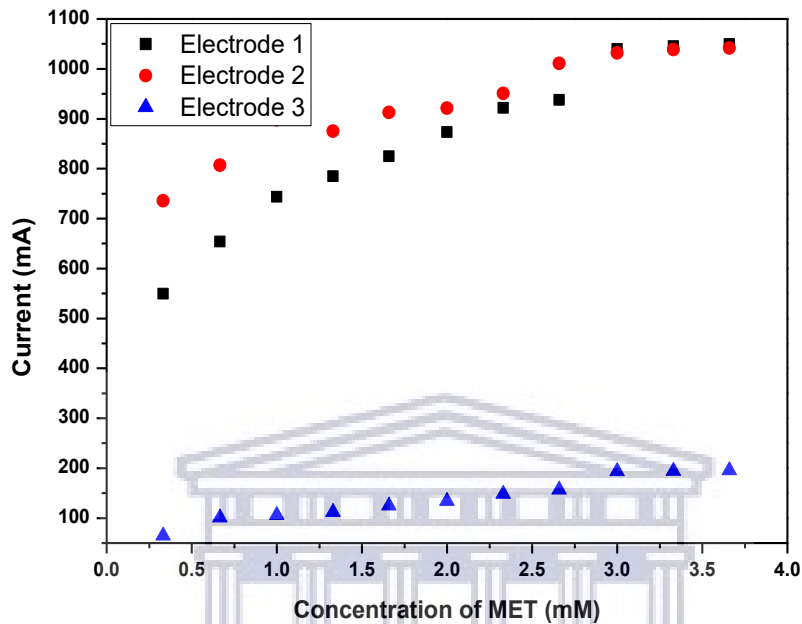


Figure 47: Calibration curve for the detection of metformin (0.01 - 0.13 mM) at CuNP-PPy/GCE, at a potential between -0.4 to 1.0 V (Ag/AgCl), 50 mV/s in 0.1 M HCl.

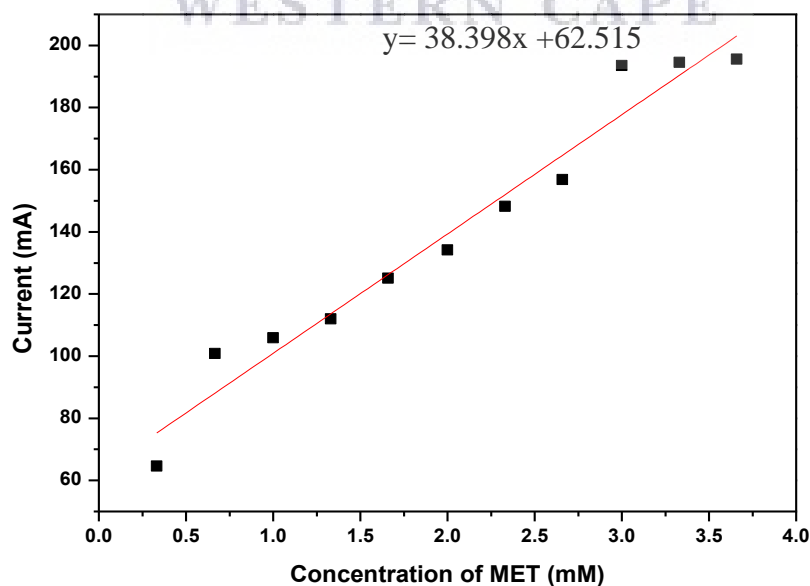


Figure 48: Linear plot of the current response of metformin within the concentration range of 0.33- 3,66 Mm at CuNP-PPy/GCE in 0.1 M HCl, scan rate of 50 mV/s.

Figure 47, demonstrate the calibration curves of CuNP-PPy/GCE at different concentrations of metformin in 0.1 M HCl, at scan rate of 50 mV/s. The calibration curves indicated a linear relationship as metformin concentrations increased from 0.01 mM- 0.11 mM. The electrochemical analysis of metformin in aqueous solution was performed n=3 by cyclic voltammetry (Figure 48). The current response of two electrodes were observed to be higher than the current response previously reported in literature. The processing factors such as temperature and time may be the contributing factors to the high background current of the electrodes. The linear plot in figure 43 was used to investigate the analytical performance of CuNP-PPy/GCE composite in 0.1 M HCl at 50 mV/s for the detection of metformin in aqueous solution. Thus, the calculated limit of detections from the experiments was  $9.0454 \times 10^{-5} M$ ,  $4.0142 \times 10^{-5} M$  and  $2.3749 \times 10^{-5} M$  respectively. The average LOD for CuNP-PPy/GCE sensor towards the detection of metformin was found to be  $5.1448 \times 10^{-5} M$  and the sensitivity of the sensor 38.3900 mA/M. Thereafter, the analytical performance of the electrochemical sensor was compared with the nanomaterial-based sensors in literature.

Table 11: Analytical performance of CuNP-PPy/GCE sensor compared to published data for MET detection.

| Electrode   | LOD                       | Author                  |
|---|---------------------------|-------------------------|
| PPy-RGO-(AuNPs-GOD) n/GCE                             | $5.6000 \times 10^{-6} M$ | Wu, 2018                |
| Fe <sub>3</sub> O <sub>4</sub> NP/MWCNT nanocomposite | $3.0000 \times 10^{-9} M$ | Shahrokhian et al, 2012 |
| CuNP-PPy/GCE  | $2.3749 \times 10^{-5} M$ | This study              |

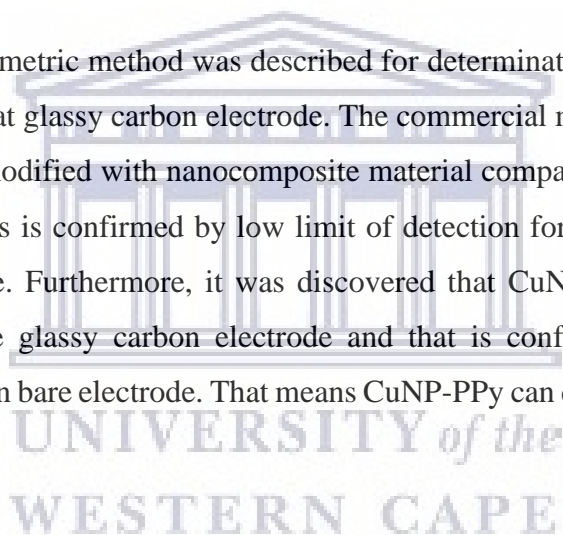
The analytical performance of CuNP-PPy/GCE sensor was compared with the work in literature, the CuNP-PPy/GCE chemical sensor was discovered to have comparable LOD which proves that

the CuNP-PPy/GCE electrochemical sensor is a stable, low cost, environmentally friendly and easy alternative method in detecting metformin in an aqueous medium (Table 11).

Table 12: Comparison of the analytical performance of the CuNP-PPy/GCE.

| Electrode      | Sensitivity (mA/mM) | LOD (M)                 | LOQ (M)                 | R-Square |
|----------------|---------------------|-------------------------|-------------------------|----------|
| CuNP-PPy/GCE 1 | 38.3900             | $9.0454 \times 10^{-5}$ | $2.7410 \times 10^{-4}$ | 0,9565   |
| CuNP-PPy/GCE 2 | 86.5250             | $4.0142 \times 10^{-5}$ | $1.2164 \times 10^{-4}$ | 0,9141   |
| CuNP-PPy/GCE 3 | 146.2580            | $2.3749 \times 10^{-5}$ | $7.1965 \times 10^{-5}$ | 0,9558   |

An electroanalytical voltammetric method was described for determination of MET in bulk drug, based on its redox reaction at glassy carbon electrode. The commercial metformin showed a good response on the electrode modified with nanocomposite material compare to a polymer electrode and bare GC electrode. This is confirmed by low limit of detection for CuNP-PPy compared to PPy and bare GC electrode. Furthermore, it was discovered that CuNP-PPy electrode is more sensitive compared to bare glassy carbon electrode and that is confirmed by lower limit of detection for CuNP-PPy than bare electrode. That means CuNP-PPy can detect the analyte at lower concentration.



# Conclusion

Metformin is classified as the best recommended anti-diabetic drug, particularly for individuals with type 2 diabetes mellitus disease which is considered a worldwide epidemic. The wide use of this anti-diabetic drug with bioavailability below 60% for a broadening variety of health problems globally, result to it being regarded as an emerging pollutant found in large quantities in wastewater. Previously, different methods were utilized for the early detection of metformin in wastewater, however they proved to suffer from several disadvantages such as long chromatographic run times, low sensitivity, and complicated sample preparation procedures before analysis. Developing a sensitive electrochemical sensor will make it easy to quantify metformin concentration in aqueous systems.

In this work, the first part focused on synthesising metformin derivatives with better bioavailability. However, the full synthesis was not completed since it was costly and complicated. Nonetheless, the starting material, 2-Amino-3-methylbutanoic acid **A1** (DL-Valine) was synthesised following **Scheme 2**. Characterisation of 2-Amino-3-methylbutanoic acid **A1** (DL-Valine) with column chromatography, thin layer chromatography, confirmed the starting material to be synthesized successfully. The chemical structure of the above-mentioned compound was fully elucidated by analysis of spectroscopic data with  $^1\text{H}$  NMR and  $^{13}\text{C}$  NMR. Notwithstanding of the incomplete organic synthesis of metformin derivatives, the main aim of this study was to evaluate the electroanalytical behaviour as well as the concentration profile of metformin in aqueous matrices. Thus, a commercial metformin drug was made in use to proceed with the experiment.

Metformin solutions were prepared from the commercial tablets (Glucophage, 500mg) and were characterised using cyclic voltammetry (CV) square wave voltammetry (SWV). For comparison purposes MET was also analysed using a standard analytical method, Ultraviolet Visible spectroscopy (UV-Vis). The limit of detection determined from UV-Vis for metformin was  $5.2660 \times 10^{-3}\text{M}$ . A conductive polymer, polypyrrole was synthesised electrochemically following Bozzini's methods for some nitrogens and was characterized using Cyclic Voltammetry (CV) and Square Wave Voltammetry (SWV). Cyclic voltammograms confirmed synthesis to be a success

since the peak potential observed agreed with literature. The calculated limit of detection for PPy/GCE was  $2.0431 \times 10^{-2} M$  which is high compared to the ones previously reported in literature.

Copper nanoparticles were synthesized using chemical reduction method. Copper nanoparticles were characterized by Scanning Electron Microscopy (SEM), Fourier Transform infrared spectroscopy (FTIR), Transform Electron Microscopy (TEM). The SEM was used to study the morphology of copper nanoparticles, the SEM image of CuNP, a typical clustered structure confirmed the successful synthesis of the nanoparticles. Fourier transform infrared spectroscopy (FTIR) confirmed the functional groups associated with copper nanoparticles. Moreover, Small Angled X-ray Scattering (SAXS) was utilized for the size of nanoparticles, which was found to be 37 nm. The composite of CuNP-PPy/GCE was formed by combining copper nanomaterial and polypyrrole. CuNP-PPy/GCE was then characterised using Cyclic voltammetry (CV). The main purpose of the composite was to increase sensitivity of the sensor. Cyclic voltammograms observed confirmed a success synthesis of the composite by studying its electrochemical behaviour. Literature agreed with the electrochemistry of composite.

Metformin was successfully detected by the sensor designed, with the average limit of detection of  $5.1448 \times 10^{-5} M$ . Meaning the designed sensor can detect low concentrations of metformin in the presence of the 0,1m Hydrochloric acid as an electrolyte. This was demonstrated by the small standard deviation per sample set ( $n=3$ ) with a relative standard deviation (RSD) of 47%. Even though the electrochemistry of metformin on Cu-PPy/GCE is limited, the analytical performance of the Cu-PPy/GCE sensor in this work in terms of LOD, LOQ and sensitivity illustrates that the sensor provides a cost-effective, reproducible and is a fast analytical tool for the detection of metformin in waste water.

## Future Works

The motivation of this work was synthesis metformin analogues since metformin's bioavailability was 60%, with large amounts of it being excreted in wastewater unchanged. Due to time and cost effectiveness of the process we could not finish. Thus, in future we will focus on synthesizing metformin analogues with high bioavailability in human system such that small amounts of this anti-diabetic drug are excreted in wastewater. Additionally, in the future we will focus more on applying the novel electrochemical sensor to real sample analysis and develop a portable monitoring tool to evaluate the concentration levels of metformin in wastewater. Collaboration with water and sanitation department form the municipality will be a necessity to develop sampling protocols and evaluating on site analysis efficiency and reliability.





# References

- Abdelmoneim, A.S., Hasenbank, S.E., Seubert, J.M., Brocks, D.R., Light, P.E., (2012), Simpson SH. Variations in tissue selectivity amongst insulin secretagogues: a systematic review. *Diabetes Obesity and Metabolism*, 14, pp 130-138. doi:10.1111/j.1463-1326.2011.01496.
- Abdulfatai, B.O., Olusegun, A.O., Lateef, B.O., (2012). Type 2 diabetes mellitus: A review of current trends. *Medical Journal*. 27. pp. 269-273. DOI: [10.5001/omj.2012.68](https://doi.org/10.5001/omj.2012.68)
- Agbabiaka, A., Wilfong, M. and Park, C., (2013). Small angle X-ray scattering technique for the particle size distribution of nonporous nanoparticles. *Journal of Nanoparticles*, 2013.
- Aroon, M., Ismail, A., Montazer-Rahmati, M., Matsuura, T. (2010). Morphology and permeation properties of polysulfone membranes for gas separation: Effects of non-solvent additives and co-solvent. *Separation and purification technology*, 72(2), pp. 194-202. aspects and contemporary approaches to tackling solubility and permeability hurdles. *Acta Pharmaceutica Sinica B*, 7(3), pp 260-280. <http://dx.doi.org/10.1016/j.apsb.2016.09.005>.
- Attia, A.K, Salem, W.M., Mohamed, M.A., (2015), Voltammetric assay of metformin hydrochloride using pyrogallol modified carbon paste electrode. *Acta Chimica Slovenica*, 62, pp 1-7. DOI: 10.17344/acsi.2014.950.
- Bakhashab, S., Ahmed, F., Schulten, H.J., Ahmed, F.W., Glanville, M., Al-Qahtani, Weaver, J.U., (2018), Proangiogenic effect of metformin in endothelial cells is via upregulation of VEGFR1/2 and their signaling under hyperglycemia-hypoxia. *Intermolecular Journal of Molecular Science*. **19**, 1–18. <https://doi.org/10.3390/ijms19010293>
- Bele, A.A., Khale A., (2010). *An Overview on Thin Layer Chromatography*, *International Journal of Pharmaceutical Sciences and Research*, Vol. 2, Issue 2, Available online on [www.ijpsr.com](http://www.ijpsr.com)
- Bellisola, G., Sorio, C., (2012), Infrared spectroscopy and microscopy in cancer research and diagnosis. *America Journal of Cancer*. *American Journal of Cancer Research*, 2(1), pp 1-21.

- Bitinis, N., Hernandez, M., Verdejo, R., Kenny, J.M., Lopez-Manchado, M.A., (2011). Recent advances in clay/polymer nanocomposites. *Advanced Materials*. 23, pp. 5229-5236.
- Bozzini, B., Bocchetta, P., Kourousias, G., Gianoncelli, A., (2017). Electrodeposition of Mn-Co/Polypyrrole nanocomposite: An electrochemical and in situ soft-X-ray microscopic investigation. *Polymer Journal*, 9(17), pp. 1–22 doi:10.3390/polym9010017. [www.mdpi.com/journal/polymers](http://www.mdpi.com/journal/polymers).
- Bradshaw, D., Norman, R., Pieterse, D., (2007) Estimating the burden of disease attributable to diabetes in South Africa in 2000. *South Afr. Med Journal*, **97** pp. 700–6.
- Burlibasa, L., Chifiriuc, M.C., Lungu, M.V., Lungulescu, E.M., Mitrea, S., Sbarcea, G., Popa, M., Marutescu, L., Constantin, N., Bleotu, C., Hermanean, A., (2020), Synthesis, physico-chemical characterization, antimicrobial activity and toxicological features of Ag-ZnO nanoparticles. *Arabian Journal of Chemistry*, 13(2), pp 4180-4197. <https://doi.org/10.1016/j.arabjc.2019.06.015>
- Cetin, M., Sahin, S., (2015). Microparticulate and nanoparticulate drug delivery systems for metformin hydrochloride. *Drug Delivery*, 23(8), Page 2796-2805, <https://doi.org/10.3109/10717544.2015.1089957>.
- Chakravarti, B., Mallik, B., Chakravarti, D.N., (2016), Column chromatography. *Curr. Protoc. Essential Lab. Tech.* doi: 10.1002/cpet.6.
- Chatterjee, S., Khunti, K., Davies, M.J., (2017). Type 2 diabetes. *Lancet Lond Engl*. 389, pp. 2239-2251.
- Chaudhury A., (2017), “Clinical Review of Antidiabetic Drugs: Implications for Type 2 Diabetes Mellitus Management”. *Frontiers in Endocrinology*, 8(6), pp 1-12. doi: 10.3389/fendo.2017.00006
- Chen, X., Schröder, J., Hauschild, S., Rosenfeldt, S., Dulle, M., Förster, S., (2015). Simultaneous SAXS/WAXS/UV–vis Study of the Nucleation and Growth Of nanoparticles: A Test of Classical nucleation theory. *Langmuir*, **31**(42), pp. 11678–11691.
- Chhetri, H.P., Thapa, P., Schepdael, A.V., (2013), Simple HPLC-UV method for the quantification of metformin in human plasma with one step protein precipitation. *Saudi Pharmaceutical Journal*. 22, pp. 483-487. <http://dx.doi.org/10.1016/j.jsps.2013.12.011>

- Cid-Hernández, M., Dellamary-Toral, F.A.L, González, L.J., Sánchez-Peña, M.J., Pacheco-Moises, F.P., (2018). International Journal of Analytical Chemistry, pp 1-9. <https://doi.org/10.1155/2018/4605373>
- Coskun, O., (2016). *Separation techniques: Chromatography*, North Clin Istanbul. **3**(2), page 156-160. [doi: 10.14744/nci.2016.32757](https://doi.org/10.14744/nci.2016.32757).
- Dang, T.M.D., Thu Le, T.T., (2011). Synthesis and optical properties of copper nanoparticles prepared by a chemical reduction method, *Advances in natural sciences: nanoscience and nanotechnology*, **2**, pp 1-6, <http://doi:10.1088/2043-6262/2/1/015009>.
- De Oliveira, A.D., Beatrice, C.A.G., (2018), Polymer Nanocomposites with Different Types of Nanofiller, *Nanocomposites - Recent Evolutions*, Technology Development Centre, Federal University of Pelotas, Pelotas, RS, Brazil, (5<sup>th</sup> Ed.). pp. 103-128.
- Dehdashtian, S., Gholivand, M. B., Shamsipur, M., Karimica, Z., (2015). Sensor Actuators B Chem., **221**, pp. 807–815.
- Devine, R., Stephens, J., (2013), Design, synthesis and biological evaluation of antidiabetic agents, PhD thesis, National University of Ireland Maynooth.
- Dey, S. (2015), A Review on nucleophilic substitution reactions at P=O substrates of organophosphorus compounds. *American Journal of Organic Chemistry*, **5**(3), pp. 83-94.
- Doomkaew, A., Prapatpong, P., Buranphalin, S., Heyden, Y.V., and Suntornsuk, L., (2015), Fast and Simultaneous Analysis of Combined Anti-Diabetic Drugs by Capillary Zone Electrophoresis. *Journal of Chromatographic Science*, **53**, pp. 993-999. [doi:10.1093/chromsci/bmu138](https://doi.org/10.1093/chromsci/bmu138).
- Douros, A., Dell’Aniello, S., Hoi Yun Yu, O., Fillion, K.B., Azoulay, L., Suissa, S. (2018). Sulfonylureas as second-line drugs in type 2 diabetes and the risk of cardiovascular and hypoglycaemic events: a population-based cohort study. *British Medical Journal*, **392**, <http://www.bmj.com/BMJ: first published as 10.1136/bmj.k2693 on 18 July 2018>.
- Dwyer-Lindgren, L., Mackenbach, J.P., Van Lenthe, F.J., Flaxman, A.D., Mokdad, A.H., (2016) “Diagnosed and undiagnosed diabetes prevalence by county in the U.S., 1999–2012,” *Diabetes Care*, **39**(9), pp. 1556–1562,
- Espinoza, E.M., Clark, J.A., Soliman, J., Derr, J.B., Morales M., Vullev, V.I., (2019), Practical Aspects of Cyclic Voltammetry: How to Estimate Reduction Potentials When

Irreversibility Prevails. *Journal of The Electrochemical Society*, 166(5), pp 3175-3187. DOI: 10.1149/2.0241905jes.

- Evans, J.M., Ogston, S.A., Emslie-Smith A., Morris A.D., (2006), Risk of mortality and adverse cardiovascular outcomes in type 2 diabetes: a comparison of patients treated with sulfonylureas and metformin. *Diabetologia*, 49, pp. 930-936. doi:10.1007/s00125-006-0176-9.
- Foretz M.,Guigas, B., Pollak, L.M. Viollet, B., (2014), Metformin: From mechanisms of action to therapies. 20(6), pp 953-966. <https://doi.org/10.1016/j.cmet.2014.09.018>
- Gholivand, M.B., (2014), Synthesis of Fe-Cu/TiO<sub>2</sub> nanostructure and its use in the construction of a sensitive and selective sensor for metformin determination, *Material Science and Engineering C*, **42**, pp. 791-798. <http://dx.doi.org/10.1016/j.msec.2014.05.077>.
- Gholivand, M.B., Mohammadi-Behzad, L., (2013). Differential pulse voltammetric determination of metformin using copper-loaded activated charcoal modified electrode. *Journal of Analytical Biochemistry*. **438**, pp. 53-60. DOI:[10.1016/j.ab.2013.03.019](https://doi.org/10.1016/j.ab.2013.03.019).
- Goedecke, C., Fettig, I., Piechotta, C., Philippa, R., S. U. Geissenc, (2013), A novel GC-MS method for the determination and quantification of metformin in surface water, *Analytical Methods*, pp. 1-8.
- Graham, G.G., Punt, J., Arora, M., Day, R.O., Doogue, M.P., Duong, J.K., Furlong, T.J., Greenfield, J.R., Greenup, L.C., Kirkpatrick, C.M., Ray, J.E., Timmins, P., Williams, K.M. (2011). Clinical Pharmacokinetics of Metformin, *Clin Pharmacokinetic*, **50**(2), pp. 81-98.
- Guariguata L., Whiting, D.R., Hambleton, I., Beagley, J., Linnenkamp, U., Shaw, J.E., (2014), Global estimates of diabetes prevalence for 2013 and projections for 2035, *Diabetes Research and Clinical Practice*. 103, pp 137-149.
- Gupta A, Bisht B, Dey CS: Peripheral insulin-sensitizer drug metformin ameliorates neuronal insulin resistance and Alzheimer's-like change. *Neuropharmacology* 2011, 60:910–920.
- Hadi, M., Poorgholi, H., Mostaanzader, H., (2016). Determination of metformin at metal-organic framework (Cu-BTC) nanocrystals/ multi-walled carbon nanotube modified glassy electrode. **69**, pp. 132-139. <http://dx.doi.org/10.17159/0379-4350/2016/v69a16>.

- Han, T.K., Proctor W.R., Costales C.L., Cai, H., Everett, R.S., Thakker, D.R., (2015) Four cation-selective transporters contribute to apical uptake and accumulation of metformin in Caco-2 cell monolayers. *J Pharmacol Exp Ther*, 352, pp 519–528.
- Hernandez-Vargas, G., Sosa-Hernández, J.E., Saldarriaga-Hernandez, S., Villalba-Rodríguez, A.M., Parra-Saldivar, R., Iqbal, H.M.N., (2018). Electrochemical Biosensors: A Solution to Pollution Detection with Reference to Environmental Contaminants. *Biosensors* **8**(29), pp. 1 – 21. doi:10.3390/bios8020029.
- Huttunen, K. M. et al. (2009). The first bio reversible prodrug of metformin with improved lipophilicity and enhanced intestinal absorption. *J. Med. Chem.* **52**, pp. 4142–4148.
- International Diabetes Federation. *IDF Diabetes Atlas*, 8th ed. Brussels, Belgium: International Diabetes Federation; 2017.
- Jiang, S., Luo, J.J., (2012). *A novel non-enzymatic glucose sensor based on Cu nanoparticles modified graphene sheet electrode*, *Analytical Chemical Acta.*, **709**, pp. 47-53. DOI: [10.1016/j.aca.2011.10.025](https://doi.org/10.1016/j.aca.2011.10.025).
- Kabel, A.M., Altowirqi, R., Thobiti, H.A., Althumali, A., and Alharthi, E., (2017), *Pharmacological Therapy of Type 2 Diabetes Mellitus: New Perspectives*. *EC pharmacology and toxicology*, 4.1, pp 12-19.
- Kagan, I.A., Flythe, M.D., (2014). Thin-layer Chromatographic (TLC) Separations and Bioassays of Plant Extracts to Identify Antimicrobial Compounds. *Journal of Visualized Experiments*, Issue 85, pp. 1-8. doi:10.3791/51411.
- Kaul, K., Tarr, J.M., Ahmad, S.I., Kohner, E.M. and Chibber, R., (2012), introduction to diabetes mellitus, in Shamim, I. (ed), *diabetes*, United Kingdom, pp. 1-10.
- Kaur, G., Adhikar, R., Cass, P., Bown, M., Gunatillake, P., (2015), Electrically conductive polymers and composites for biomedical applications. *RSC Advances*, 5, pp. 37553 – 37567. DOI: 10.1039/c5ra01851j.
- Khan, A., Rashid, A., (2016). *A chemical reduction approach to the synthesis of copper nanoparticles*, *International Nano Letters*, 6, pp. 21-26, DOI [10.1007/s40089-015-0163-6](https://doi.org/10.1007/s40089-015-0163-6).
- Kibirige, D., Lumu, W., Jones, A.G., Smeeth, L., Hattersley, A.T., and Nyirenda, M.J., (2019), Understanding the manifestation of diabetes in sub Saharan Africa to inform

therapeutic approaches and preventive strategies: a narrative review. *Clinical Diabetes and endocrinology*, 5(2), pp. 1-8.

- Kim, BE, Turski, ML, Nose, Y, Casad, M, Rockman, HA, Thiele, DJ. (2010). *Cardiac copper deficiency activates a systemic signaling mechanism that communicates with the copper acquisition and storage organs*. *Cell Metab*, **11**, pp. 353-363. [CrossRefPubMedWeb of ScienceGoogle Scholar](#)
- Kinaan, M., Hong, D., Triggler, C.R., (2015). Metformin: An old drug for the treatment of diabetes but a new drug for the protection of endothelium. DOI:[10.1159/000381643](#)
- Kohda, K., Tada, M., Hakura, A., Kasai, Hiroshi, Kawazoe, Y., (1987), Formation of 8-hydroxyguanine residues in DNA treated with 4-hydroxyaminoquinoline 1-oxide and its related compounds in the presence of seryl-AMP. *Biochemical and Biophysical Research Communications*, 149(3), pp. 1141-1148.
- Labuschagne, Q., Boikgantsho, M., Kamogetso, M., (2017). Overview and management of type 2 diabetes mellitus. **84**, pp 29-36.
- Li, J., Sha, Y., (2008), A Convenient Synthesis of Amino Acid Methyl Esters. *Molecules*, 13, pp 1111-1119. DOI: [10.3390/molecules13051111](#)
- Lin, P.C., Lin, S., Wang, P.C., Sridhar, R., (2014), Techniques for physicochemical characterization of nanomaterials. *Biotechnology Advances*, 32(4), pp. 711-726. <https://doi.org/10.1016/j.biotechadv.2013.11.006>
- Logie, L., Harthill, J., Patel, K., Bacon, S., Hamilton, D.L., Macrae, K., McDougall, G., Wang, H. H., Xue, L., Jiang, H., Sakamoto, K., Prescott, A. R., Rena, G. (2012). *Cellular responses to the metal-binding properties of metformin*. *Journal of Diabetes*, **61**(6), pp. 1423–1433.
- Machini, W.B.S., Fernandes, I. P. G., and Oliveira-Brett, A. M., (2019), Antidiabetic Drug Metformin Oxidation and in situ Interaction with dsDNA Using a dsDNA-electrochemical Biosensor. *Electroanalysis*, 31, pp 1977-1987. DOI: [10.1002/elan.201900162](#)
- MacLaren, R.D., Wisniewski, K., MacLaren, C., (2018), Environmental concentrations of metformin exposure affect aggressive behaviour in the

Siamese fighting fish, *Betta splendens*. Pone journal, **13**, pp. 1-13, <https://doi.org/10.1371/journal.pone.0197259>.

- Mahdi, M.F., Arif, I.S., Jubair, N.K., (2017). Design, synthesis, and preliminary pharmacological evaluation of new metformin derivatives. International Journal of pharmacy and pharmacological science. **9**, page 239-245. doi: <http://dx.doi.org/10.22159/ijpps.2017v9i1.15250>.
- Malin, S.A., Malin, A.S., Laskin, B.M., (2008), Synthesis of  $\alpha$ -bromoisovaleric acid in the polyphosphoric acid medium. Russian Journal of Applied Chemistry, 81(3), pp. 511-512.
- Mazzola, N., (2012), Review of current and emerging Therapies in Type 2 diabetes mellitus. The American Journal of Managed Care, **18**(1), pp. 17-26.
- McCreight, L.J., Clifford, J.B., Ewan, R.P. (2016), Metformin and gastrointestinal tract. Diabetologia Journal. **59**, pp 426-435. Published online 2016 Jan 16. DOI: [10.1007/s00125-015-3844-9](https://doi.org/10.1007/s00125-015-3844-9)
- Mery, H.A., Ramadan, N.K., Diab, S.S., Mustafa, A.A., (2018), Chromatographic Methods for the Simultaneous Determination of Binary Mixture of Sitagliptin HCl and Metformin HCl. Bulletin of Faculty of Pharmacy. Cairo University. 55(2), pp. 311–317. DOI: [10.1016/j.bfopcu.2017.04.002](https://doi.org/10.1016/j.bfopcu.2017.04.002).
- Miller, R.A., Chu, Q., Xie, J., Foretz, M, Viollet, B, Birnbaum, M.J., (2013). Biguanides suppress hepatic glucagon signalling by decreasing production of cyclic AMP. Nature. **494**, pp. 256–260. doi: 10.1038/nature11808.
- Mohamed, D., Elshahed, M.S., Nasr, T., Aboutaleb, N., Zakaria, O., (2019), Novel LC–MS/MS method for analysis of metformin and canagliflozin in human plasma: application to a pharmacokinetic study. BMC Chemistry, 13(82). pp. 1-11. doi: [10.1186/s13065-019-0597-4](https://doi.org/10.1186/s13065-019-0597-4)
- Mohanty, B., (2018), *Choosing the Best Oral Diabetic Agents in T2 Diabetes Mellitus Physicians Challenge*, Journal of Diabetes and Metabolism, **9**(6), pp. 1-7, DOI: 10.4172/2155-6156.1000797.
- Moniri, S., Ghoranneviss, M., Hantehzadeh, M.R., Asadi, M., Asadabad, (2017), Synthesis and optical characterization of copper nanoparticles prepared by laser ablation. Bulletin of Materials Science Journal, 40(1), pp. 37-43. DOI 10.1007/s12034-016-1348-y

- Müller, K., Bugnicourt, E., Latorre, M., Jorda, M., Echegoyen, S.Y., Lagaron, J., (2017), Review on the processing and properties of polymer nanocomposites and nano coatings and their applications in the packaging, automotive and solar energy fields. *Nanomaterials*, **7**, page 74-121.
- Naveed, S., Shafiq, A., Khan, M., Zafar, H., Hashim, H., Urooj, L., (2014). Degradation study of available brands of metformin in Karachi using UV spectrophotometer. *Journal of diabetes* 5(1), pp 1-3. DOI: [10.4172/2155-6156.1000328](https://doi.org/10.4172/2155-6156.1000328)
- Ngema, X.T., Baker, P., Aubert P.H., (2018), ‘Metallic nanoparticles with polymeric shell: A multifunctional platform for application to biosensor.’ PhD, University of Cergy-Pontoise and University of the Western Cape, Cape Town.
- Niemuth, J.N, Jordan, R., (2015). Metformin Exposure at Environmentally Relevant Concentrations Causes Potential Endocrine Disruption in Adult Male Fish. *Environmental Toxicology and Chemistry Journal*. **34**, pp 291-296, DOI: 10.1002/etc.2793.
- Ouellette, Robert J., Rawn, J. David, (2018), *Nucleophilic Substitution and Elimination Reactions*, in *Organic Chemistry* (2<sup>nd</sup> Edition), Towson University.
- Patel, M., (2018). Review Article: Chromatography Principle and Applications, *International journal of pharmacy and pharmaceutical research*, **13**(4), pp. 288-293.
- Pettit, D.J., Talton, J., Dabelea, Dana, Divers, Jasmin, Imperatore, G., Lawrence, J.M., Liese, A.D., Linder, B., Mayer-Davis, E.J., Pihoker, C., Saydah, S.H., Standiford, Debra A., and Hamman, R.F., (2014), Prevalence of Diabetes in U.S. Youth in 2009: The SEARCH for Diabetes in Youth Study. *Diabetes Care*, **37**, pp 402-408.
- Pheiffer, C., Wyk, V.P., Joubert, J.D., Levitt, N., Nglazi M.D., Debbie, B., (2017), The prevalence of type 2 diabetes in South Africa: a systematic review protocol. *British Medical Journal*, **8**, pp 1-4. doi:10.1136/bmjopen-2017-021029.
- Pursat, B.A.J., Spanning, R.J.M., Braster, M., Helmus, R., Voogt, P., Parsons, J.R., (2019), *Biodegradation of metformin and its transformation product, guanylurea, by natural and exposed microbial communities*, *Ecotoxicology and Environmental Safety Journal*, **182**, pp 1-10.
- Qian, C., Gong, L., Chen, X.Z., (2009). Preparation of optically active aliphatic  $\alpha$ -amino acid from fatty acid: synthesis of L-norvaline and D-norvaline, *Research on Chemical Intermediates*, DOI [10.1007/s11164-008-0013-5](https://doi.org/10.1007/s11164-008-0013-5)



- Rahaman, M., Aldalbahi, A., Almoqli, M., Alzahly, S., (2018), Chemical and Electrochemical Synthesis of Polypyrrole Using Carrageenan as a Dopant: Polypyrrole/Multi-Walled Carbon Nanotube Nanocomposites. *Polymers*, 10 (632), pp. 1-20.
- Rathod, A.P., Wasewar, K.L., Yoo, C.K., (2014), Enhancement of Esterification of Propionic Acid with Isopropyl Alcohol by Pervaporation Reactor. *Journal of Chemistry*, 14, pp. 1-4. <http://dx.doi.org/10.1155/2014/53934>
- Rena, G., Hardie, D.G., Pearson, E.R., (2017), The mechanisms of action of metformin. *Diabetologia*, 60, pp. 1577-1585.
- Repiščák, P., Erhardt, S., Rena, G., Paterson, M. J., (2014). Biomolecular mode of action of metformin in relation to its copper binding properties. *Biochemistry journal*, **53**(4), pp. 787–795.
- Rojas, L.B.A., Gomes, M.B., (2013), Metformin: an old but still the best treatment for type 2 diabetes. *Diabetology & Metabolic Syndrome*, 5(6), pp 1- 15. <http://www.dmsjournal.com/content/5/1/6>
- Roy, T., Lloyd, C.E., (2012). Epidemiology of depression and diabetes: a systematic review. *Journal of Affective Disorders*. **142**, pp. 8-21. [https://doi.org/10.1016/S0165-0327\(12\)70004-6](https://doi.org/10.1016/S0165-0327(12)70004-6).
- Santarino, I.B., Oliveira, S.C.B., Oliveira-Brett, A.M., (2014), *Electroanalysis*. 26, pp 1304–1311.
- Sayyah S.M., Abd El-Rehim S.S., El-Deep M.M., (2003), *Electro polymerization of pyrrole and characterisation of the obtained polymer films*. *Journal of Applied Polymer Science*, **90**, pp. 1783-1792.
- Schnablegger, H. and Singh, Y., (2013). *The SAXS guide: getting acquainted with the principles*. Austria: Anton Paar GmbH.
- Shahrokhian, S., Rastgar S., (2012). Fabrication of a modified electrode based on Fe<sub>3</sub>O<sub>4</sub>NPs/MWCNT nanocomposite: Application to the simultaneous determination of guanine and adenine in DNA, *Bio electrochemistry*, **86**, pp. 78-86. [DOI: 10.1016/j.bioelechem.2012.02.004](https://doi.org/10.1016/j.bioelechem.2012.02.004).

- Shaw, J.E, Sicree R.A., Zimmet P.Z., 2010, Global estimate of the prevalence of diabetes for 2010 and 2030. *Diabetes Atlas*, **85**(1), pp.4-14. <https://doi.org/10.1016/j.diabres.2009.10.007>.
- Shekhawat, P.B., Pokharkarn, V.B., (2017), Understanding peroral absorption: regulatory
- Siddiqui, M.R., AL Othman, Z.A., Rahman, N., (2013), Analytical techniques in pharmaceutical analysis: A review. *Arabian Journal of Chemistry*, pp 1-14. DOI: 10.1016/j.arabjc.2013.04.016.
- Sierra-Ávila, R., Pérez-Alvarez, M., Cadenas-Pliego, G., Padilla, V.C., Ávila-Orta, C., Camacho, O.P., Jiménez-Regalado, E., Hernández-Hernández, E., Jiménez-Barrera, R.M., (2015), Synthesis of Copper Nanoparticles Using Mixture of Allylamine and Polyallylamine. *Journal of Nanomaterials*, pp. 1-9. Article ID 367341 <http://dx.doi.org/10.1155/2015/367341>.
- Soloduch, J., Cabaj, J., (2016), Conducting polymers in sensor design, Wroclaw University of Science and Technology, Poland, pp 27 to 48. <http://dx.doi.org/10.5772/63227>.
- Stephenie, X., Foretz, M., Taleux, N., van der Zon G.C., Sokal, E., Hue, L., Viollet, B., Guigas, B., (2011), Metformin activates AMP-activated protein kinase in primary human hepatocytes by decreasing cellular energy status. *Diabetologia*, **54**, pp. 3101-3143. DOI: [10.1007/s00125-011-2311-5](https://doi.org/10.1007/s00125-011-2311-5). Epub 2011 Sep 23.
- Straub, J.O., Caldwell D.J., 2019, Environmental risk assessment of metformin and its transformation product Guanylurea. I. Environmental fate, *Chemosphere Journal*, **216**, pp. 844-854, <https://doi.org/10.1016/j.chemosphere.2018.10.036>.
- Suramwar, N.V., Thakare, S.R., Khaty, N.T., (2016), One pot synthesis of copper nanoparticles at room temperature and its catalytic activity. *Arabian Journal of Chemistry*, **9**, pp 1807-1812. <http://dx.doi.org/10.1016/j.arabjc.2012.04.034>
- Suresh Y., Annapurna S., Bhikshamaiah G., Singh A.K., Green Luminescent Copper Nanoparticles, *Materials Science and Engineering* **149**, pp 1-8. doi:10.1088/1757-899X/149/1/012187.
- Swinnen, S.G., Hoekstra M.J.B., Devries J.H., 2009, Insulin Therapy for Type 2 Diabetes, **32**, pp. 253-259. DOI: 10.2337/dc09-S318.

- Thulé, P.M., 2012, Mechanisms of current therapies for diabetes mellitus type 2. *Advances in Physiology Education*, Volume 36. Page 275-283, doi:10.1152/advan.00094.2012.
- Tisler, S., Zwiener, C., 2018. Formation and occurrence of transformation products of metformin in wastewater and surface water. *Sci. Total Environ.* 628–629, pp.1121–1129. <https://doi.org/10.1016/j.scitotenv.2018.02.105>.
- Trautwein C., Kümmerer K., 2011. Incomplete aerobic degradation of the antidiabetic drug Metformin and identification of the bacterial dead-end transformation product Guanylurea. *Chemosphere*, **85**, pp. 765–773. <https://doi.org/10.1016/j.chemosphere.2011.06.057>.
- Tsopela, A., Laborde, A., Salvagnac, L., Ventalon, V., Bedel-Pereira, E., Séguy, I., Temple-Boyer, P., P. Juneau, Izquierdo, R., Launay, J., (2016), Development of a lab-on-chip electrochemical biosensor for water quality analysis based on microalgal photosynthesis. *Biosensors and Bioelectronics*, 79, pp 568-573.
- Uddin R., Habiba N.E., Rena G., Hwu E., Boisen A., 2017, New Evidence for the Mechanism of Action of a Type-2 Diabetes Drug Using a Magnetic Bead-Based Automated Biosensing Platform. *Journal of American Chemical Society*, **2**, page 1329-1336. DOI:10.1021/acssensors.7b00384.
- Ulubay, S., Dursun, Z., (2010), Cu nanoparticles incorporated polypyrrole modified GCE for sensitive simultaneous determination of dopamine and uric acid. *Talanta*, 80, pp 1461-1466. doi:10.1016/j.talanta.2009.09.054
- Vigneshvar, S, Sudhakumarl C.C., Senthilkumaral B, Prakash H, 2016. Recent advances in biosensors technology for potential application-Overview. *Frontiers in bioengineering and biotechnology*, **4**(11), pp. 1-9. Doi:10.3389/fbioe.2016.00011.
- Viollet, B., Andreelli, F., (2011). *AMP-Activated Protein Kinase and Metabolic Control*, Diabetes - Perspectives in Drug Therapy, Handbook of Experimental Pharmacology 203. pp. 303-330. DOI 10.1007/978-3-642-17214-4\_13.
- Wang S., Q. Xu, 2008, *Sensitive electrochemical determination of calcium desolates on the carbon-iron nanoparticle modified glassy carbon electrode*. *Electrochemistry Communications*, **10**, pp. 411-415. doi: 10.1016/j.elecom.2007.12.028.
- Whitting, D.R., Guariguata L., Weil C., Shaw J., 2011, Global estimate of the prevalence of diabetes for 2010 and 2030. *Diabetes Atlas*, **94**(1), pp. 311-321. <https://doi.org/10.1016/j.diabres.2011.10.029>.

- Wu, B., Hou, S., Xue, Y., Chen, Z., (2018), *Electrodeposition–Assisted Assembled Multilayer Films of Gold Nanoparticles and Glucose Oxidase onto Polypyrrole-Reduced Graphene Oxide Matrix and Their Electrocatalytic Activity toward Glucose*. *Nanomaterials*, **8**, <https://doi.org/10.3390/nano8120993>
- Xiaofeng, L., Zhang, W., Wang, C., Wen, T.C., Wei, Y., (2011), One-dimensional conducting polymer nanocomposites: Synthesis, properties and applications. *Progress in Polymer Science*, 36(5), pp 671-712. <https://doi.org/10.1016/j.progpolymsci.2010.07.010>
- Yakaryılmaz, F.D., Öztürk, Z.A., (2017), *Treatment of type 2 diabetes mellitus in the elderly*, *World Journal of Diabetes*, **8**(6), pp. 278-285. DOI: 10.4239/wjd. v8.i6.278.
- Yoon, K.H., Lee J.H., Kim J.W., Cho J.H., Choi Y.H., Ko, S.H., (2006). *Epidemic obesity and type 2 diabetes in Asia*. *Lancet* 368(9548), pp. 1681-1688.



UNIVERSITY of the  
WESTERN CAPE